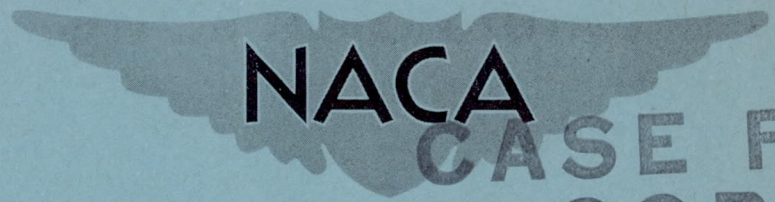


FILE COPY
NO 5



RM No. L9B23

NACA RM No. L9B23



NACA
CASE FILE
COPY
RESEARCH MEMORANDUM

TWO-DIMENSIONAL WIND-TUNNEL INVESTIGATION OF TWO
NACA 7-SERIES TYPE AIRFOILS EQUIPPED WITH
A SLOT-LIP AILERON, TRAILING-EDGE FRISE
AILERON, AND A DOUBLE SLOTTED FLAP

By

Albert L. Braslow and Fioravante Visconti

Langley Aeronautical Laboratory
Langley Air Force Base, Va.

THIS DOCUMENT ON LOAN FROM THE FILES OF
NATIONAL ADVISORY COMMITTEE FOR AERONAUTICS
LANGLEY AERONAUTICAL LABORATORY
LANGLEY FIELD, HAMPTON, VIRGINIA

RETURN TO THE ABOVE

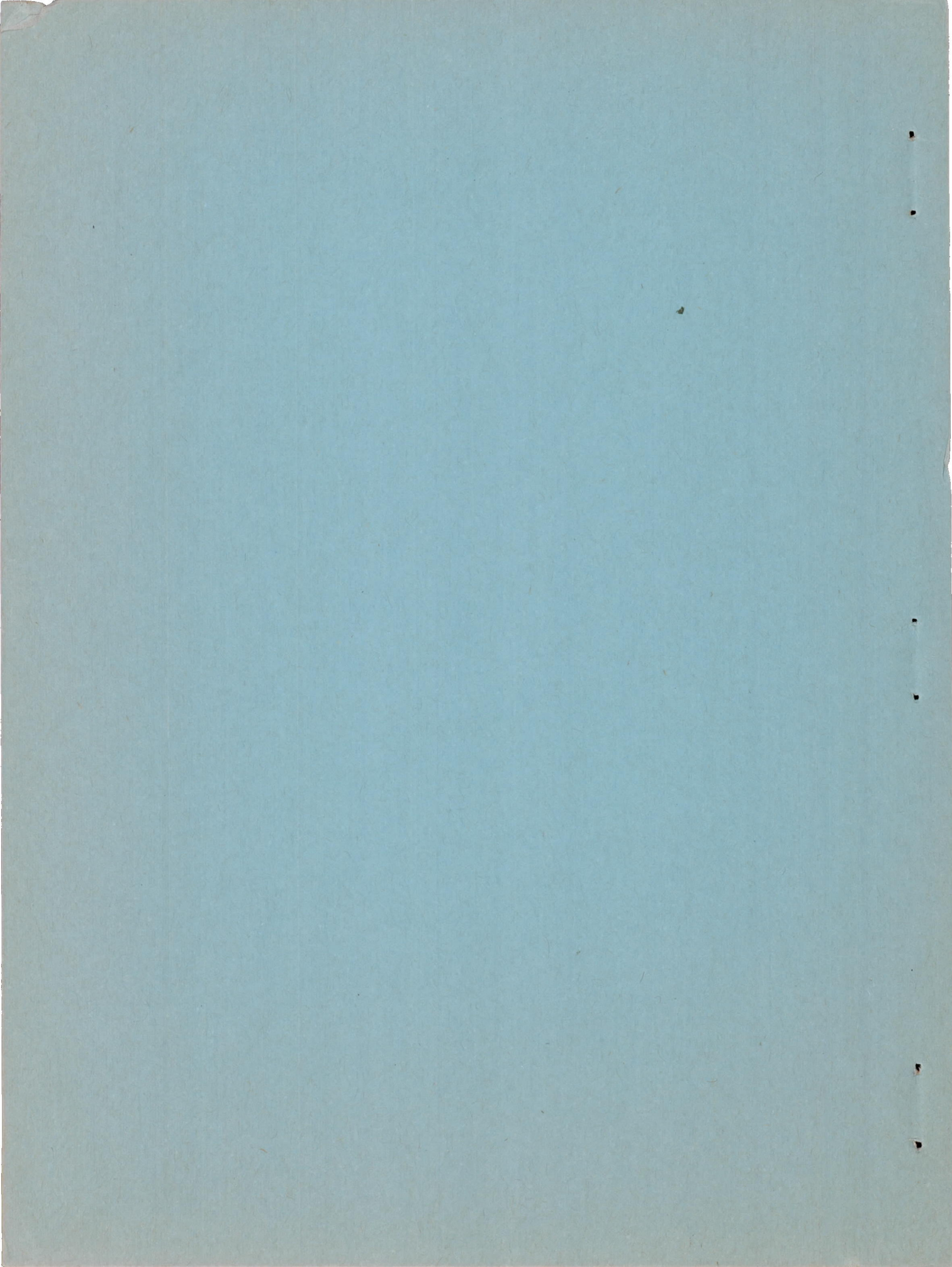
REQUESTS FOR PUBLICATIONS SHOULD BE ADDRESSED
AS FOLLOWS:

NATIONAL ADVISORY COMMITTEE FOR AERONAUTICS
1512 H STREET, N. W.
WASHINGTON 25, D. C.

**NATIONAL ADVISORY COMMITTEE
FOR AERONAUTICS**

WASHINGTON

March 28, 1949



NATIONAL ADVISORY COMMITTEE FOR AERONAUTICS

RESEARCH MEMORANDUM

TWO-DIMENSIONAL WIND-TUNNEL INVESTIGATION OF TWO
NACA 7-SERIES TYPE AIRFOILS EQUIPPED WITH
A SLOT-LIP AILERON, TRAILING-EDGE FRISE
AILERON, AND A DOUBLE SLOTTED FLAP

By Albert L. Braslow and Fioravante Visconti

SUMMARY

A two-dimensional wind-tunnel investigation was made of two NACA 7-series type airfoils of approximate 17.7-percent chord and 15.4-percent chord thickness, each equipped with a 30-percent-airfoil-chord double slotted flap, a slot-lip aileron, and a trailing-edge Frise aileron with two amounts of aerodynamic overhang balance. Airfoil lift and drag, Frise aileron hinge moment, and slot-lip aileron hinge moment were measured for both airfoils through a large range of deflection of flap, Frise aileron, and slot-lip aileron and section angle of attack. The data presented indicate that for a wing having a profile of the NACA 7-series type, a slot-lip aileron can be combined with a trailing-edge Frise aileron on a full-span double slotted flap so as to provide satisfactory lateral control characteristics at large flap deflections.

INTRODUCTION

The use of full-span flaps on large airplanes with high wing loadings to obtain the required high values of maximum lift coefficient for landing and take-off has complicated the problem of obtaining satisfactory lateral control during both the high-lift and high-speed flight conditions. A collection of available test data on lateral-control devices used in conjunction with full-span flaps is presented in reference 1. A system consisting of plain trailing-edge ailerons for the flaps-up condition and slot-lip ailerons for the flaps-down condition has proven satisfactory. Only a limited amount of data is available, however, on this type of lateral-control system on low-drag-type airfoils equipped with double slotted flaps.

A two-dimensional investigation was made in the Langley two-dimensional low-turbulence pressure tunnel of two NACA 7-series-type airfoils of approximate 15.4-percent chord and 17.7-percent chord thickness, each equipped with a double slotted flap, slot-lip aileron, and straight-sided trailing-edge Frise aileron. The Frise ailerons were tested with overhang balances of 35.1 percent and 40.8 percent of the aileron chord. Tests were made at a Reynolds number of 6×10^6 and included measurements of airfoil lift, drag, and aileron hinge moments through a wide range of deflection of flap and ailerons.

SYMBOLS

The symbols used in the presentation of results are defined as follows:

c_l	airfoil section lift coefficient
c_d	airfoil section drag coefficient
Δc_l	increment of airfoil section lift coefficient
c_{h_a}	Frise aileron section hinge-moment coefficient $\left(\frac{h_a}{qc_a^2} \right)$
c_{h_l}	slot-lip aileron section hinge-moment coefficient $\left(\frac{h_l}{qc_l^2} \right)$
α_0	airfoil section angle of attack measured with respect to wing reference line, degrees (fig. 2)
$\Delta \alpha_0$	increment of airfoil section angle of attack, degrees
c	chord of airfoil with movable surfaces neutral; measured parallel to wing reference line
c_a	chord of Frise aileron measured parallel to wing reference line from hinge axis to airfoil trailing edge
c_l	chord of slot-lip aileron measured parallel to wing reference line from hinge axis to aileron trailing edge
c_b	chord of Frise aileron overhang measured parallel to wing reference line from aileron hinge axis to aileron leading edge

- δ_f flap deflection with respect to wing reference line; positive when trailing edge is deflected downward, degrees
- δ_a Frise aileron deflection with respect to flap; positive when trailing edge is deflected downward, degrees
- δ_l slot-lip aileron deflection with respect to wing reference line; positive when trailing edge is deflected downward, degrees
- R Reynolds number based on airfoil chord
- q free-stream dynamic pressure
- h_a Frise aileron hinge moment per unit span; positive when trailing edge tends to deflect downward
- h_l slot-lip aileron hinge moment per unit span; positive when trailing edge tends to deflect downward

$$c_{n_a \alpha_0} = \left(\frac{\partial c_{n_a}}{\partial \alpha_0} \right)_{\delta_a, \delta_l, \delta_f}$$

$$c_{n_a \delta_a} = \left(\frac{\partial c_{n_a}}{\partial \delta_a} \right)_{\alpha_0, \delta_l, \delta_f}$$

The subscripts to the partial derivatives denote the variables held constant when the partial derivatives were taken. The derivatives were measured at zero angle of attack and at zero aileron deflection.

MODELS

The airfoils tested were of approximate 15.4-percent chord and 17.7-percent chord thickness and were of the NACA 7-series type (reference 2). Ordinates of the basic airfoils are given in tables I and II. The cusps near the trailing edge were removed by drawing straight lines from the trailing edge tangent to the airfoil contour. A photograph and profile sketches of the models showing the double slotted flap, straight-sided Frise aileron, and slot-lip aileron, hereinafter referred to as "flip," are presented in figures 1 and 2.

The arrangement and pertinent dimensions of the flap and control surfaces are shown in figure 3. The vane of the double slotted flap was fixed with respect to the remainder of the flap and the total flap rotated

as a unit about the hinge axis shown in figure 3. The over all length of the aileron remained constant and the percentage of overhang balance with respect to the aileron chord behind its hinge axis was changed by changing the position of the hinge axis. Overhang balances of 35.1 percent and 40.8 percent of the aileron chord were tested with resulting aileron chords of 0.150c and 0.144c, respectively. The angle of attack of the models was measured with respect to the wing reference line as shown in figure 2. The angle of attack during previous lift tests of the 0.154c thick airfoil with a double slotted flap, contour Frise aileron, and flip (reference 3) was measured with respect to a different reference line also indicated on figure 2.

The models had chords of 24 inches measured parallel to the wing reference lines and were tested in an aerodynamically smooth condition. All slots were unsealed except for a few tests in which the aileron slot was sealed with modeling clay.

APPARATUS AND TESTS

The models were tested in the Langley two-dimensional low-turbulence pressure tunnel. A description of this tunnel and of the methods by which the lift and drag data were measured and corrected to free-air conditions is given in reference 4. Hinge moments of the Frise aileron and of the flip were measured with resistance-type electrical strain gages. The corrections to the hinge moments are very small (in the order of 0.003c_l) and, therefore, were not applied.

Drag measurements were made on both airfoils with all movable surfaces neutral and on the 0.177c thick airfoil with only the flap deflected. Lift, aileron hinge moment, and flip hinge moment were measured for both airfoils with the ailerons having overhang balances of either 0.351c_a or 0.408c_a. The measurements were obtained for a large range of deflection of flap, Frise aileron, and flip. The scope of the investigation is outlined in table III which may also be used as a figure index for the basic data. The basic lift and flip hinge-moment data obtained on the airfoils equipped with the aileron of larger balance are not presented inasmuch as these data are very similar to the data presented for the smaller aileron balance.

During each test run, the deflections of the movable surfaces were held constant while the angle of attack was varied in both an increasing and a decreasing direction. For some combinations of movable-surface deflection a difference in lift or hinge-moment values existed at the same angle of attack. For these conditions arrows are drawn along the curves to indicate the direction of the change in angle of attack.

The Reynolds number for all tests was approximately 6×10^6 and the Mach number was less than 0.13.

RESULTS AND DISCUSSION

The basic data are presented in figures 4 to 14 and analysis curves are presented in figures 15 to 23.

Lift Characteristics

The existence of sharp breaks in the lift curves of the 0.154c thick airfoil equipped with a true-contour aileron was indicated in reference 3 for flap deflections of 50° and greater. For this investigation, therefore, the flap deflection of the 0.154c thick airfoil was limited to 40° . A few tests of the 0.177c thick airfoil with a flap deflection of 50° indicated that sharp breaks in the lift curves and unsteady flow conditions also existed (fig. 4(1)). The remainder of the tests on the thicker airfoil, therefore, were limited also to a maximum flap deflection of 40° .

The variations of maximum lift coefficient with flap deflection for the neutral aileron condition are presented in figure 15 for both airfoils tested and for the 0.154c thick airfoil with the true-contour aileron (reference 3). The change in the aileron profile from true to straight-sided contour has no effect on the airfoil maximum lift coefficients at all the flap deflections tested.

The rate of change of maximum lift coefficient with flap deflection for the 0.177c thick airfoil decreases through a range of flap deflection from approximately 20° to 25° , and then increases when the flap is deflected more than 25° . A discontinuity also occurs near this range for the thinner airfoil. This discontinuity is probably caused by the lower-surface skirt of the airfoil which blocks the flow of air through the slot between the flap and the vane of the double slotted flap at low flap deflections. When the flap deflection is large enough to permit better air flow conditions through this slot over the vane, the maximum lift is increased. A similar variation of maximum lift coefficient with flap deflection was shown by tests of a double-slotted-flap model with lower-surface airfoil skirts of different lengths as reported in reference 5.

The maximum section lift coefficients of the 0.177c thick airfoil are lower than those of the thinner airfoil at flap deflections less than approximately 18° . At flap deflections greater than approximately 30° , however, higher values of maximum section lift coefficients were obtained on the thicker airfoil. Values of maximum section lift coefficient of 2.92 and 2.85 were obtained on the 17.7-percent and 15.4-percent thick airfoils, respectively, at a flap deflection of 40° with both ailerons neutral.

Aileron and Flip Lift Effectiveness

The variations of section lift coefficient with aileron deflection and with flip deflection are presented in figures 16 and 17, respectively, for the airfoil at zero angle of attack. In order to facilitate an analysis of the aileron and flip lift effectiveness, values of the increment of section angle of attack required to maintain a constant lift coefficient are plotted against aileron deflection in figure 18 for various flip deflections on both airfoils with the double slotted flap retracted and deflected 25° and 40° . The lift coefficient chosen at each flap deflection for this analysis corresponds to approximately the minimum value of maximum lift obtained throughout the range of deflection of the aileron and flip.

At the double-slotted-flap deflections of 25° and 40° the Frise aileron was generally more effective for negative aileron deflections than for positive aileron deflections on both airfoils with flip neutral. At a flap deflection of 40° on the 15.4-percent-chord thick airfoil, the air flow over the aileron became unsteady and erratically stalled and unstalled at aileron deflections of 5° and greater (figs. 5(g), 5(h), 6, and 18(e)). The effect of sealing the aileron slot was investigated at a flap deflection of 40° , and the results are presented in figures 5(h), 6, and 18(f). Sealing the aileron slot precipitated aileron stall at aileron deflections of 10° and 15° with the flip neutral but tended to prevent the aileron stall at an aileron deflection of 5° with the flip neutral and at an aileron deflection of 10° with the flip deflected -3° . The data for the true-contour Frise aileron (reference 3) indicated that sealing the aileron slot also precipitated aileron stall at aileron deflections of 10° and 15° with the flip neutral at flap deflections of 45° and 50° . Fairing the aileron slot to the aileron contour, however, in addition to sealing the slot eliminated the aileron stall at flap, aileron, and flip deflections of 40° , 10° , and 0° , respectively (figs. 6 and 18(f)).

The variation of flip effectiveness with flap deflection is shown by comparison of figures 18 and 19. With the flap retracted the flip is very ineffective in producing a change in angle of attack at a section lift coefficient of 0.4. A large increase in flip effectiveness occurs with increasing flap deflection with the result that at a flap deflection of 40° the flip is more effective than the aileron. The flip is more effective on the 0.154c thick airfoil than on the 0.177c thick airfoil through the complete range of flip deflection at a flap deflection of 25° . With a 40° deflection of the flap and with the aileron neutral the flip on the thinner airfoil is also more effective than the flip on the thicker airfoil only for flip deflections greater than -10° .

Inasmuch as the change in angle of attack required to maintain a constant lift coefficient is a measure of the rolling effectiveness of a control-surface installation, a study of figure 18 indicates that use of

the flip in combination with the aileron will most likely result in a rolling effectiveness at a flap deflection of 40° equal to or greater than the effectiveness of the aileron alone with the flap retracted.

Hinge-Moment Characteristics

A large quantity of basic hinge-moment data of the straight-sided Frise aileron and of the flip is presented as an aid in the design of similar complex control-surface installations. The discussion of these data is restricted to the general trends of the hinge-moment parameters and hinge-moment characteristics that are instrumental in determining the design of control surfaces and the lateral-control linkage systems.

Frise aileron.—The variations of the straight-sided Frise aileron section hinge-moment coefficient with aileron deflection are presented in figure 20 for flap deflections of 0° , 25° , and 40° . A summary of the basic aileron hinge-moment parameters $c_{h\alpha_0}$ and $c_{h\delta_a}$ is presented in

table IV for a range of double slotted flap and flip deflections. All values of $c_{h\alpha_0}$ and $c_{h\delta_a}$ were determined at zero aileron deflection and zero angle of attack.

For the 17.7-percent-thick airfoil with the double slotted flap and flip neutral, an increase in aileron overhang balance chord from $0.351c_a$ to $0.408c_a$ increased positively the values of $c_{h\alpha_0}$ and $c_{h\delta_a}$ from 0.0003 to 0.0008 and from -0.0034 to -0.0013 , respectively. On the 15.4-percent-thick airfoil, the values of $c_{h\alpha_0}$ and $c_{h\delta_a}$ increased positively from -0.0013 to -0.0002 and from -0.0060 to -0.0037 , respectively, with the increased aileron overhang balance. The increase in aileron overhang balance on both airfoils also increased the values of $c_{h\delta_a}$ positively at double-slotted-flap deflection of 25° and 40° with the flip neutral, but generally increased the values of $c_{h\alpha_0}$ negatively for the same double slotted flap and flip configurations.

Deflection of the double slotted flap with flip neutral, generally resulted in a negative increase in $c_{h\alpha_0}$ and $c_{h\delta_a}$ with maximum values resulting at a flap deflection of 25° . At double-slotted-flap deflections of 25° and 40° , however, the values of $c_{h\alpha_0}$ and $c_{h\delta_a}$ varied inconsistently with flip deflection for all configurations investigated.

The effects of flip deflection on the neutral aileron hinge-moment characteristics at double-slotted-flap deflections of 25° and 40° are presented in figure 21 for both airfoils investigated. In general, low flip deflections appear to have little effect on the neutral aileron hinge-moment coefficients; however, an increase in the magnitude of the aileron hinge moments occurs at the high flip deflections.

As mentioned in the discussion of the lift characteristics, the aileron stalled on the 15.4-percent-thick airfoil at a flap deflection of 40° and aileron deflections of 5° and greater. At these combinations of control-surface deflection, values of the lift coefficient measured when the angle of attack was increased differed from those measured when the angle of attack was decreased. This hysteresis effect is caused by a change in air flow conditions through the various control-surface slots when the airfoil is stalled. The irregular nature of the air flow is evidenced also in the aileron hinge moments which differ in value for increasing and decreasing angles of attack at the same control-surface deflections. (See figs. 9(g), 9(h), 9(i), 10(e), and 10(f).)

Flip.— The values of the flip hinge-moment coefficients are not considered to be as quantitatively accurate as the values of the Frise aileron hinge moments because of considerable difficulty experienced in eliminating friction from the flip strain-gage system. The flip hinge-moment data, however, are believed to be sufficiently accurate quantitatively to obtain indications of the order of magnitude of the flip control forces.

The flip hinge-moment coefficients for several combinations of control-surface deflection exhibited a hysteresis effect for increasing and decreasing angles of attack (figs. 11 and 12). Hysteresis loops were measured at some configurations for which a similar spread in lift or aileron hinge moments was not measured. This result seems to indicate that the flip was very sensitive to small changes in air flow conditions over the airfoil that were not large enough to affect the airfoil lift or Frise aileron hinge moments. Data not presented indicate, however, that if the angle of attack is not increased to the airfoil stall the value of the flip hinge moment will be independent of the previous direction of change in angle of attack. The flip hinge-moment hysteresis loops that occurred during these tests without a similar lift effect may not be serious, therefore, under actual flight conditions.

Cross plots of the basic data showing the effect of aileron deflection and flip deflection on the flip hinge-moment coefficients are presented in figures 22 and 23, respectively. With the double slotted flap retracted, intermediate and large positive deflections of the Frise aileron cause an opening tendency of the slot-lip aileron which would add to the stick force if the flip were connected in the linkage system. This opening

tendency at positive aileron deflections in addition to the poor lift effectiveness of the flip with the flaps up appear to warrant a control linkage system that would disengage the flip from the system when the flap is retracted. For both airfoils at a flap deflection of 25° and at an angle of attack of 0° , the flip has a closing tendency. For the 0.177c thick airfoil, negative aileron deflections have no appreciable effect on the closing tendency of the flip, but reduce the closing tendency for the thinner airfoil. Positive aileron deflections increase the flip closing tendency on both airfoils. Variation of flip hinge moment with flip deflection was nonlinear (fig. 23).

Deflection of the double slotted flap from 25° to 40° decreases the closing tendency of the flip at all Frise aileron deflections at an angle of attack and flip deflection of 0° . Aileron deflection has very little effect on the flip hinge moments for both airfoils at a flap deflection of 40° . An opening tendency exists at intermediate flip deflections (fig. 23) from approximately -10° to -15° on the 17.7-percent-thick airfoil and from approximately -10° to -21° on the thinner airfoil. Elimination of the opening tendency of the flip may be accomplished by modifying the flip overhang balance. In a flight investigation of a slot-lip aileron on an airplane (reference 6), a spring was incorporated into the lateral-control system to counteract an opening tendency of the slot-lip aileron.

Drag Characteristics

Profile drag characteristics of the 17.7-percent chord and 15.4-percent chord thick airfoils are presented in figures 13 and 14, respectively. With all control surfaces neutral, the drag coefficients for the 17.7-percent thick airfoil were lower than the values for the 15.4-percent thick airfoil at positive lift coefficients and greater than the values for the thinner airfoil at negative lift coefficients. The increase in section drag coefficient with flap deflection is shown in figure 13 for the 17.7-percent thick airfoil.

CONCLUDING REMARKS

Results have been presented of a two-dimensional wind-tunnel investigation of two NACA 7-series type airfoils of 17.7-percent chord and 15.4-percent chord thickness, each equipped with a double slotted flap, slot-lip aileron (flip), and trailing-edge Frise aileron with two amounts of aerodynamic overhang balance. Sharp breaks in the lift curves and irregular flow conditions occurred at a flap deflection of 50° which indicate the advisability of limiting deflection of the double slotted flap to 40° . At a flap deflection of 40° with both ailerons neutral, values of maximum section lift coefficient of 2.92 and 2.85 were obtained on the 17.7-percent and 15.4-percent thick airfoils, respectively.

The lift effectiveness of the flip increased with flap deflection and was greater than the Frise aileron effectiveness at a flap deflection of 40° . With the flap retracted, the flip lift effectiveness was negligible and the flip hinge moments indicated an opening tendency at positive deflections of the Frise aileron. This combination of flip characteristics appears to warrant a lateral control linkage system that would disengage the flip from the system when the flap is retracted.

With the flip neutral and with the flap retracted or deflected 25° and 40° , the increase in Frise aileron overhang balance was effective in reducing the negative rate of change of aileron section hinge-moment coefficient with aileron deflection $c_{ha\alpha a}$. The increase in overhang balance, however, generally caused the rate of change of aileron section hinge-moment coefficient with angle of attack $c_{ha\alpha o}$ to increase negatively at flap deflections of 25° and 40° . The values of $c_{ha\alpha a}$ and $c_{ha\alpha o}$ were largest at a flap deflection of 25° and varied inconsistently with flip deflection for the deflected flap configurations.

The data presented indicate that a slot-lip aileron can be combined with a trailing-edge Frise aileron on a full-span double slotted flap so as to provide satisfactory lateral-control characteristics at large flap deflections on a wing having a profile of the NACA 7-series type.

Langley Aeronautical Laboratory
National Advisory Committee for Aeronautics
Langley Air Force Base, Va.

REFERENCES

1. Fischel, Jack, and Ivey, Margaret F.: Collection of Test Data for Lateral Control with Full-Span Flaps. NACA TN No. 1404, 1948.
2. Abbott, Ira H., Von Doenhoff, Albert E., and Stivers, Louis S., Jr.: Summary of Airfoil Data. NACA Rep. No. 824, 1945.
3. Nuber, Robert J., and Rice, Fred J., Jr.: Lift Tests of a 0.1536c Thick Douglas Airfoil Section of NACA 7-Series Type Equipped with a Lateral-Control Device for Use with a Full-Span Double-Slotted Flap on the C-74 Airplane. NACA MR No. L5C24a, 1945.
4. Von Doenhoff, Albert E., and Abbott, Frank T., Jr.: The Langley Two-Dimensional Low-Turbulence Pressure Tunnel. NACA TN No. 1283, 1947.
5. Cahill, Jones F.: Summary of Section Data on Trailing-Edge High-Lift Devices. NACA RM No. L8D09, 1948.
6. Wetmore, Joseph W., and Sawyer, Richard H.: Flight Tests of F2A-2 Airplane with Full-Span Slotted Flaps and Trailing-Edge and Slot-Lip Ailerons. NACA ARR No. 3L07, 1943.

TABLE I.- ORDINATES FOR THE APPROXIMATELY 17.7-PERCENT-CHORD THICK
NACA 7-SERIES-TYPE AIRFOIL

[Stations and ordinates given in percent of airfoil chord
measured along wing reference line]

Station	Ordinate	
	Upper surface	Lower surface
0	2.599	2.599
.1	3.312	1.996
.25	3.754	1.713
.5	4.258	1.421
1	4.977	1.040
1.75	5.778	.633
2.5	6.419	.314
3.75	7.292	-.121
5	8.004	-.487
7.5	9.128	-1.115
10	9.986	-1.667
12.5	10.659	-2.177
15	11.186	-2.658
17.5	11.589	-3.117
20	11.882	-3.557
22.5	12.079	-3.980
25	12.189	-4.385
27.5	12.220	-4.773
30	12.177	-5.144
32.5	12.064	-5.498
35	11.885	-5.832
37.5	11.644	-6.148
40	11.343	-6.442
42.5	10.985	-6.714

Station	Ordinate	
	Upper surface	Lower surface
45	10.575	-6.960
47.5	10.113	-7.180
50	9.605	-7.368
52.5	9.050	-7.519
55	8.453	-7.616
57.5	7.816	-7.650
60	7.142	-7.616
62.678	6.383	-7.486
65	5.700	-7.280
67.5	4.943	-6.984
70	4.171	-6.656
72.5	3.391	-6.317
75	2.606	-5.967
77.5	1.824	-5.618
80	1.050	-5.276
82.5	.292	-4.951
85	-.443	-4.648
87.5	-1.143	-4.374
90	-1.796	-4.139
92.5	-2.384	-3.950
95	-2.887	-3.818
97.5	-3.284	-3.761
100.000	-3.675	-3.675

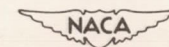


TABLE II.- ORDINATES FOR THE APPROXIMATELY 15.4-PERCENT-CHORD THICK
NACA 7-SERIES-TYPE AIRFOIL

[Stations and ordinates given in percent of airfoil chord
measured along wing reference line]

Station	Ordinate	
	Upper surface	Lower surface
0	2.044	2.044
.10	2.716	1.447
.25	3.109	1.141
.50	3.564	.840
1.00	4.219	.455
1.75	4.951	.057
2.50	5.538	-.254
3.75	6.333	-.676
5.0	6.969	-1.029
7.5	7.937	-1.631
10	8.642	-2.156
12.5	9.166	-2.633
15	9.552	-3.077
17.5	9.824	-3.497
20	10.002	-3.896
22.5	10.098	-4.275
25	10.120	-4.634
27.5	10.076	-4.973
30	9.972	-5.292
32.5	9.811	-5.590
35	9.598	-5.866
37.5	9.337	-6.121
40	9.033	-6.352

Station	Ordinate	
	Upper surface	Lower surface
42.5	8.690	-6.556
45	8.313	-6.731
47.5	7.905	-6.873
50	7.468	-6.979
52.5	7.004	-7.032
55	6.515	-6.994
57.5	6.004	-6.846
60	5.472	-6.615
62.5	4.923	-6.333
65	4.359	-6.031
67.5	3.783	-5.725
70	3.197	-5.421
72.5	2.602	-5.124
75	2.002	-4.836
77.5	1.398	-4.559
80	.795	-4.297
82.5	.196	-4.054
85	-.393	-3.834
87.5	-.960	-3.641
90	-1.490	-3.484
92.5	-1.961	-3.372
95	-2.358	-3.307
97.5	-2.699	-3.284
100	-3.010	-3.283

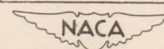


Table III.- Test program and figure index - Continued

(b) 0.154c-thick airfoil; $c_b = 0.351c_a$

δ_f		0										25						40							
		δ_a	-25	-20	-15	-10	-5	0	5	10	15	20	-20	-17	-10	-5	0	5	10	15	-15	-10	-5	0	5
0	l	5a	5a	5a	5a	5a	5a	5a	5a	5a	5a	5b	5b	5b	5b	5b	5b	5b	5g	5g	5g	5g	5g	5g	5g
	a	9a	9a	9a	9a	9a	9a	9a	9a	9a	9a	9b	9b	9b	9b	9b	9b	9b	9g	9g	9g	9g	9g	9g	9g
	f											12d	12d	12c	12c	12a	12b	12b	12b	12j	12j	12i	12e	12g	12h
-2	l														5b		5c	5d				5g	5h	5h	5h
	a														9c		9c	9c				9h	9h	9h	9h
	f														12a		12b	12b				12e	12g	12h	12h
-3	l														5b	5c	5c					5g	5h	5h	
	a														9c	9c	9c					9i	9i	9i	
	f														12a	12b	12b					12e	12g	12h	
-4	l																						5g	5h	
	a																						9i	9i	
	f																						12e	12g	
-5	l														5d	5b	5c					5g	5h		
	a														9d	9d	9d					9j	9j		
	f														12c	12a	12b					12e	12g		
-6	l														5b										
	a														9d										
	f														12a										
-7	l														5e	5d	5b					5i	5g	5h	
	a														9d	9d	9d					9j	9j	9j	
	f														12c	12c	12a					12i	12e	12g	
-10	l														5e	5e	5d	5b				5i	5g		
	a														9e	9e	9e					9k	9k		
	f														12c	12c	12a					12i	12f		
-15	l														5f	5e	5e	5b				5i	5i	5g	
	a														9e	9e	9e	9e				9k	9k	9k	
	f														12d	12d	12c	12a				12j	12i	12f	
-20	l														5f	5e		5b				5i	5i	5g	
	a														9f	9f		9f				9l	9l	9l	
	f														12d	12d		12a				12j	12i	12f	
-25	l																					5i	5i	5g	
	a																					9l	9l	9l	
	f																					12j	12j	12f	

l denotes airfoil lift data
a denotes aileron hinge-moment data
f denotes flap hinge-moment data

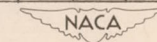


Table III.- Test program and figure index - Continued

(c) 0.177c-thick airfoil; $c_b = 0.40\delta_{c_a}$

δ_r		0										20					25					40					
δ_l	δ_a	-25	-20	-15	-10	-5	0	5	10	15	20	0	-20	-15	-10	-5	0	5	10	15	-15	-10	-5	0	5	10	15
0	l	*	*	*	*	*	*	*	*	*	*	*	*	*	*	*	*	*	*	*	*	*	*	*	*	*	*
	a	δ_a	δ_a	δ_a	δ_a	δ_a	δ_a	δ_a	δ_a	δ_a	δ_a	δ_b	δ_c	δ_c	δ_c	δ_c	δ_c	δ_c	δ_c	δ_c	δ_c	δ_c	δ_c	δ_c	δ_c	δ_c	
	f	*	*	*	*	*	*	*	*	*	*	*	*	*	*	*	*	*	*	*	*	*	*	*	*	*	*
-2	l											*						*	*				*	*	*	*	
	a											δ_b						δ_d	δ_d				δ_f	δ_f	δ_f	δ_f	
	f											*						*	*				*	*	*	*	
-5	l											*			*		*						*	*			
	a											δ_b			δ_d		δ_d						δ_f	δ_f			
	f											*			*		*						*	*			
-10	l											*		*	*							*	*				
	a											δ_b			δ_d	δ_d						δ_f	δ_f				
	f											*			*	*							*	*			
-15	l											*		*	*							*	*	*			
	a											δ_b		δ_d	δ_d							δ_g	δ_g	δ_g			
	f											*		*	*							*	*	*	*	*	
-20	l											*	*	*								*	*	*			
	a											δ_b	δ_d	δ_d								δ_g	δ_g	δ_g			
	f											*	*	*								*	*	*	*	*	
-25	l																					*	*	*			
	a																					δ_g	δ_g	δ_g			
	f																					*	*	*	*	*	

l denotes airfoil lift data
a denotes aileron hinge-moment data
f denotes flap hinge-moment data
* denotes data not presented

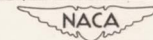


Table III.- Test program and figure index - Concluded

(d) 0.154c-thick airfoil; $c_b = 0.408c_a$

$\delta_l \backslash \delta_a$		0									25						40								
		-20	-15	-10	-5	0	5	10	15	20	-20	-15	-10	-5	0	5	10	15	-15	-10	-5	0	5	10	15
0	l	*	*	*	*	*	*	*	*	*	*	*	*	*	*	*	*	*	*	*	*	*	*	*	*
	a	10a	10a	10a	10a	10a	10a	10a	10a	10b	10b	10b	10b	10b	10b	10b	10b	10e	10e	10e	10e	10e	10e	10e	
	f									*	*	*	*	*	*	*	*	*	*	*	*	*	*		
-2	l													*		*	*					*	*	*	
	a													10c		10c	10c					10f	10f	10f	
	f															*	*					*	*	*	
-5	l												*	*	*							*	*		
	a												10c	10c	10c							10f	10f		
	f												*	*	*							*	*		
-10	l											*	*	*							*	*			
	a											10d	10d	10d							10g	10g			
	f											*	*	*							*	*			
-15	l									*	*	*	*						*	*	*				
	a										10d	10d		10d					10g	10g	10g				
	f										*	*		*					*	*	*				
-20	l									*	*			*					*	*	*				
	a										10d	10d		10d					10h	10h	10h				
	f									*	*			*					*	*	*				
-25	l																	*	*	*	*				
	a																	10h	10h		10h				
	f																	*	*						

l denotes airfoil lift data
a denotes aileron hinge-moment data
f denotes flap hinge-moment data
* denotes data not presented

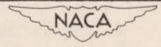
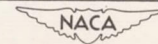


TABLE IV.- AILERON SECTION HINGE-MOMENT PARAMETERS MEASURED AT $\delta_a = 0^\circ$, $\alpha_o = 0^\circ$ $c_{h_{a\delta_o}}$

t	δ_f c_b	25						40				
		0	0	-5	-10	-15	-20	0	-5	-10	-15	-20
0.154c	0.35135c _a	-0.0013	-0.0028	-0.0026	-0.0025	-0.0039	-0.0046	-0.0018	-0.0013	-0.0019	-0.0030	-0.0022
	.40845c _a	-.0002	-.0025	-.0029	-.0035	-.0028	-.0077	-.0026	-.0017	-.0025	-.0019	-.0033
.177c	.35135c _a	.0003	-.0025	-.0031	-.0043	-.0047	-.0029	-.0016	-.0018	-.0016	-.0017	-.0024
	.40845c _a	.0008	-.0034	-----	-----	-----	-----	-.0030	-.0032	-.0028	-.0025	-.0033

 $c_{h_{a\delta_a}}$

t	δ_f c_b	25						40				
		0	0	-5	-10	-15	-20	0	-5	-10	-15	-20
0.154c	0.35135c _a	-0.0060	-0.0065	-0.0041	-0.0073	-----	-----	-0.0029	-0.0026	-0.0030	-0.0019	-0.0020
	.40845c _a	-.0037	-.0037	-.0038	-.0050	-----	-----	-.0024	-.0031	-.0041	-.0044	-.0023
.177c	.35135c _a	-.0034	-.0041	-.0043	-.0063	-0.0061	-0.0029	-.0034	-.0020	-.0034	-.0032	-.0009
	.40845c _a	-.0013	-.0019	-.0043	-.0036	-----	-----	-.0020	-.0025	-.0045	-.0045	-.0035



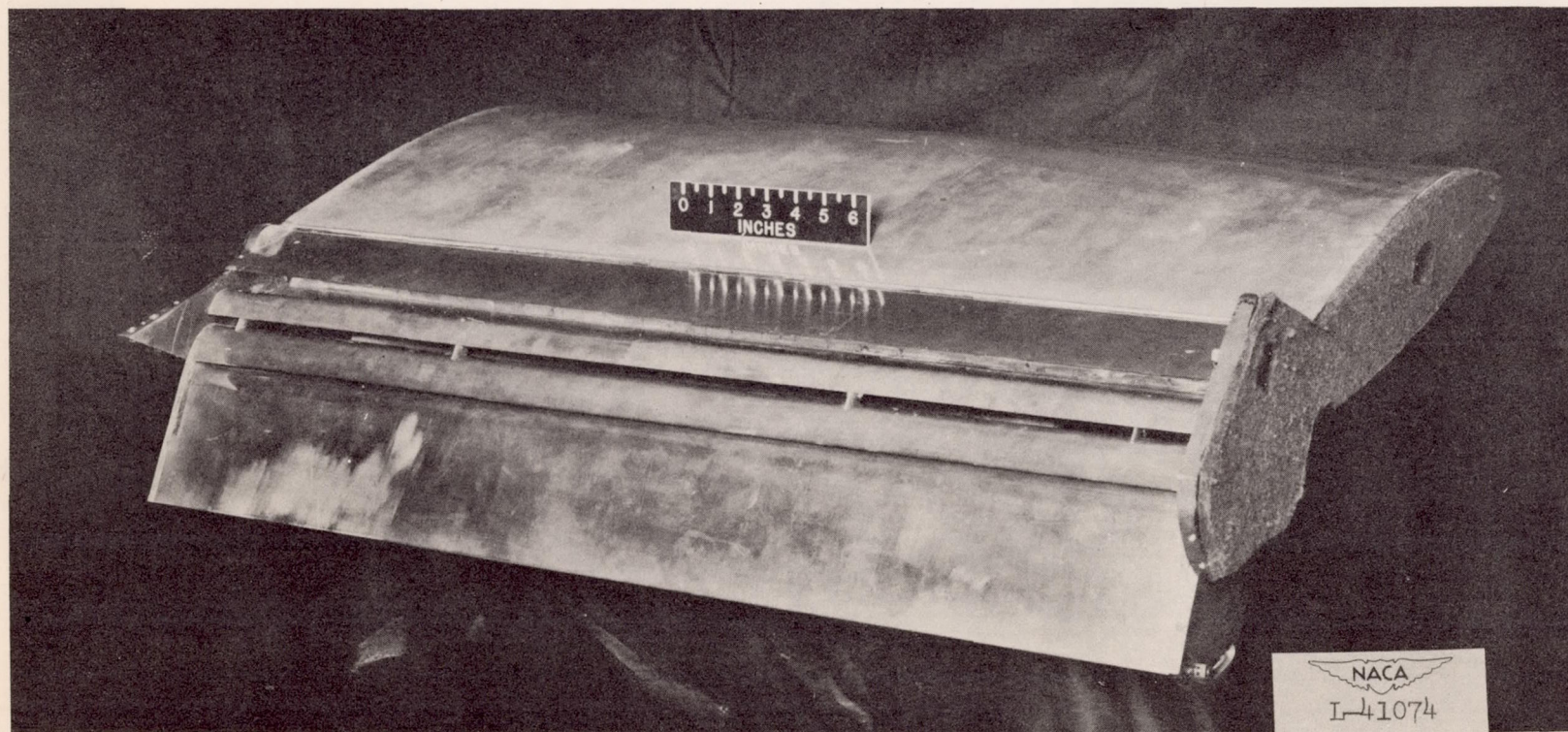
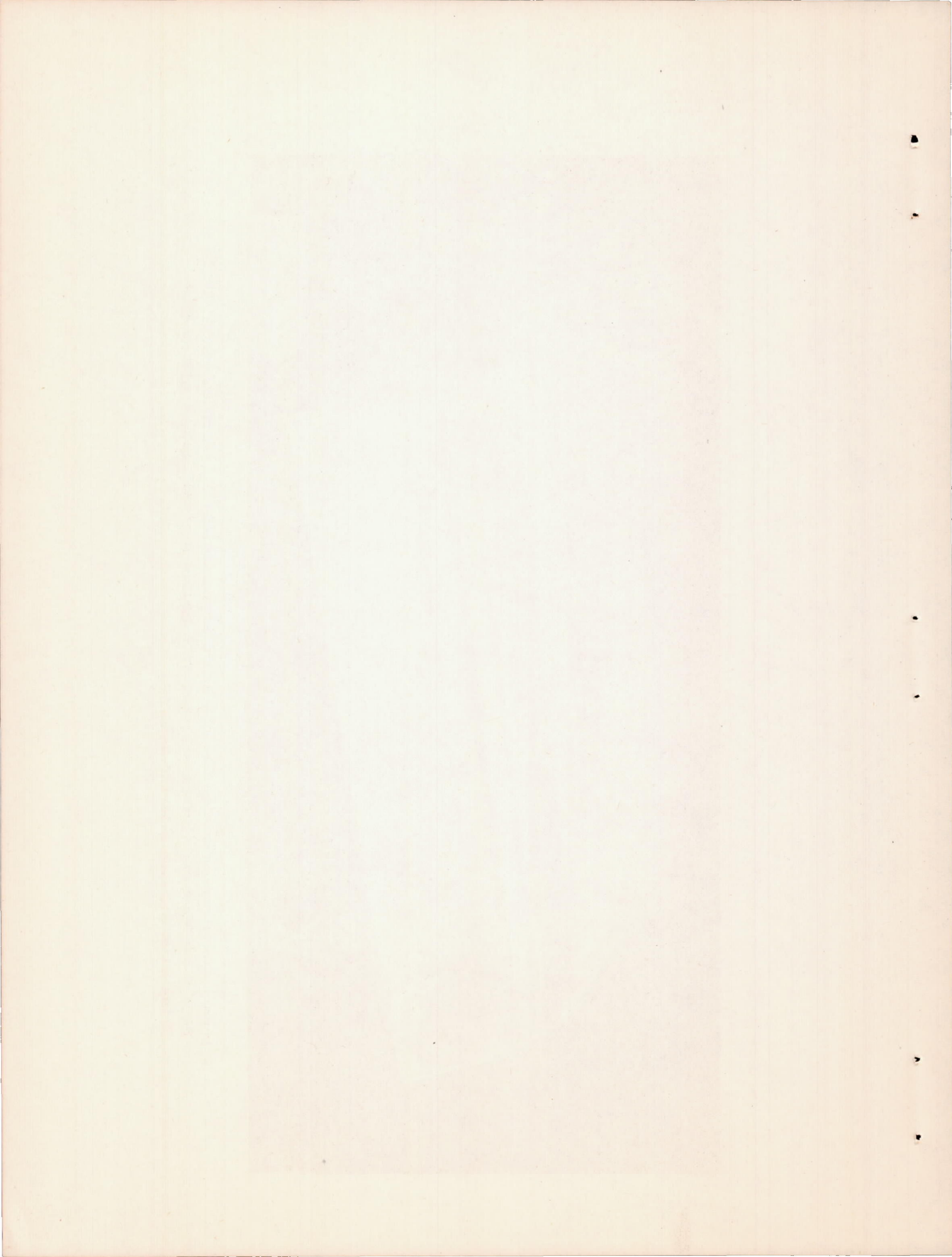


Figure 1.- Photograph of the 24-inch chord approximately 15.4-percent-chord thick NACA 7-series-type airfoil equipped with double slotted flap, trailing-edge Frise aileron, and slot-lip aileron.



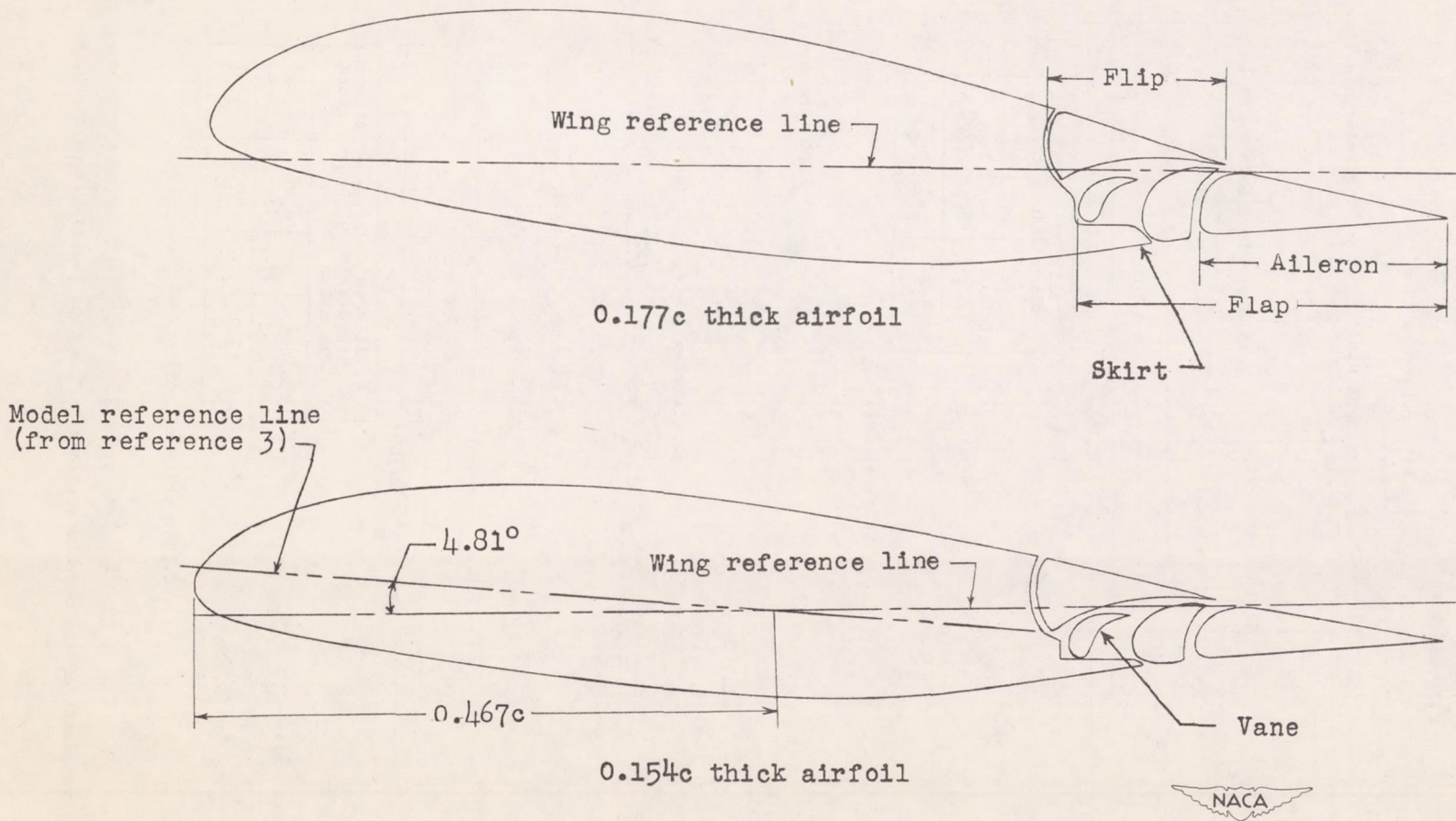


Figure 2.- Profile sketches of the NACA 7-series-type airfoils equipped with double slotted flap, trailing-edge aileron and flap.

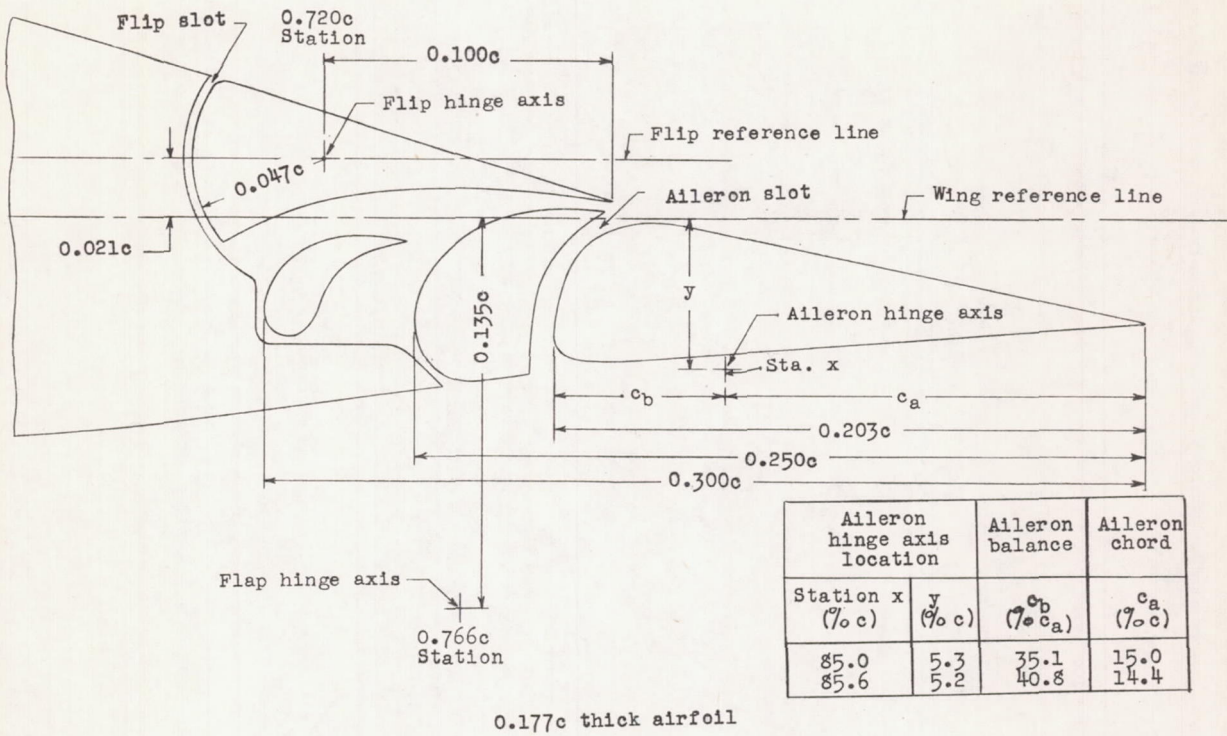
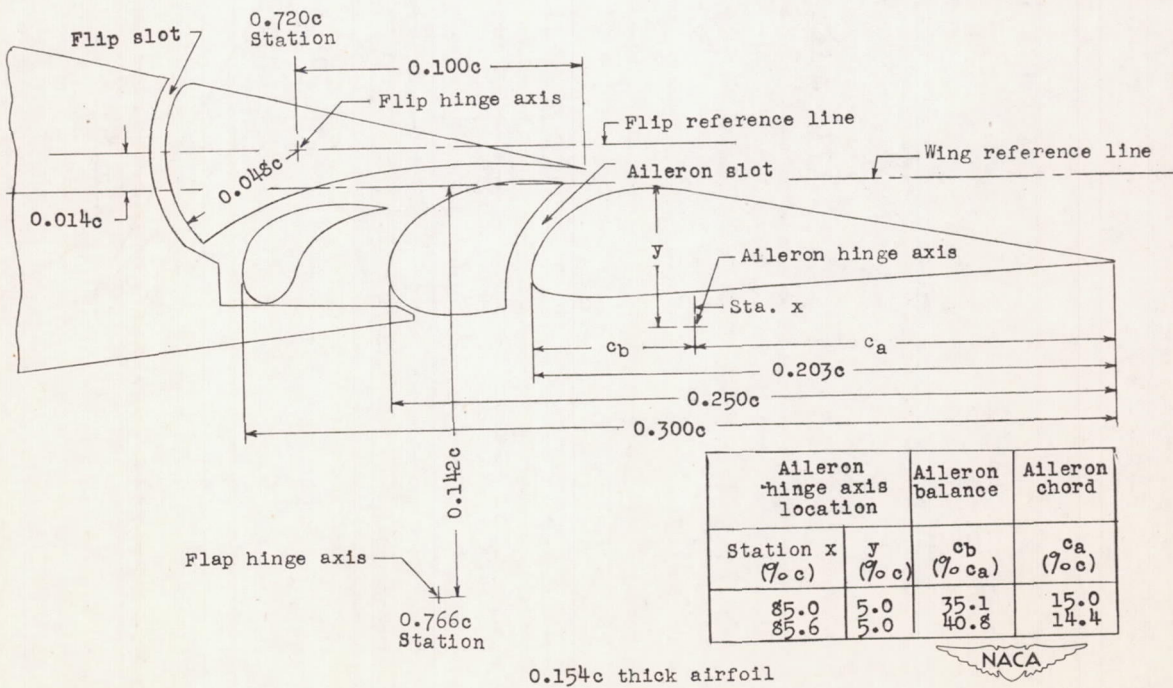
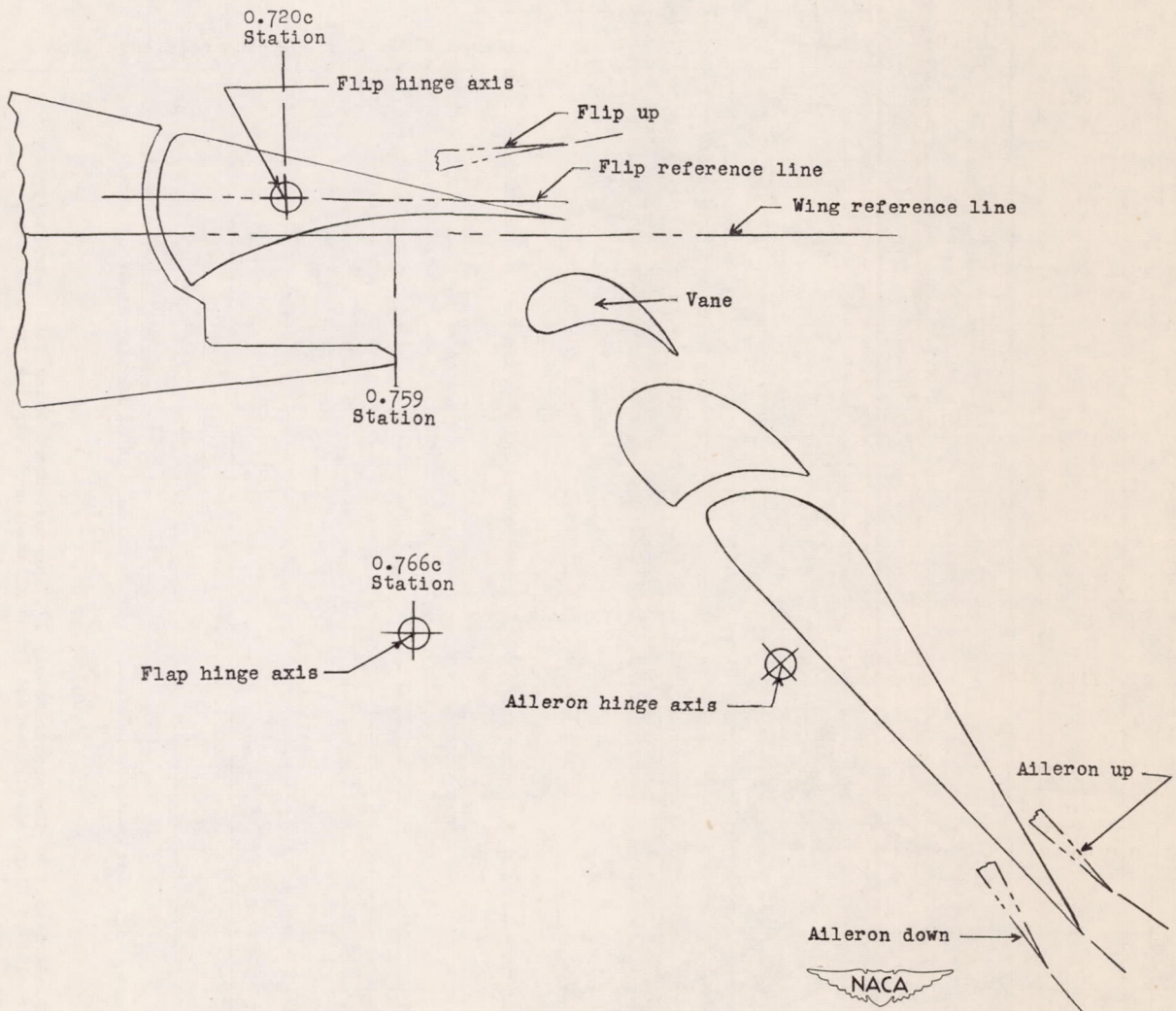


Figure to scale



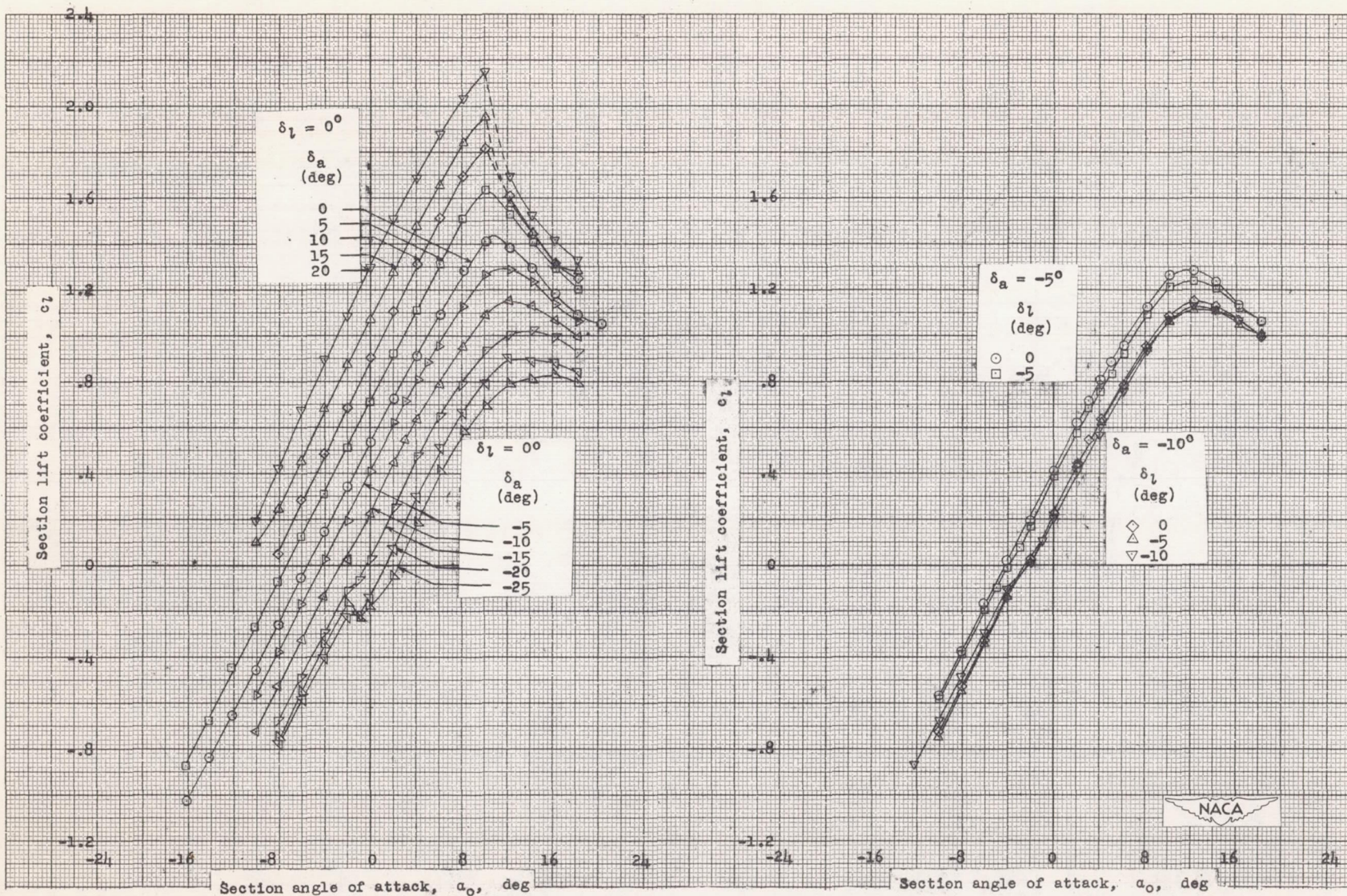
(a) $\delta_f = 0^\circ$.

Figure 3.- Arrangement of the movable surfaces on the NACA 7-series-type airfoils.



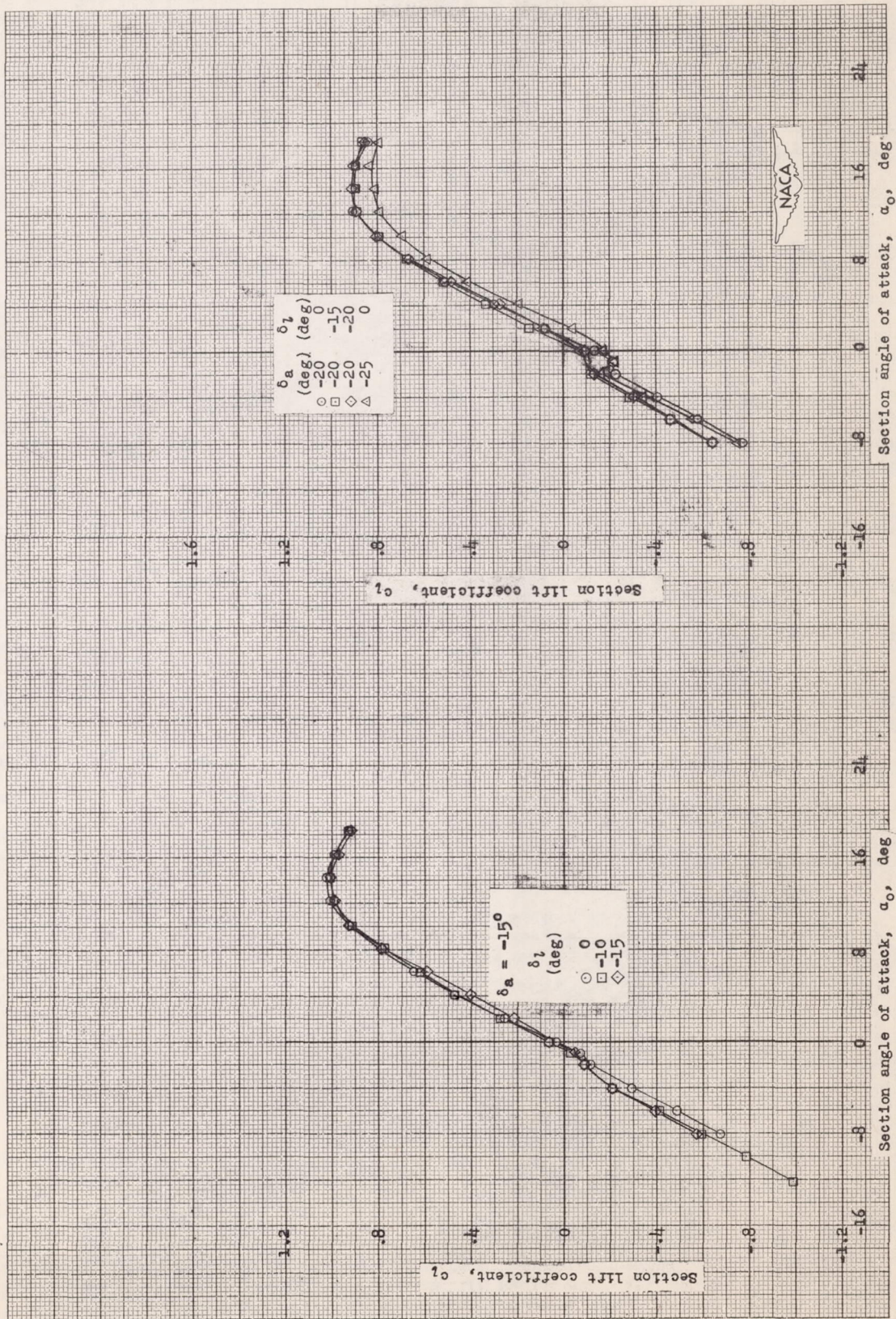
(b) $\delta_f = 50^\circ$.

Figure 3.- Concluded.

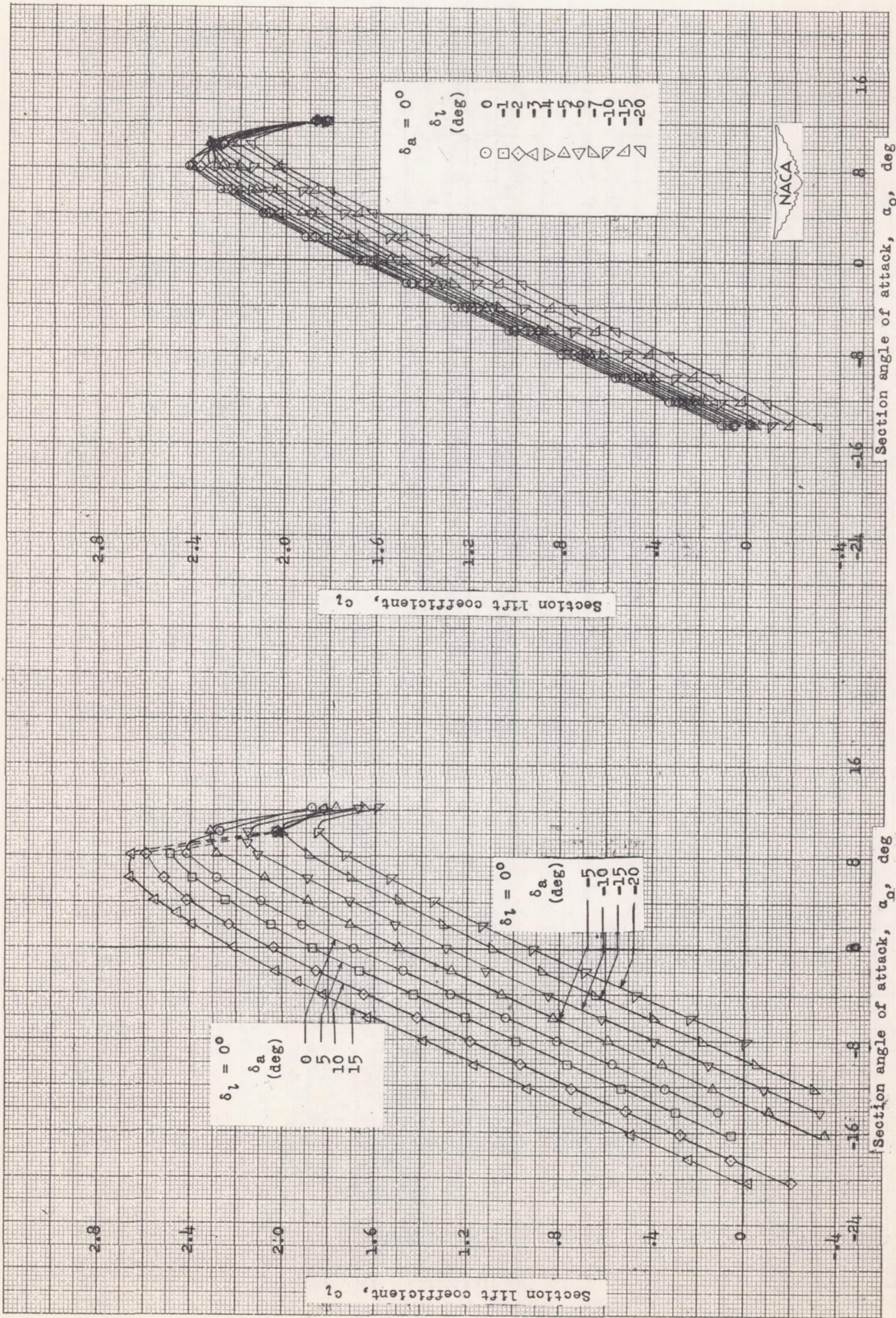


(a) $\delta_f = 0^\circ$.

Figure 4.- Lift characteristics of the approximately 17.7-percent-chord thick NACA 7-series-type airfoil with double slotted flap, straight-sided Frise aileron, and flap. Aileron balance, $0.35l_{ca}$; $R = 6 \times 10^6$ (approx.).

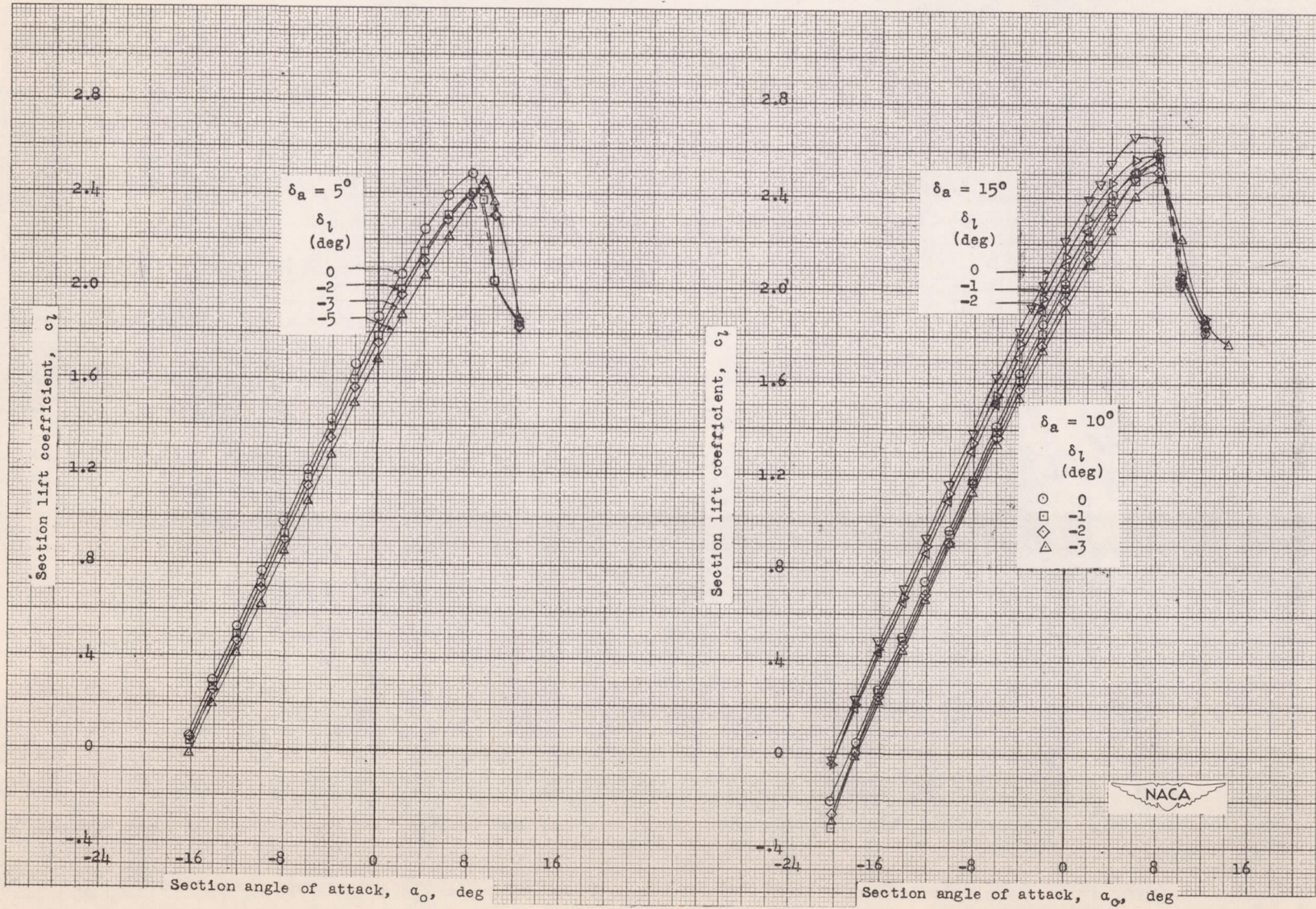


(b) $\delta_f = 0^\circ$.
Figure 4.- Continued.



(c) $\delta_f = 25^\circ$.

Figure 4.- Continued.



(d) $\delta_f = 25^\circ$.

Figure 4.- Continued.

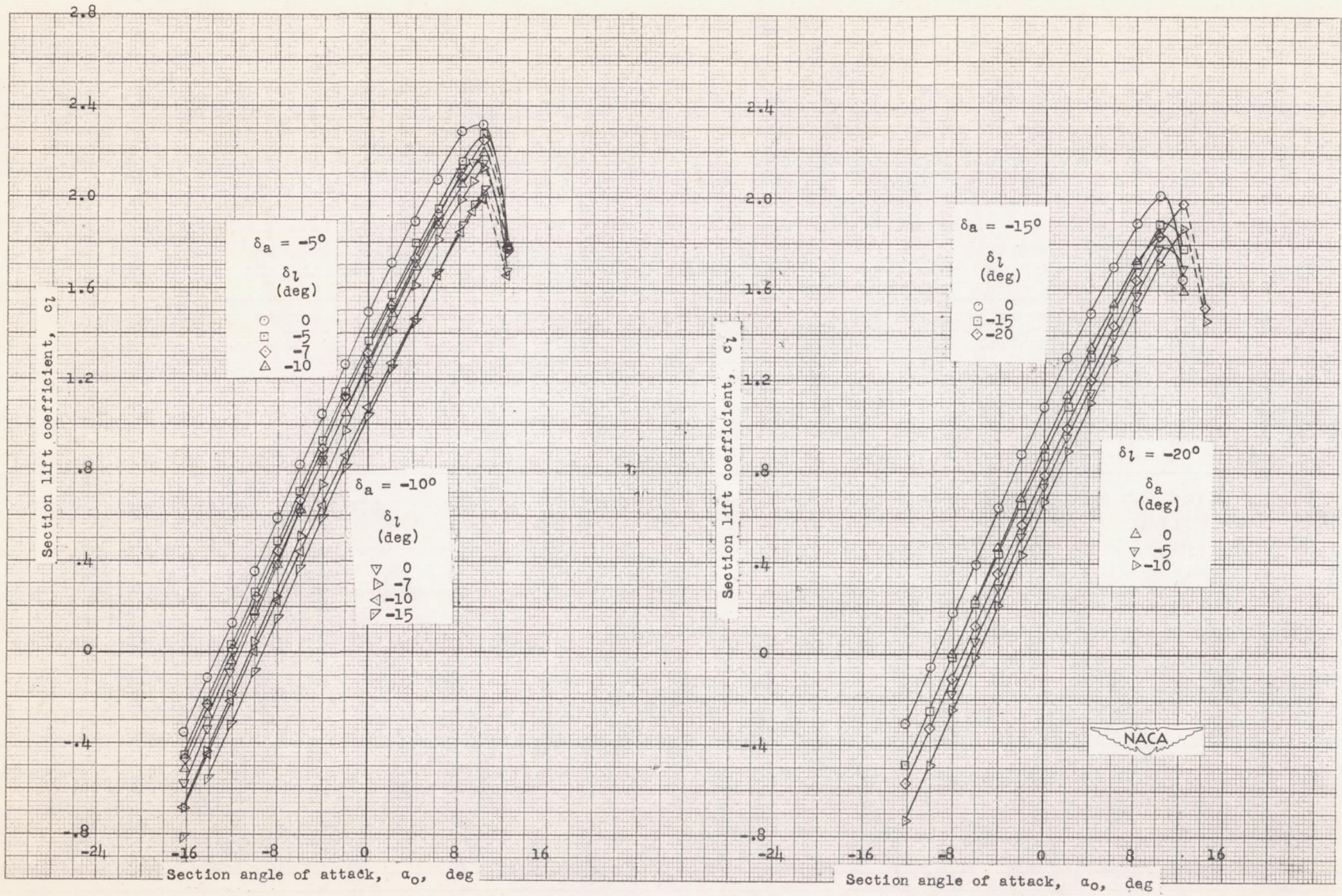
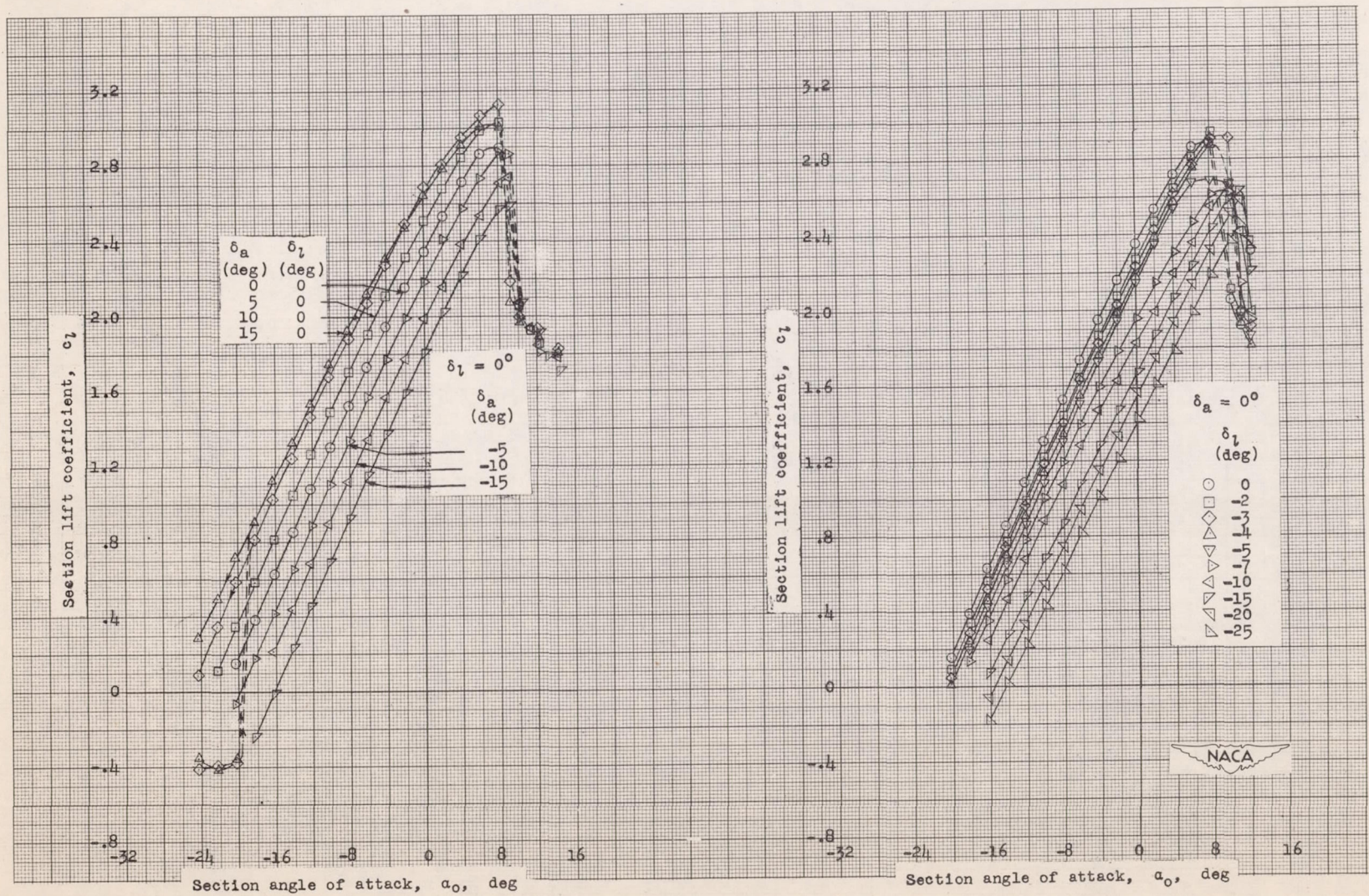
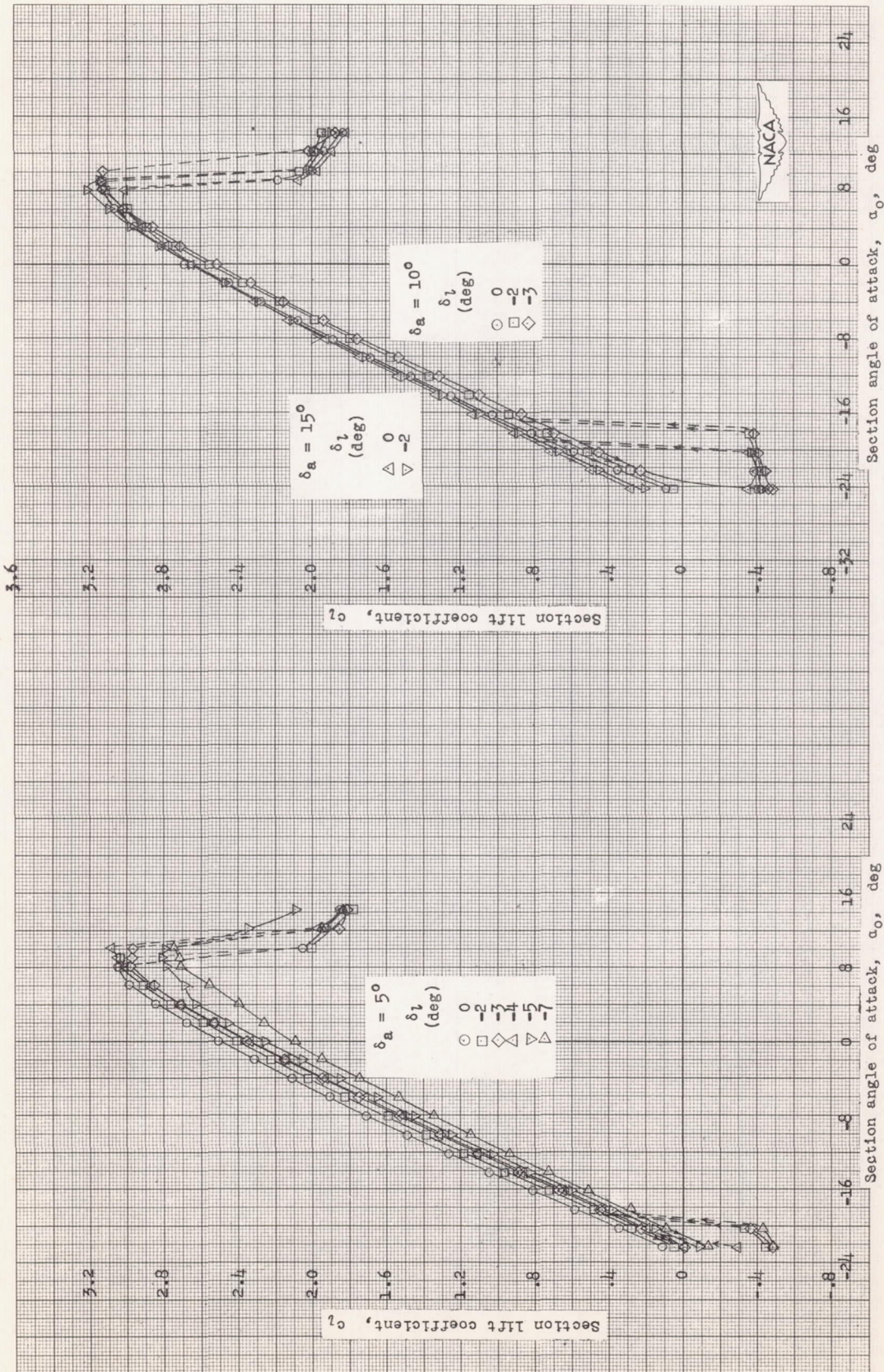
(e) $\delta_f = 25^\circ$.

Figure 4.- Continued.

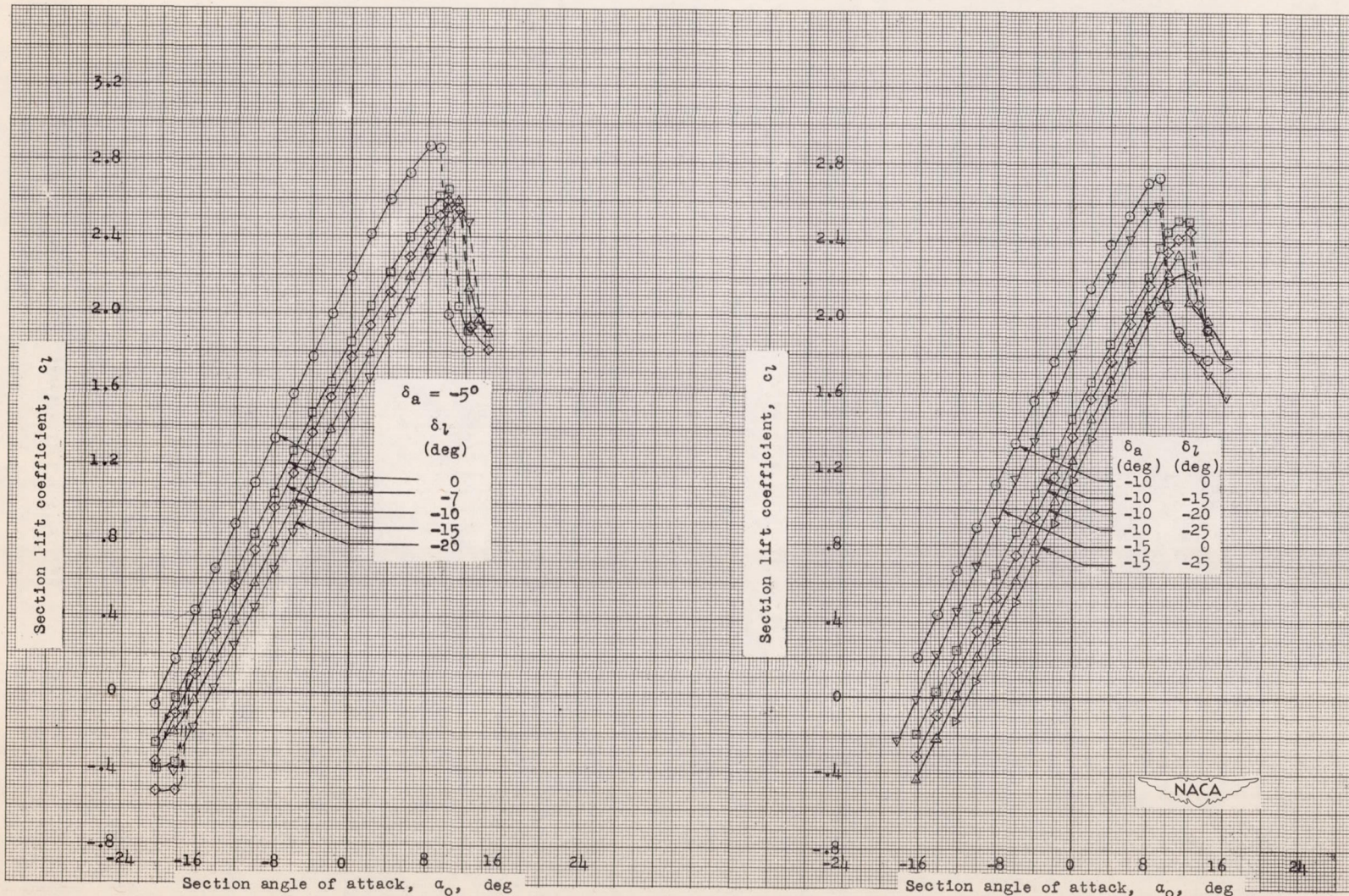


(f) $\delta_f = 40^\circ$.
 Figure 4.- Continued.



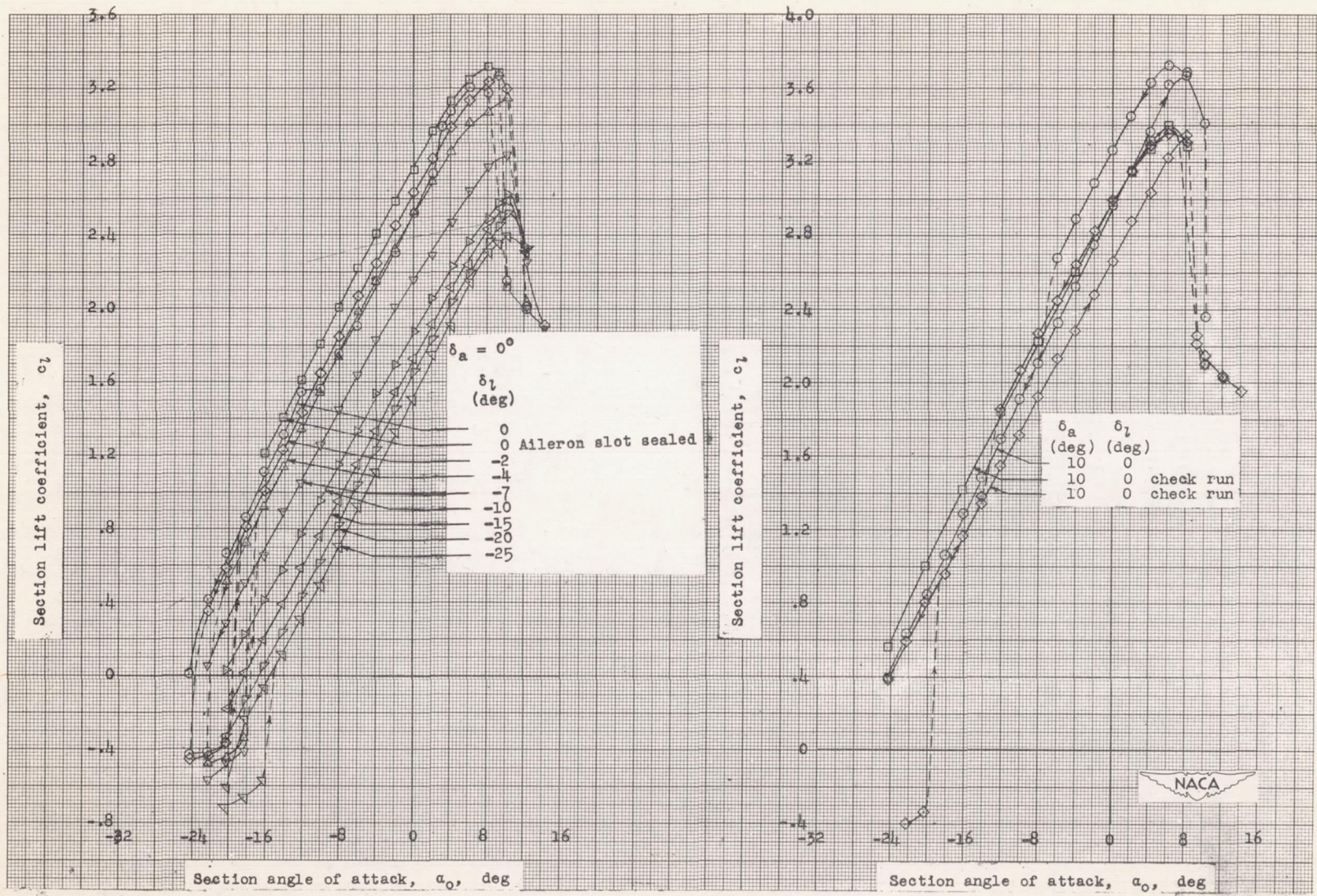
(g) $\delta_f = 40^\circ$.

Figure 4.- Continued.



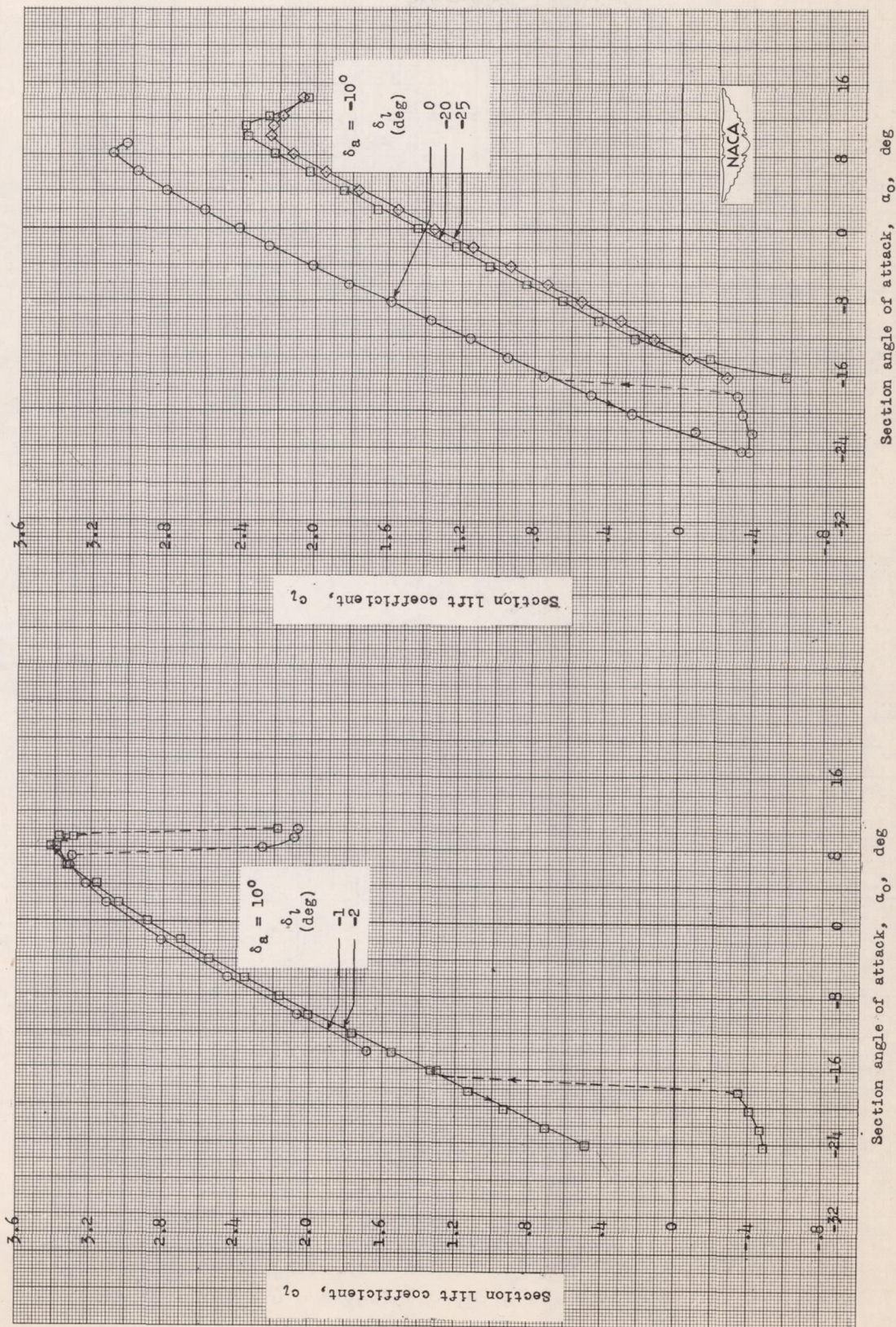
(h) $\delta_f = 40^\circ$.

Figure 4.- Continued.

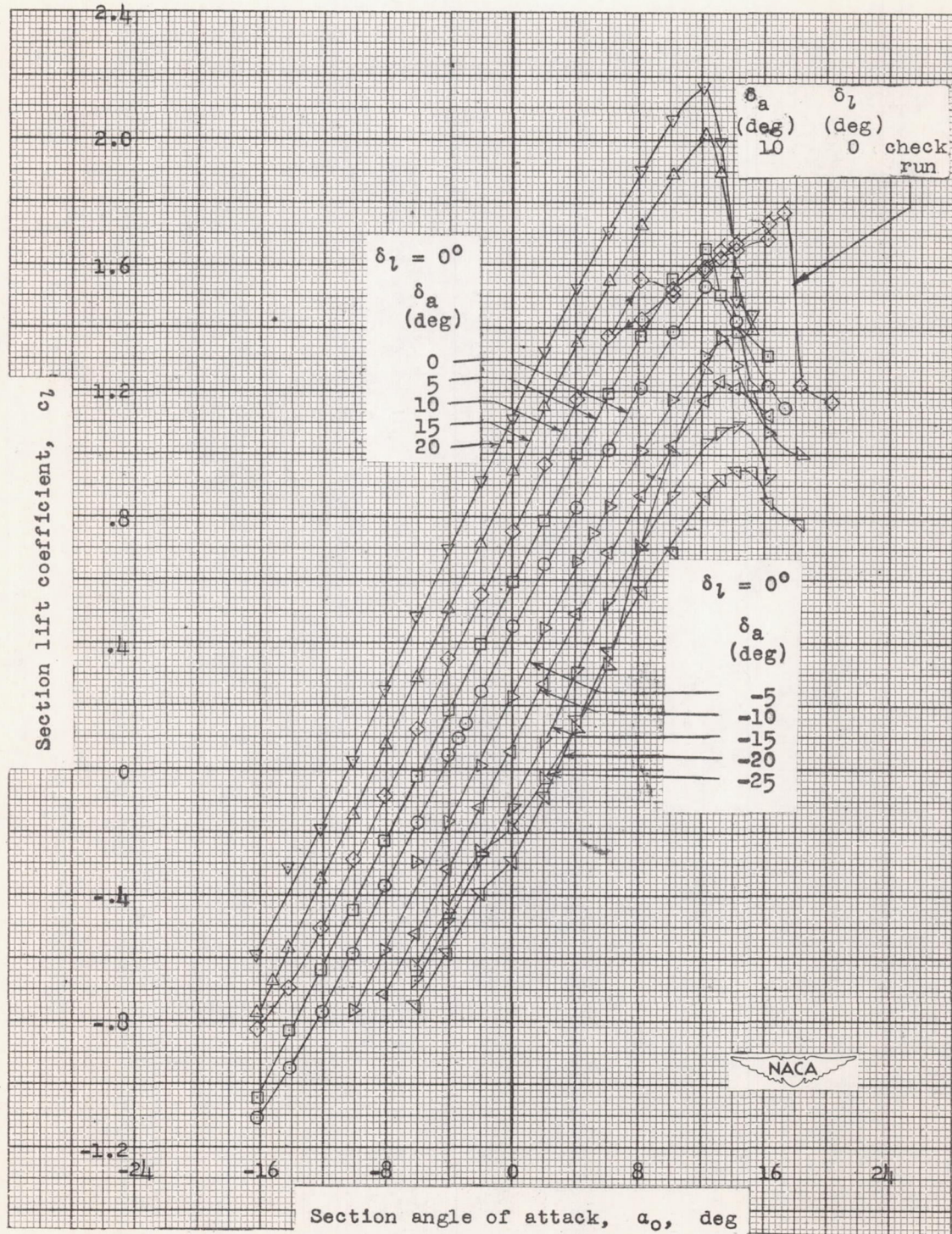


(1) $\delta_f = 50^\circ$.

Figure 4.- Continued.

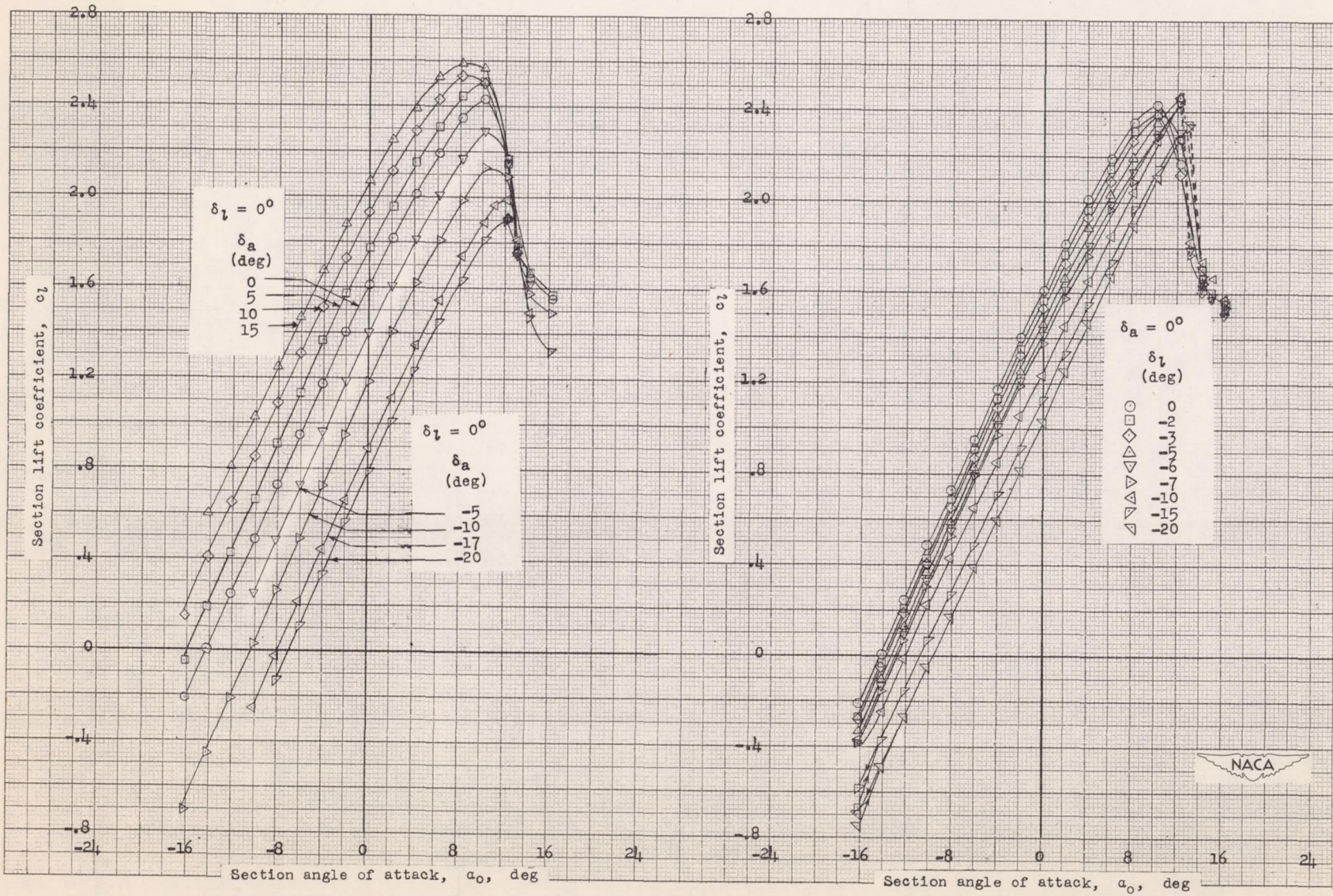


(j) $\delta_f = 50^\circ$.
Figure 4.- Concluded.



(a) $\delta_f = 0^\circ$.

Figure 5.- Lift characteristics of the approximately 15.4-percent-chord thick NACA 7-series-type airfoil with double slotted flap, straight-sided Frise aileron, and flap. Aileron balance, $0.35lca$; $R = 6 \times 10^6$ (approx.).



(b) $\delta_f = 25^\circ$.
Figure 5.- Continued.

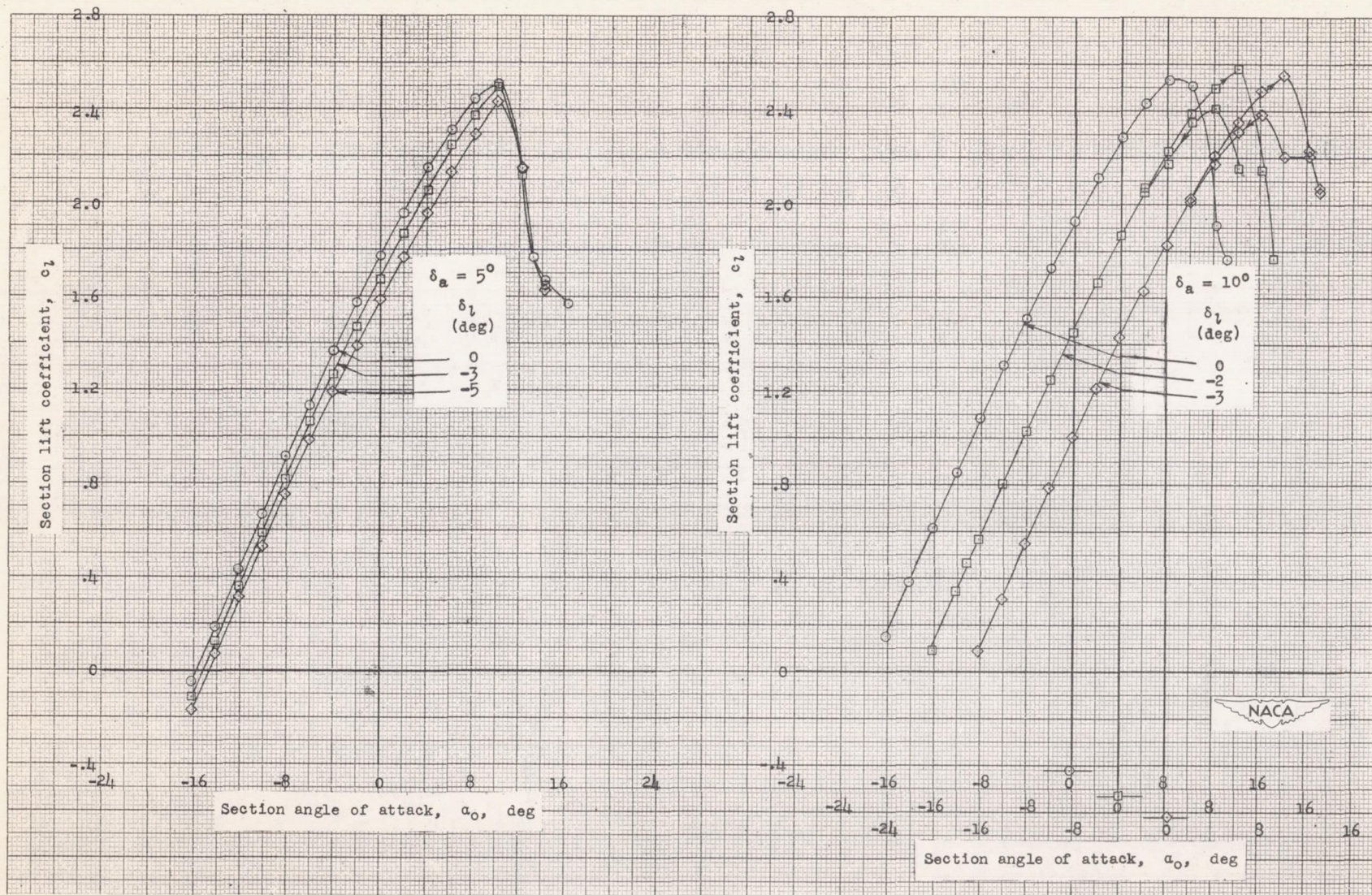
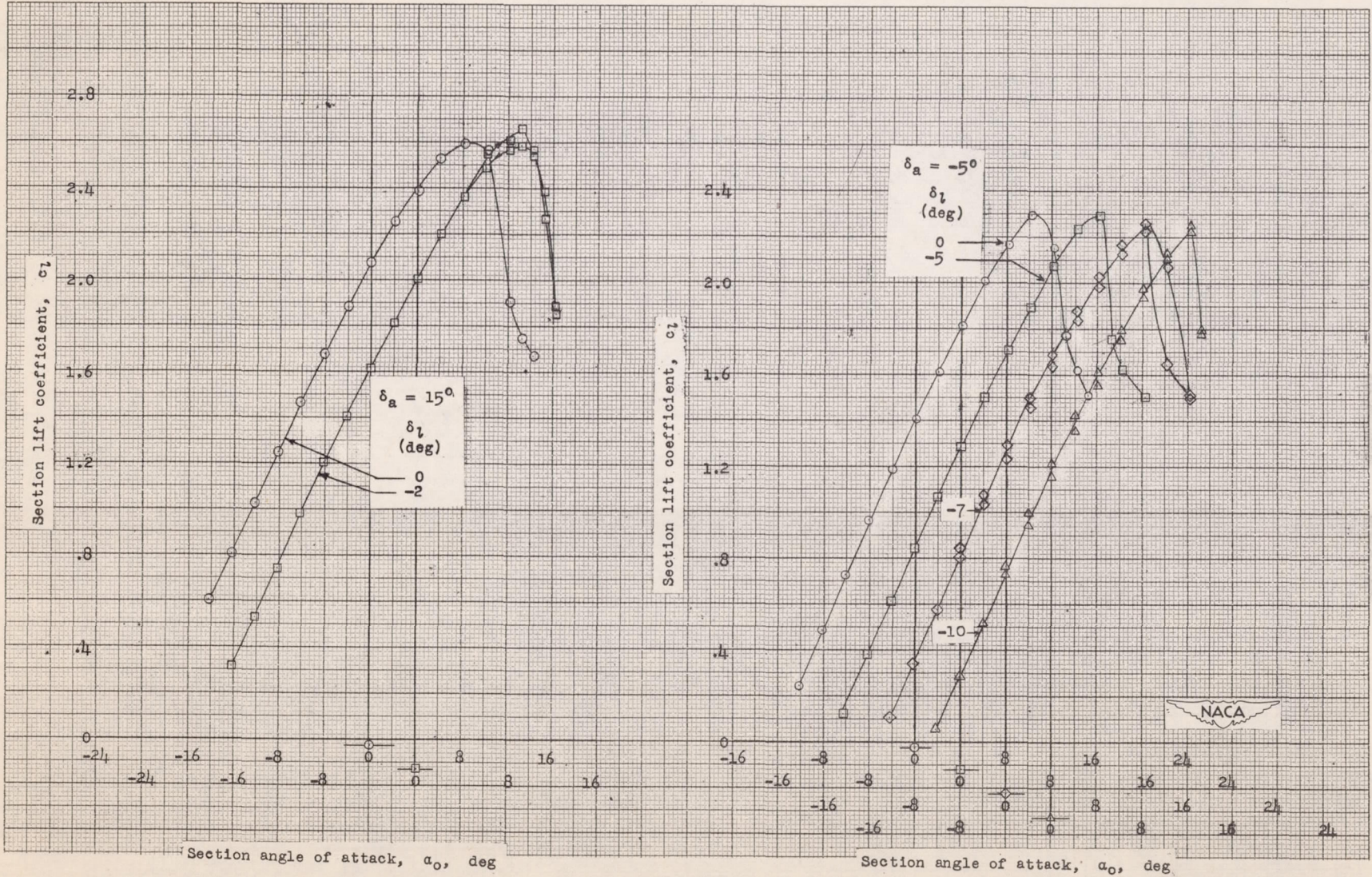
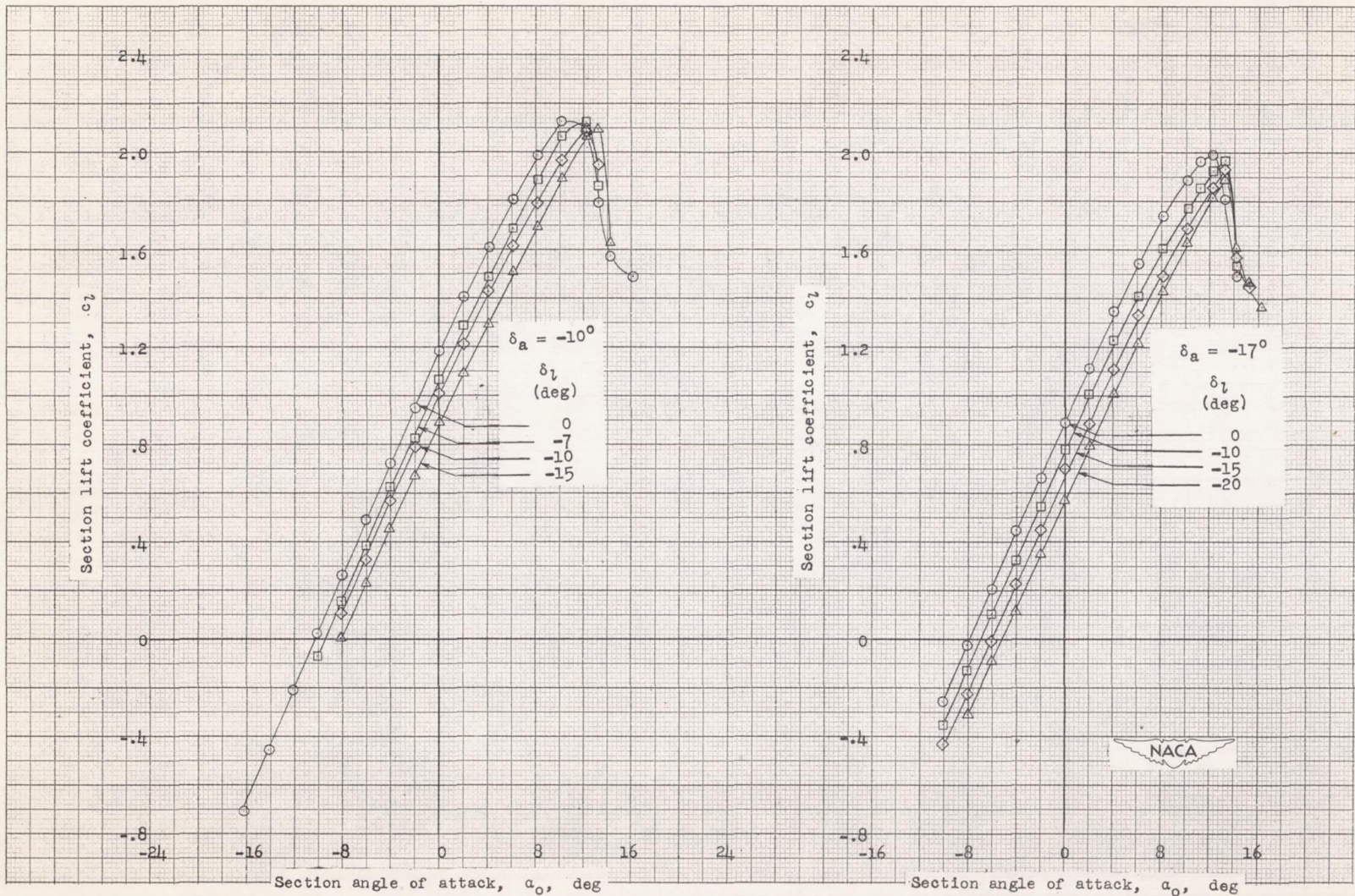
(c) $\delta_r = 25^\circ$.

Figure 5.- Continued.

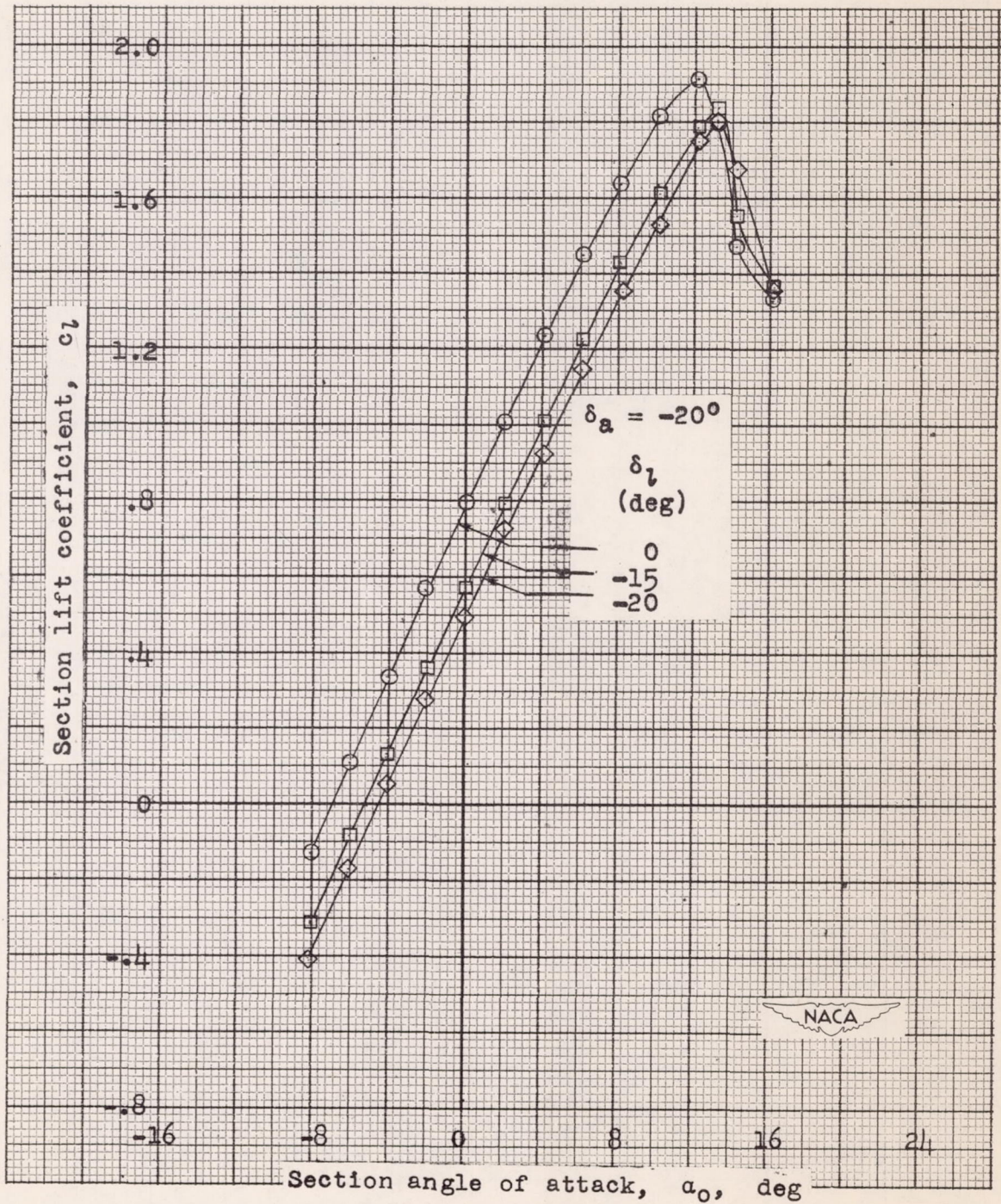


(d) $\delta_f = 25^\circ$.

Figure 5.- Continued.

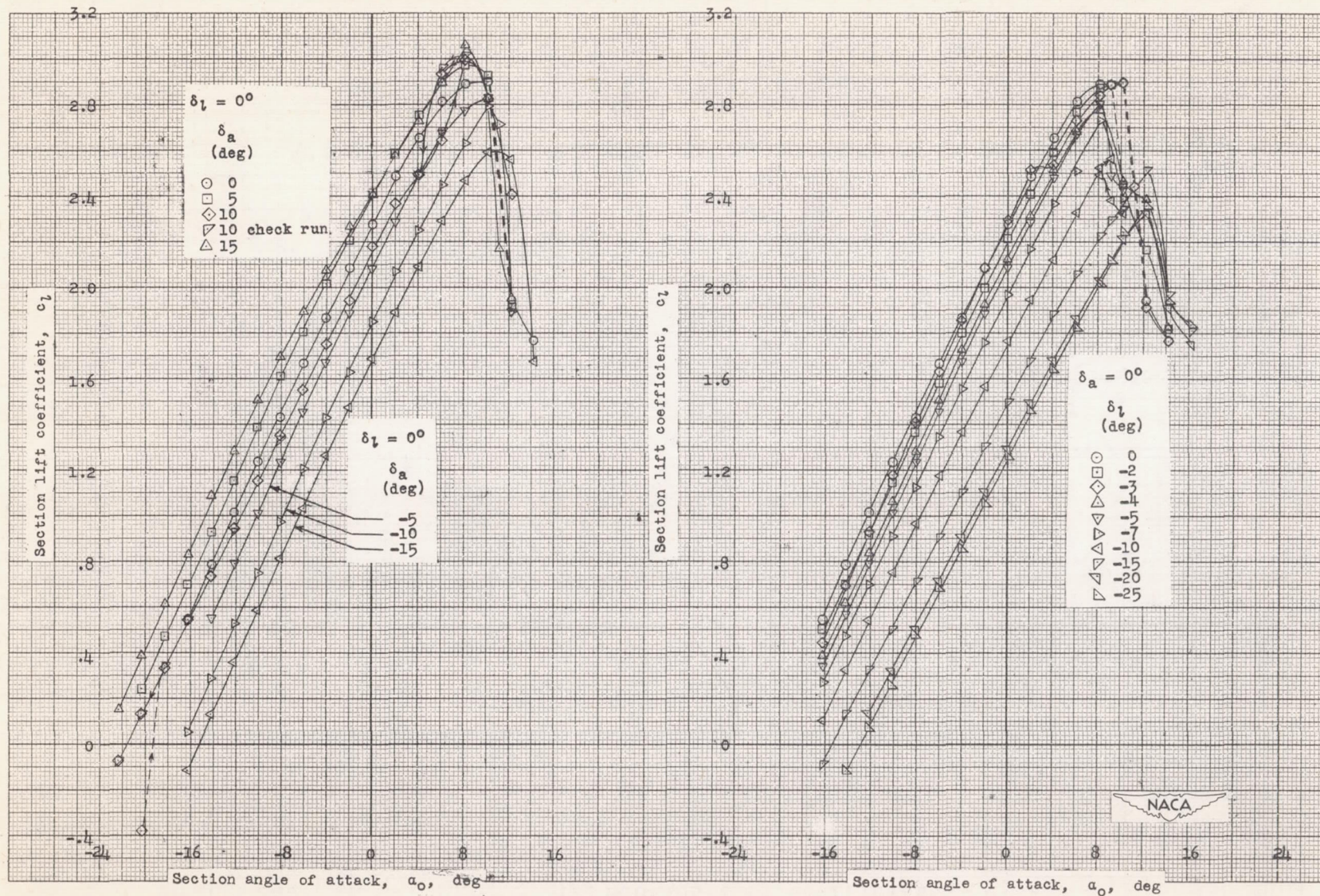


(e) $\delta_f = 25^\circ$.
 Figure 5.- Continued.



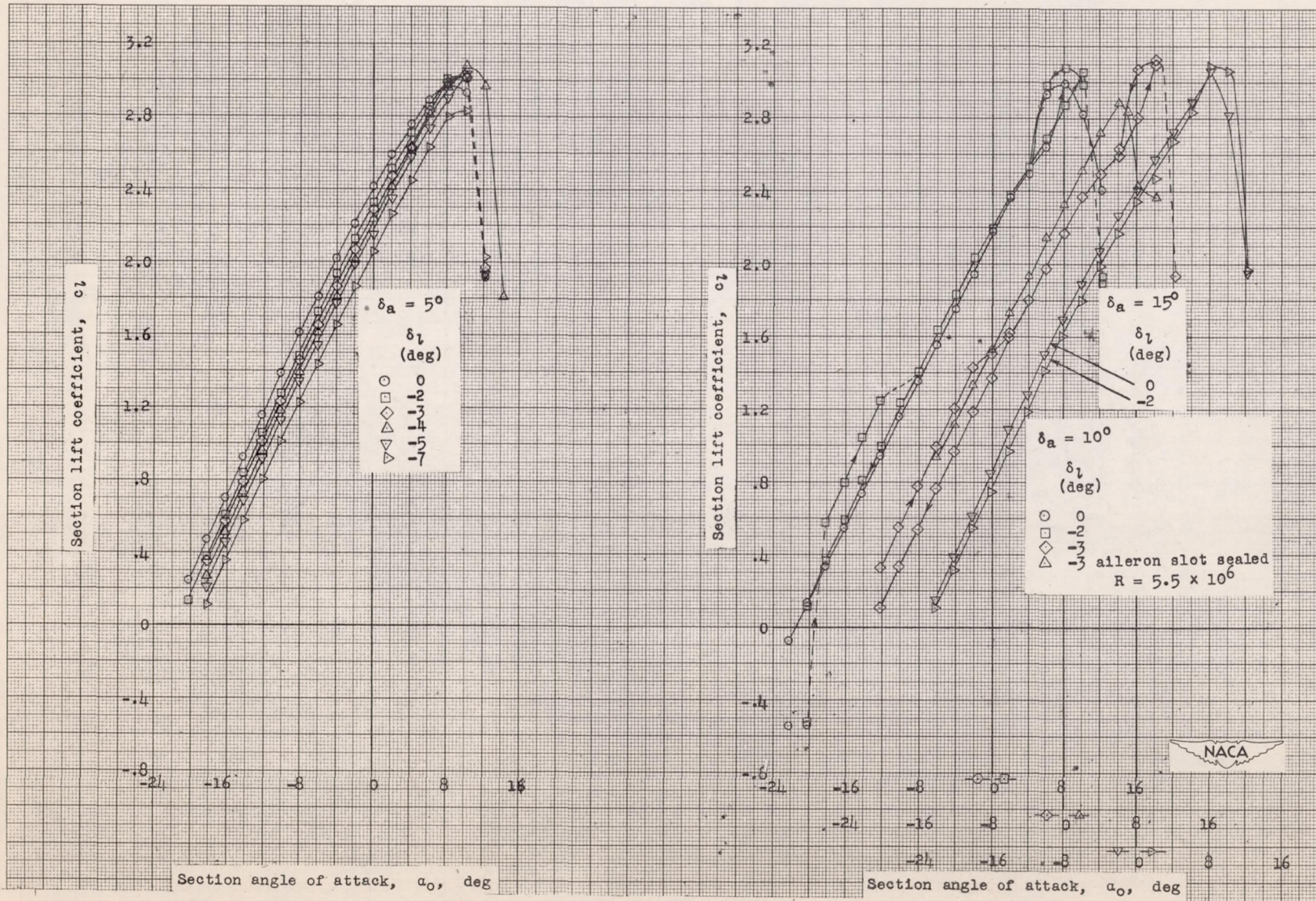
(f) $\delta_f = 25^\circ$

Figure 5.- Continued.

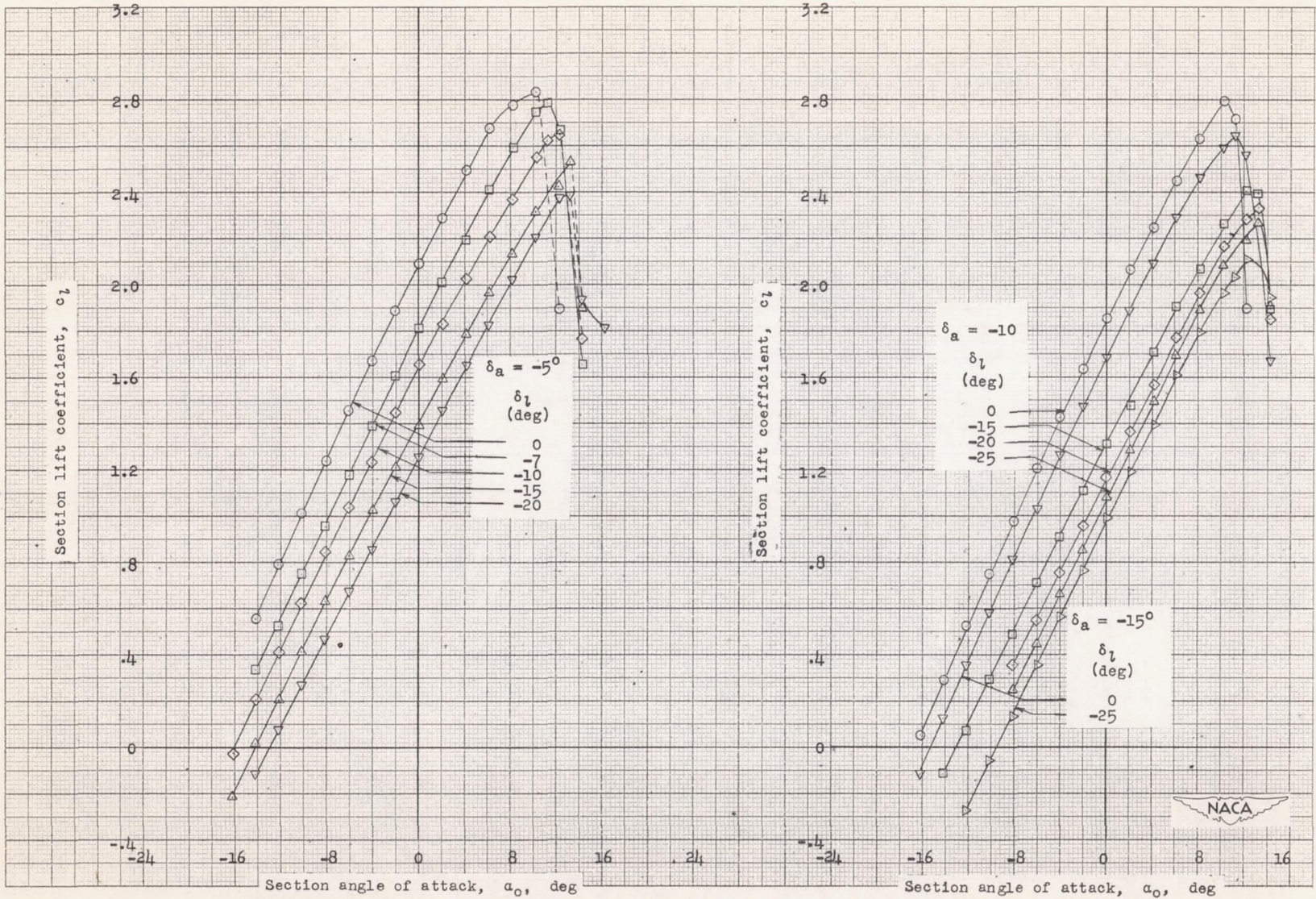


(g) $\delta_f = 40^\circ$.

Figure 5.- Continued.



(h) $\delta_r = 40^\circ$.
Figure 5.- Continued.



(1) $\delta_f = 40^\circ$

Figure 5.- Concluded.

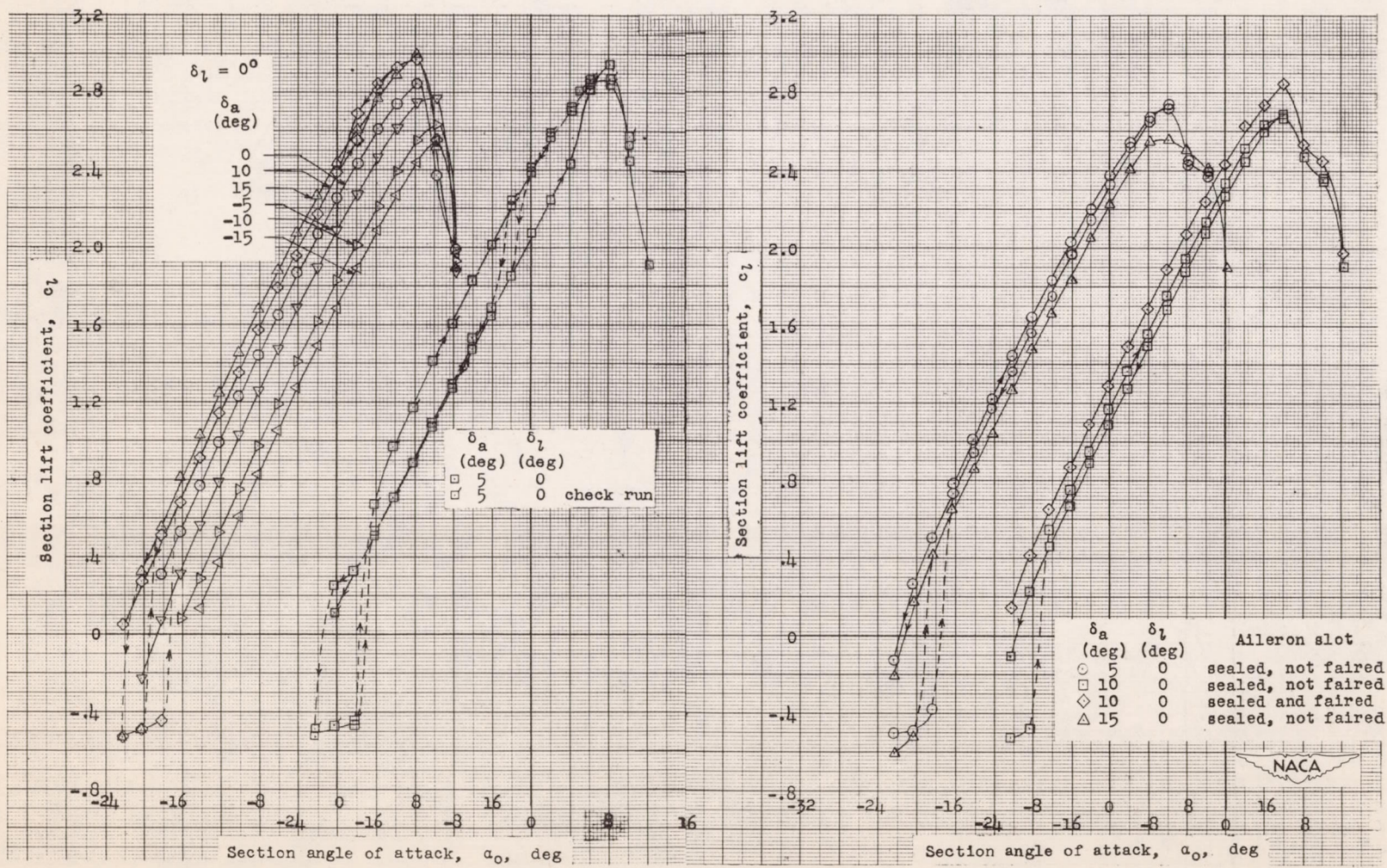


Figure 6.- The effect of sealing the aileron slot on the lift characteristics of the approximately 15.4-percent-chord thick NACA 7-series-type airfoil with double slotted flap, straight-sided Frise aileron, and flap. Aileron balance, $0.40\delta a_a$; $\delta_f = 40^\circ$; $R = 6 \times 10^6$ (approx.).

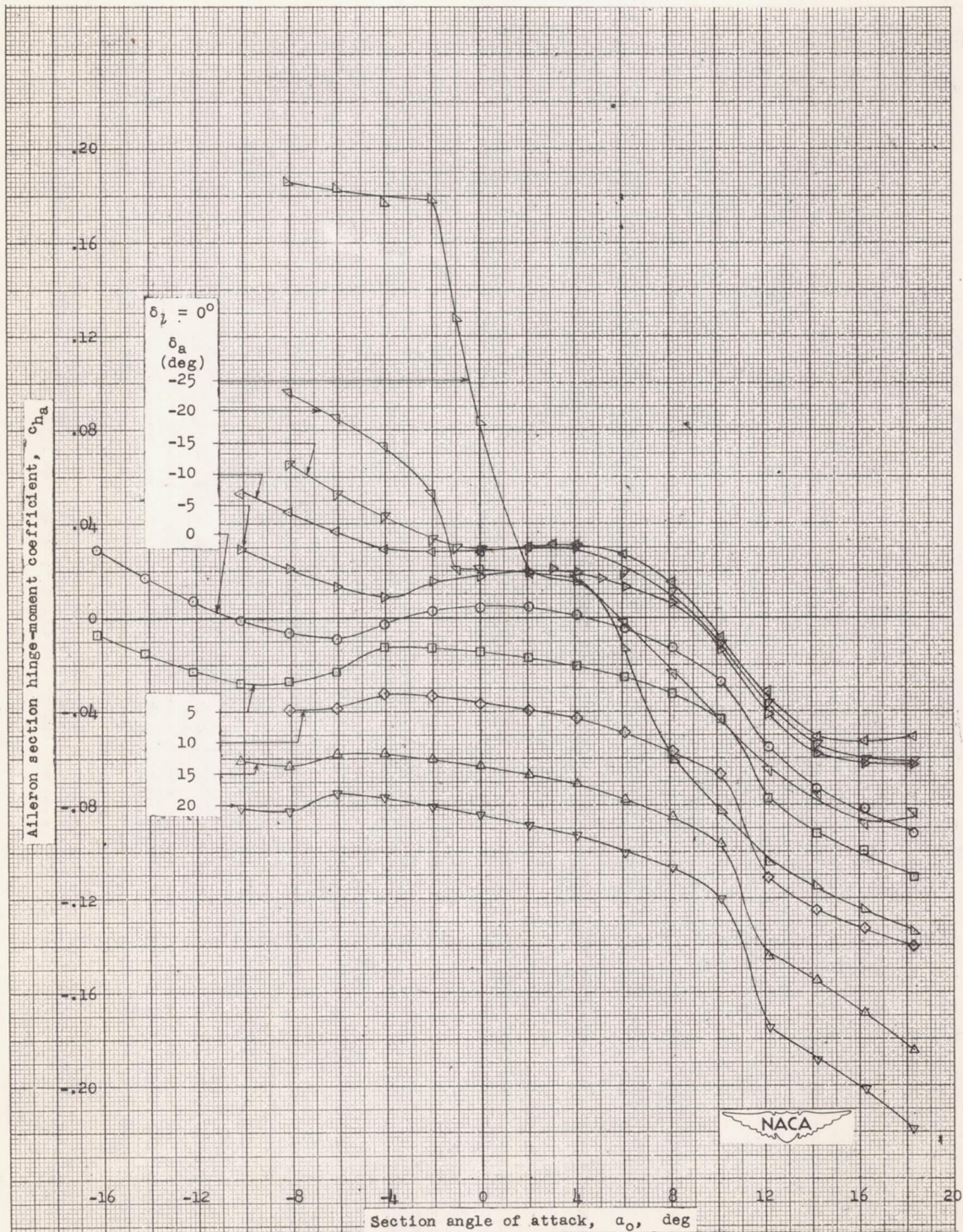
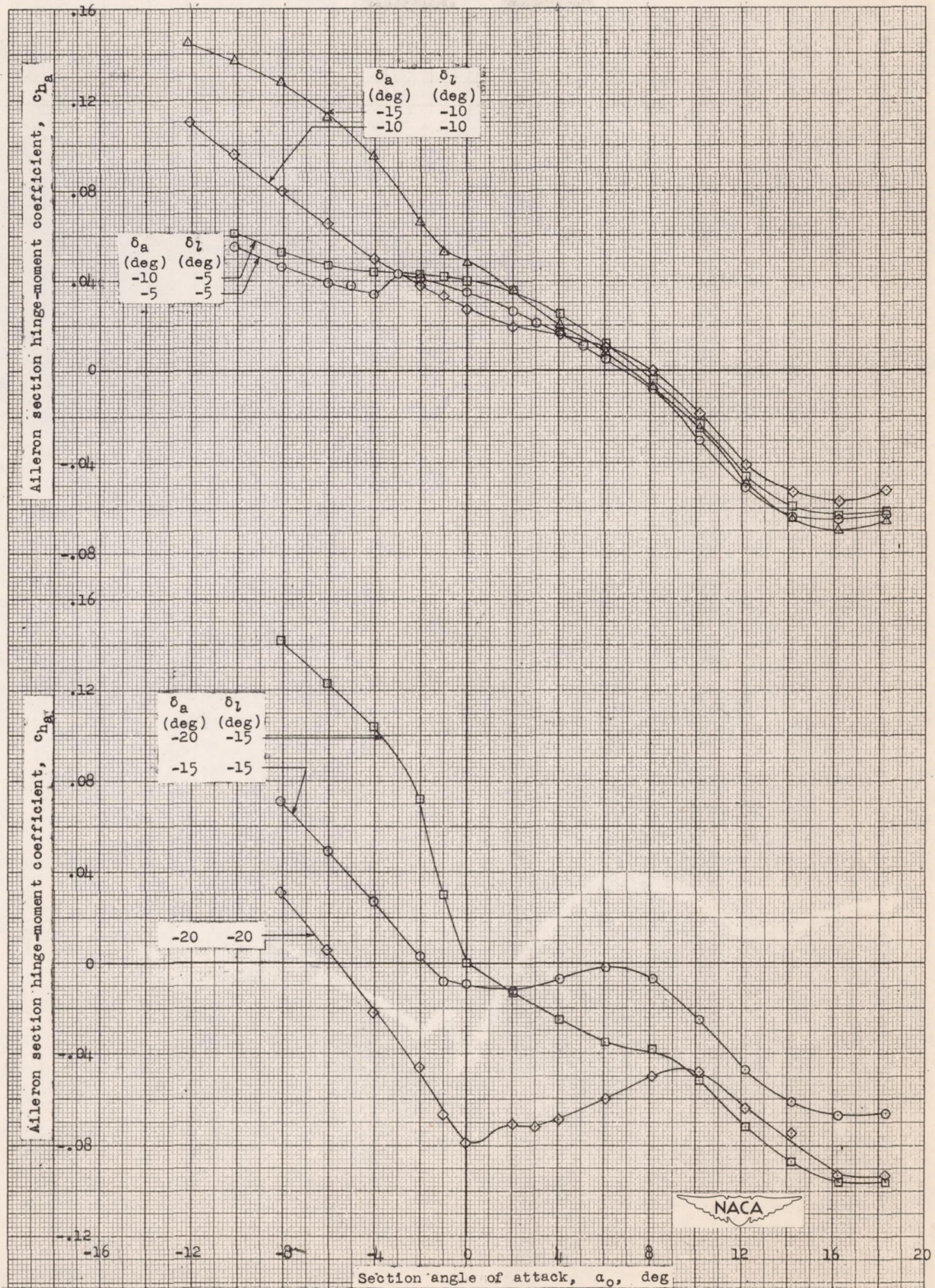
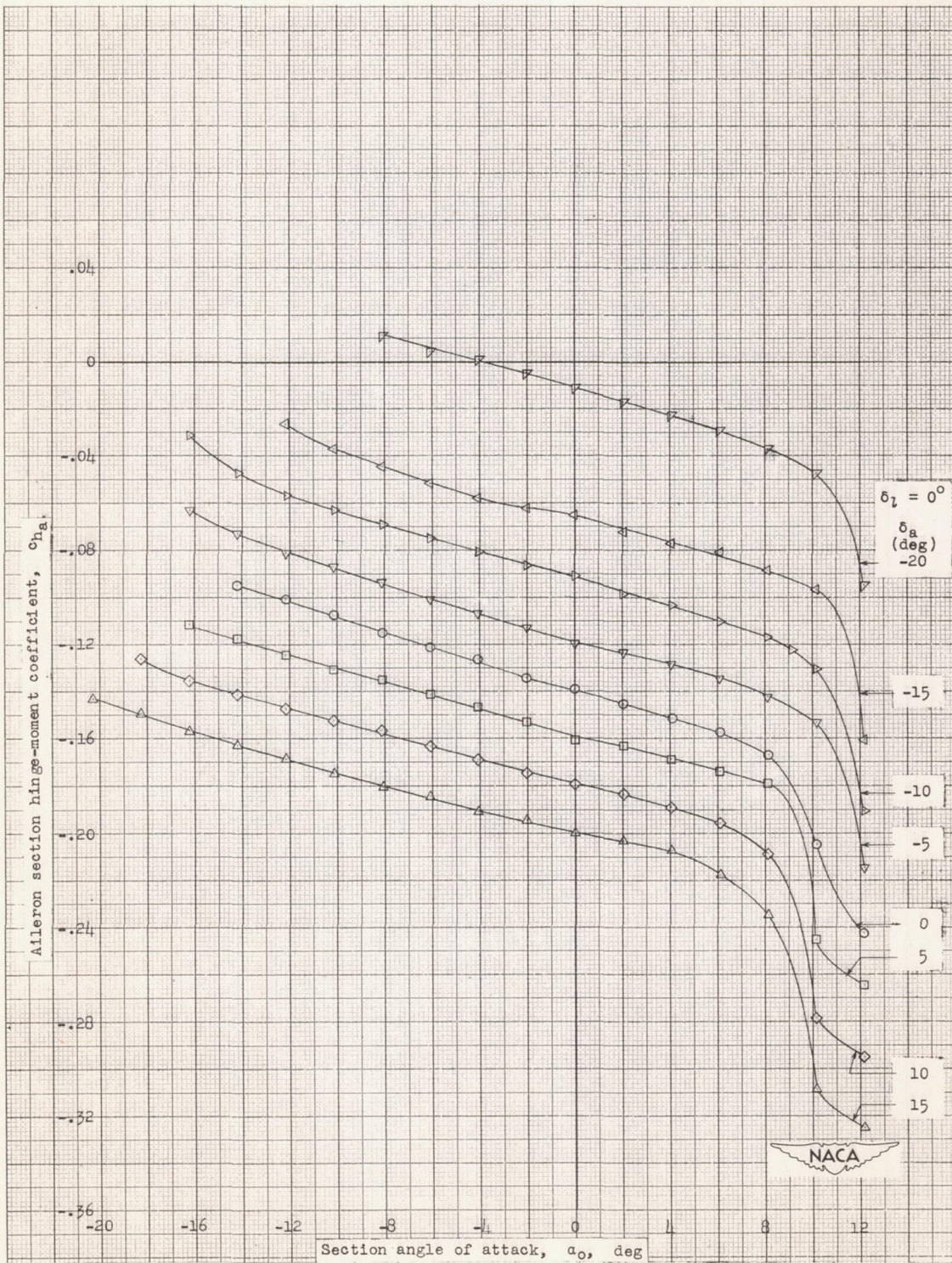
(a) $\delta_f = 0^\circ$.

Figure 7.- Hinge-moment characteristics of a straight-sided Frise aileron on the approximately 17.7-percent-chord thick NACA 7-series-type airfoil with double slotted flap and flip. Aileron balance, $0.351c_a$; $R = 6 \times 10^6$ (approx.).



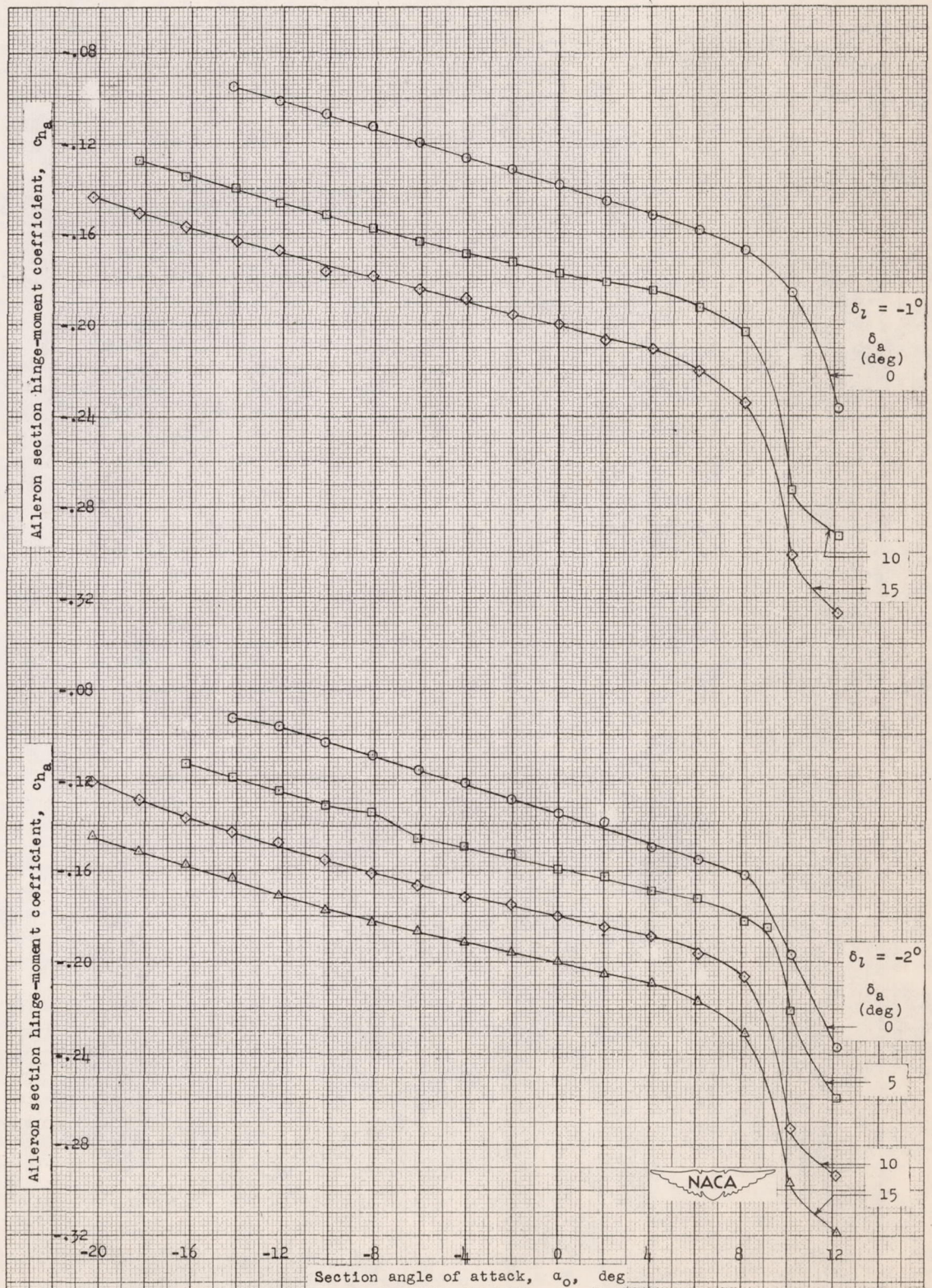
(b) $\delta_r = 0^\circ$.

Figure 7.- Continued.



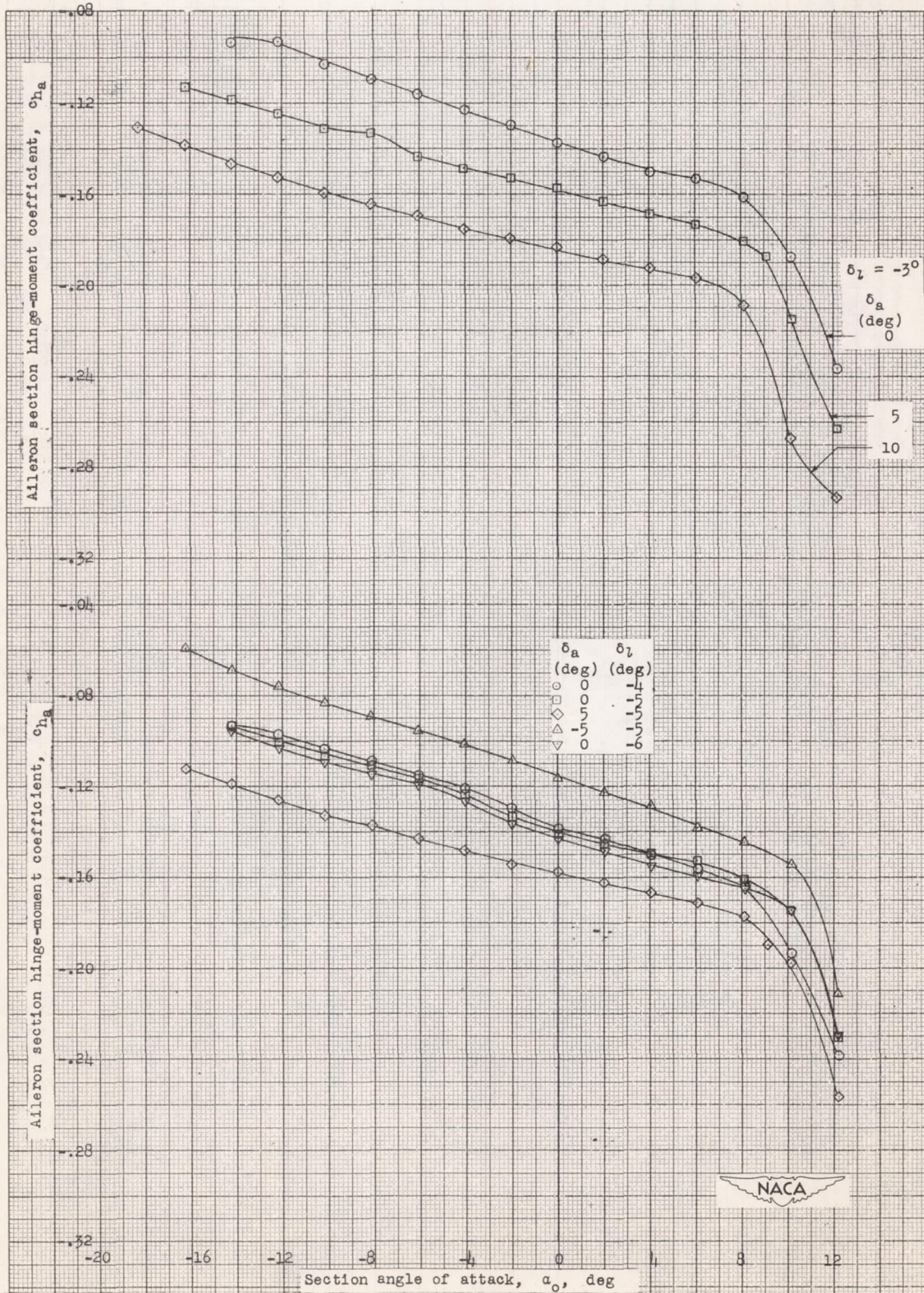
(c) $\delta_f = 25^\circ$.

Figure 7.- Continued.



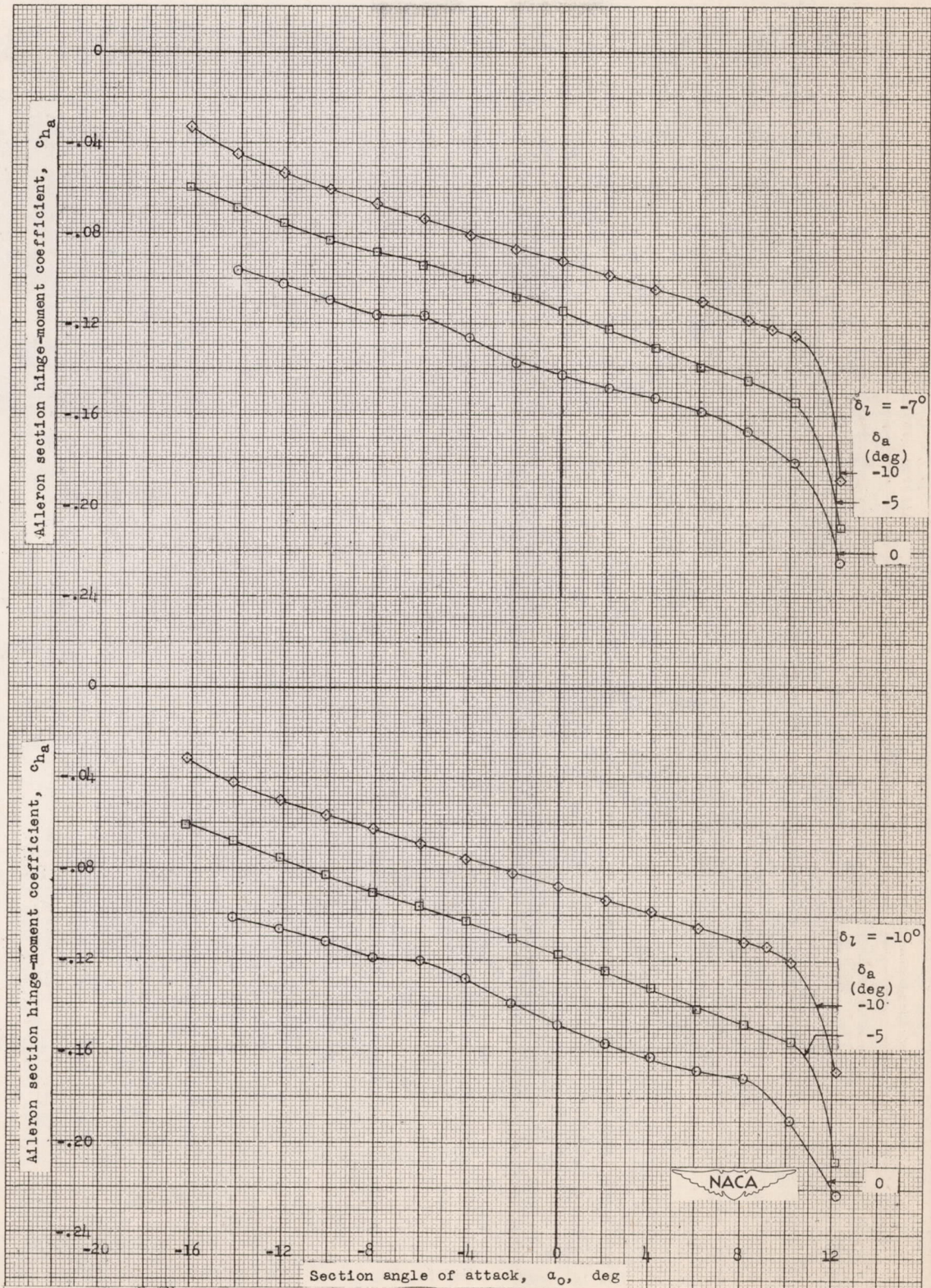
(d) $\delta_f = 25^\circ$.

Figure 7.- Continued.



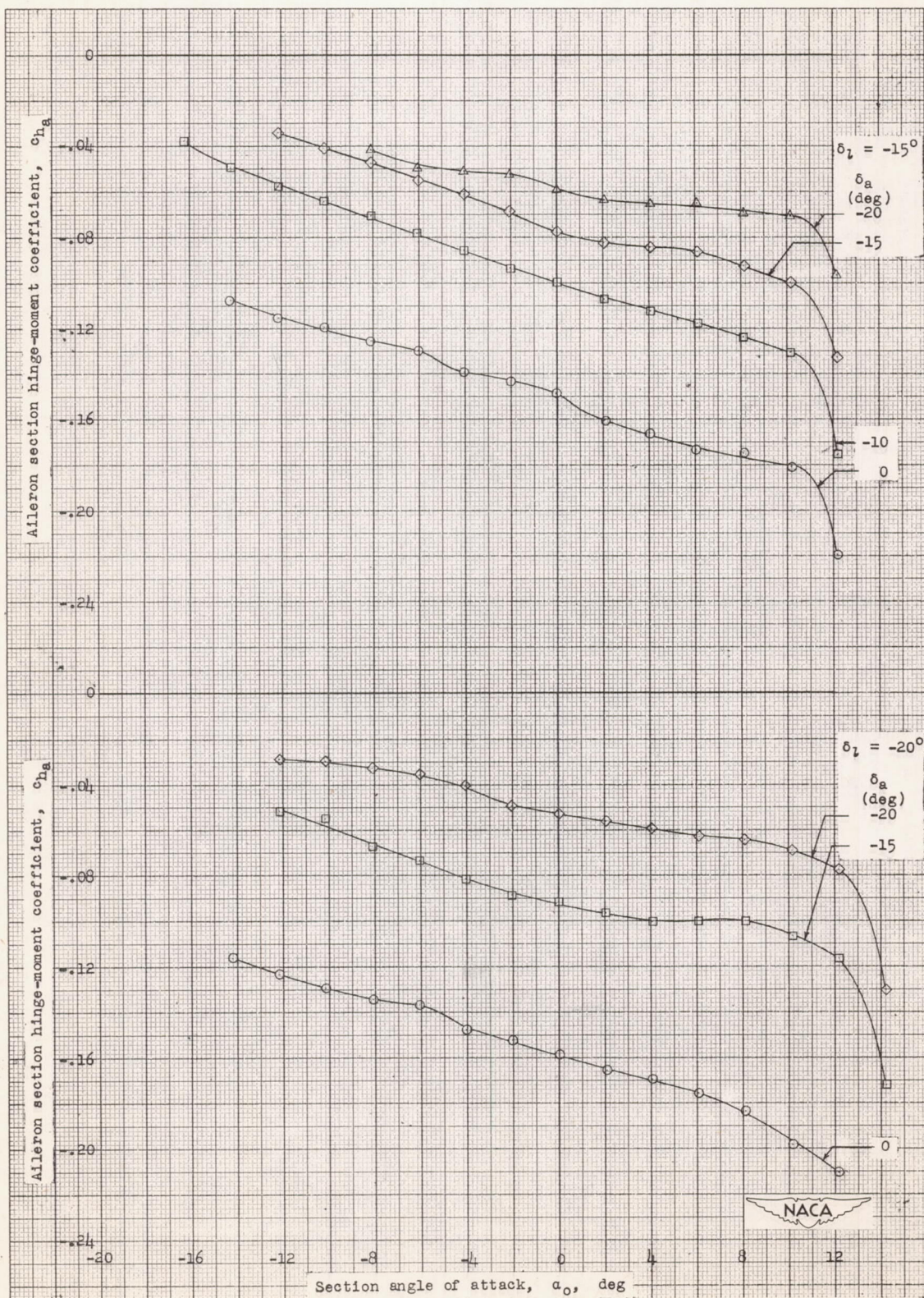
(e) $\delta_z = 25^\circ$.

Figure 7.- Continued.



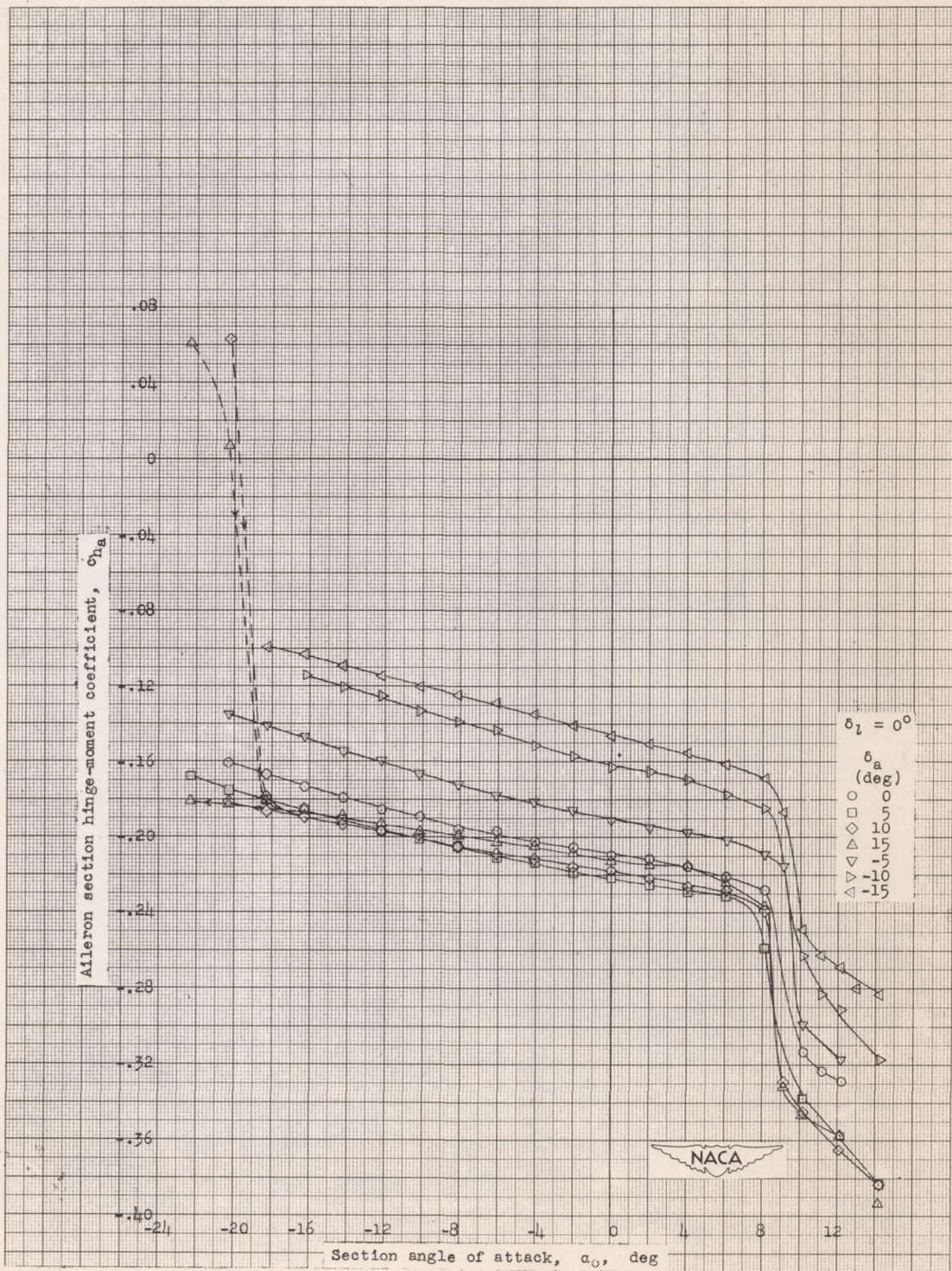
(f) $\delta_r = 25^\circ$.

Figure 7.- Continued.



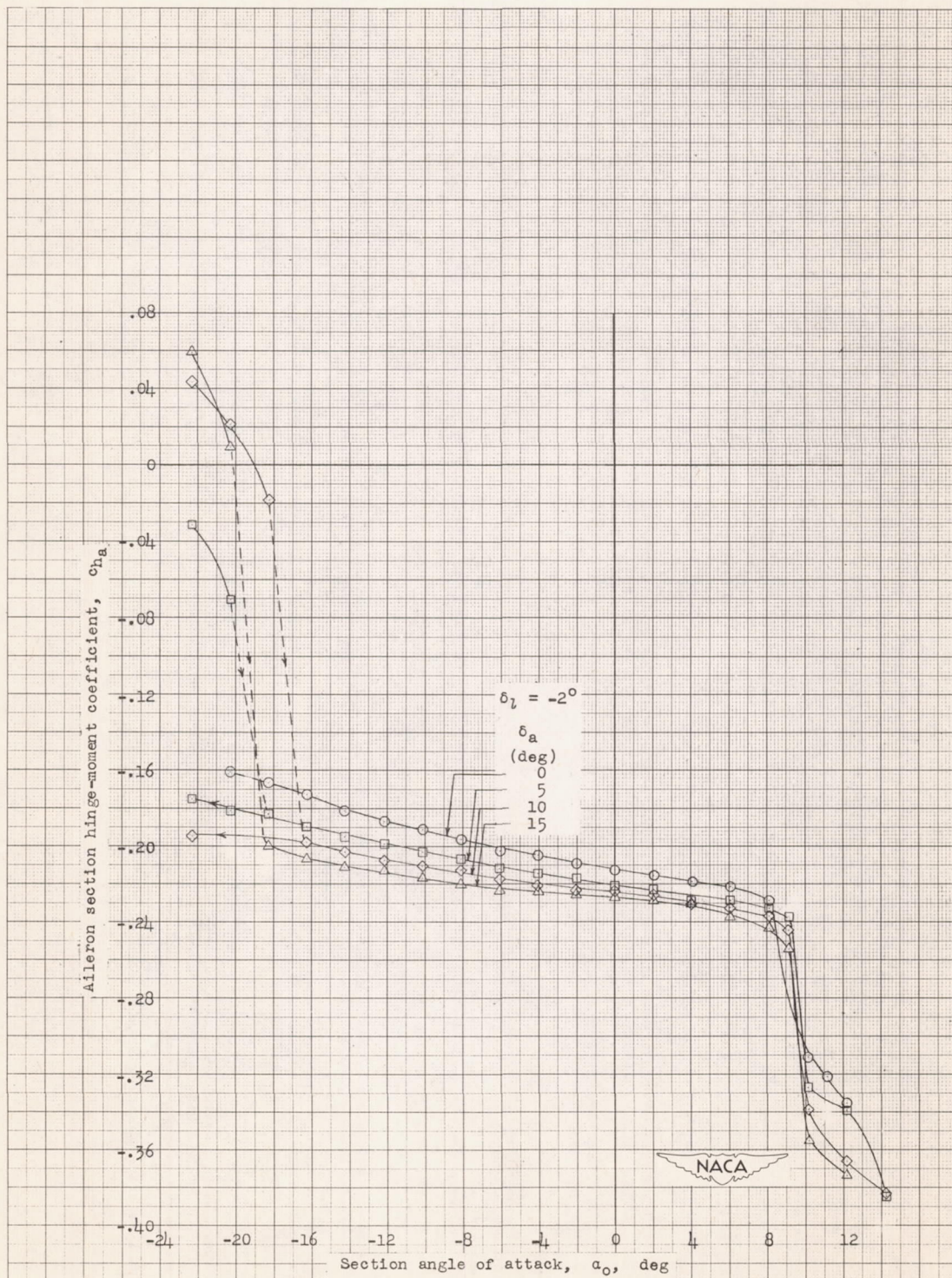
(g) $\delta_r = 25^\circ$

Figure 7.- Continued.



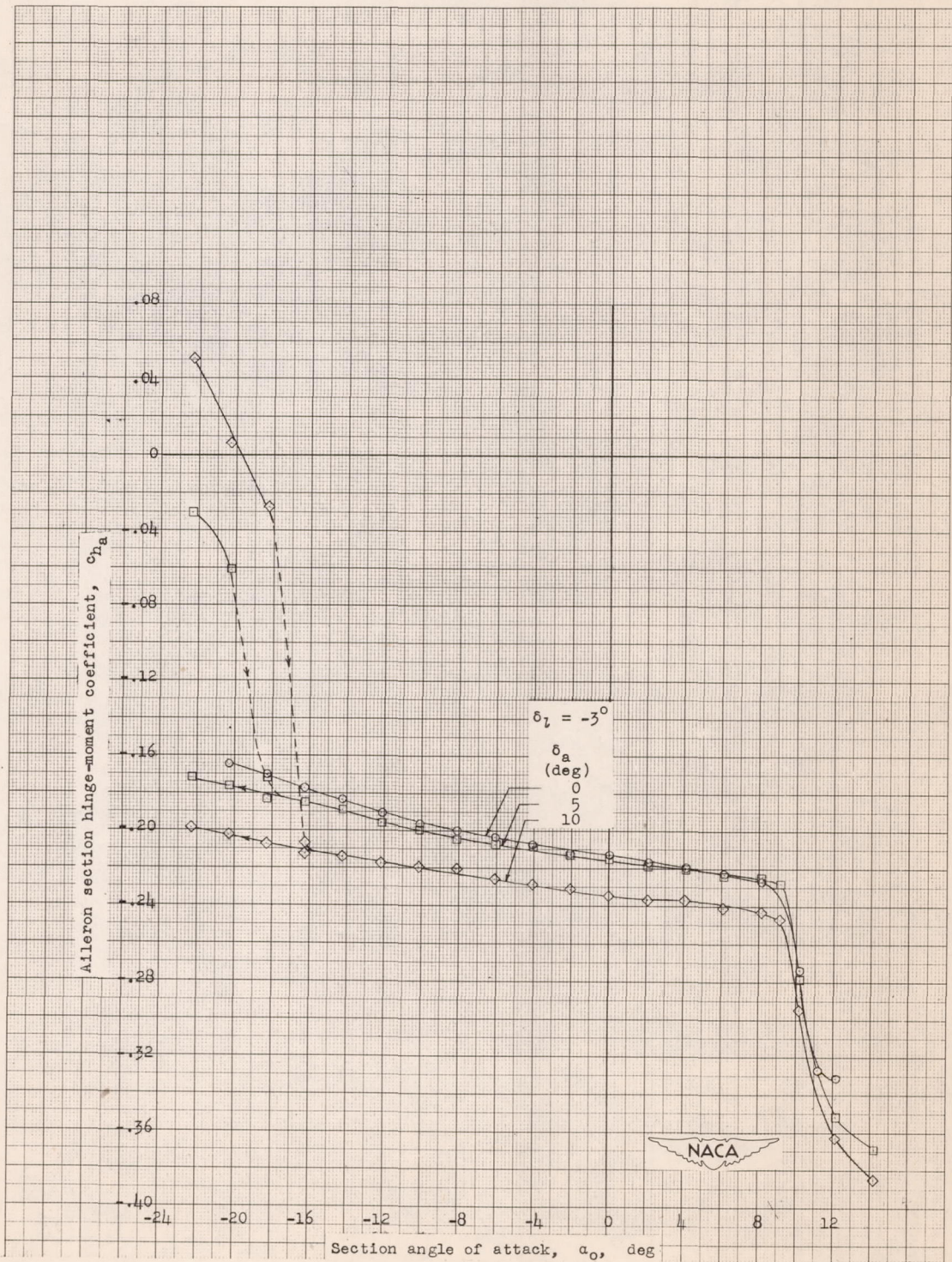
(h) $\delta_f = 40^\circ$.

Figure 7.- Continued.



(1) $\delta_r = 40^\circ$.

Figure 7.- Continued.



(j) $\delta_f = 40^\circ$.

Figure 7.- Continued.

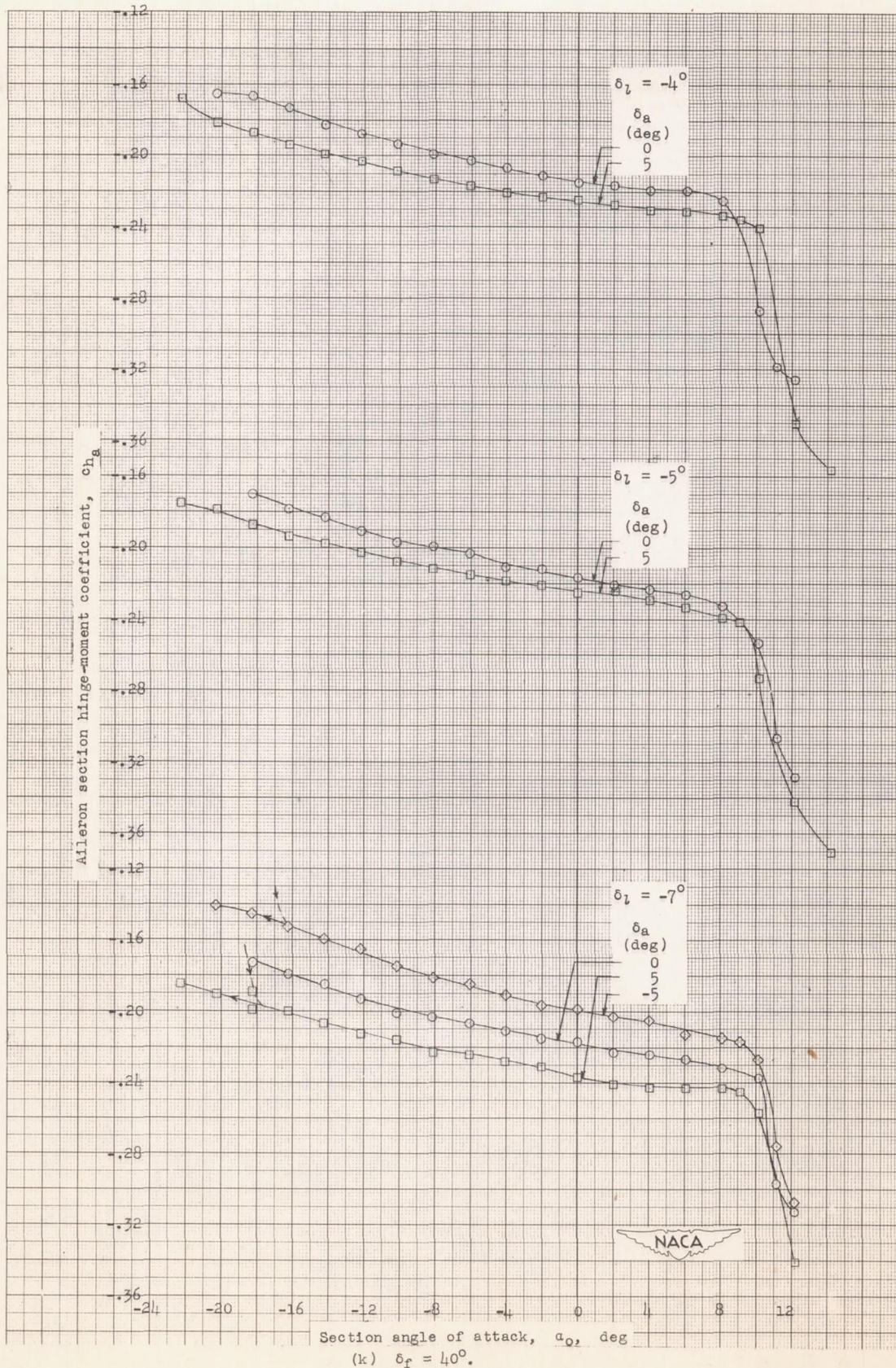
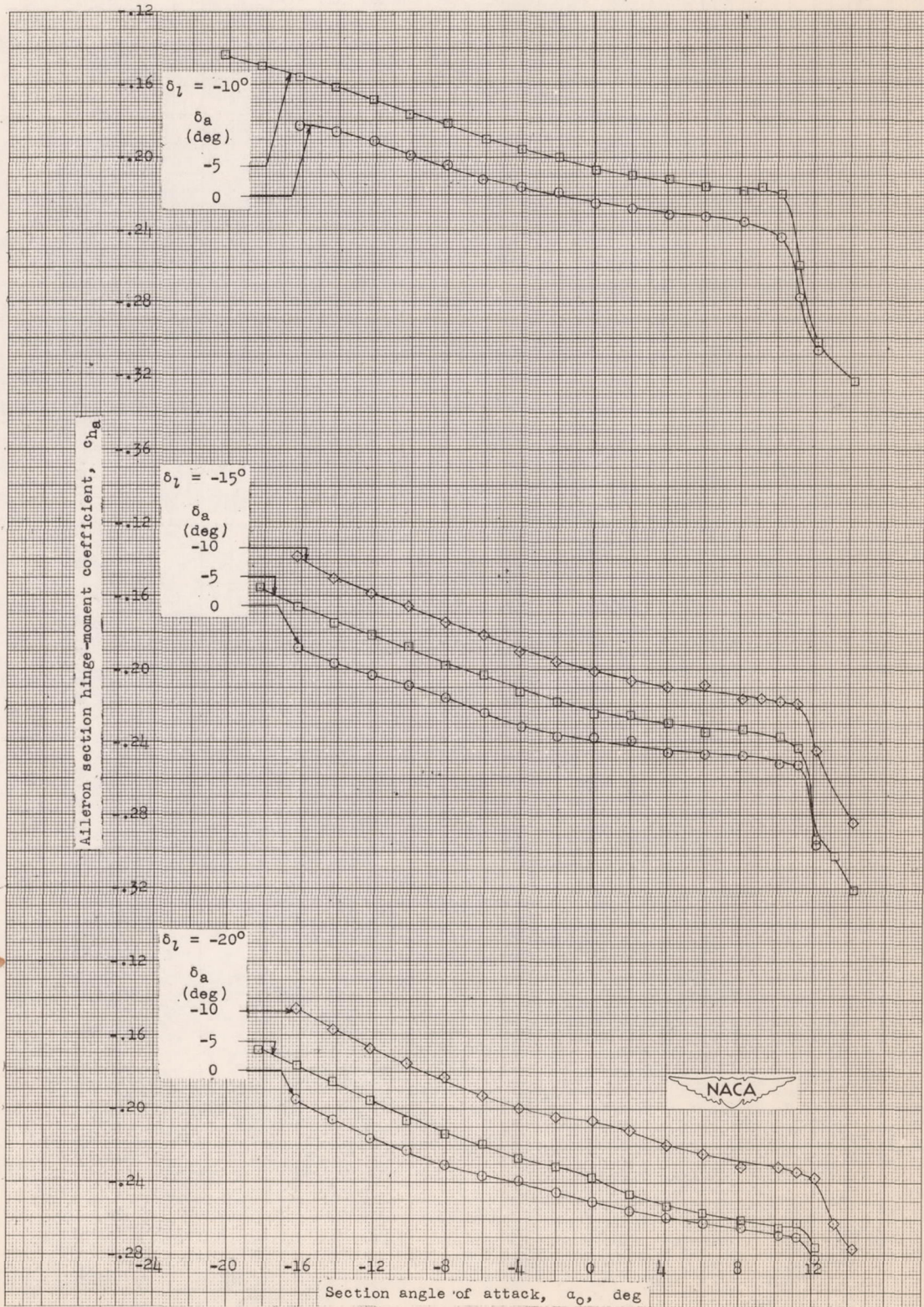
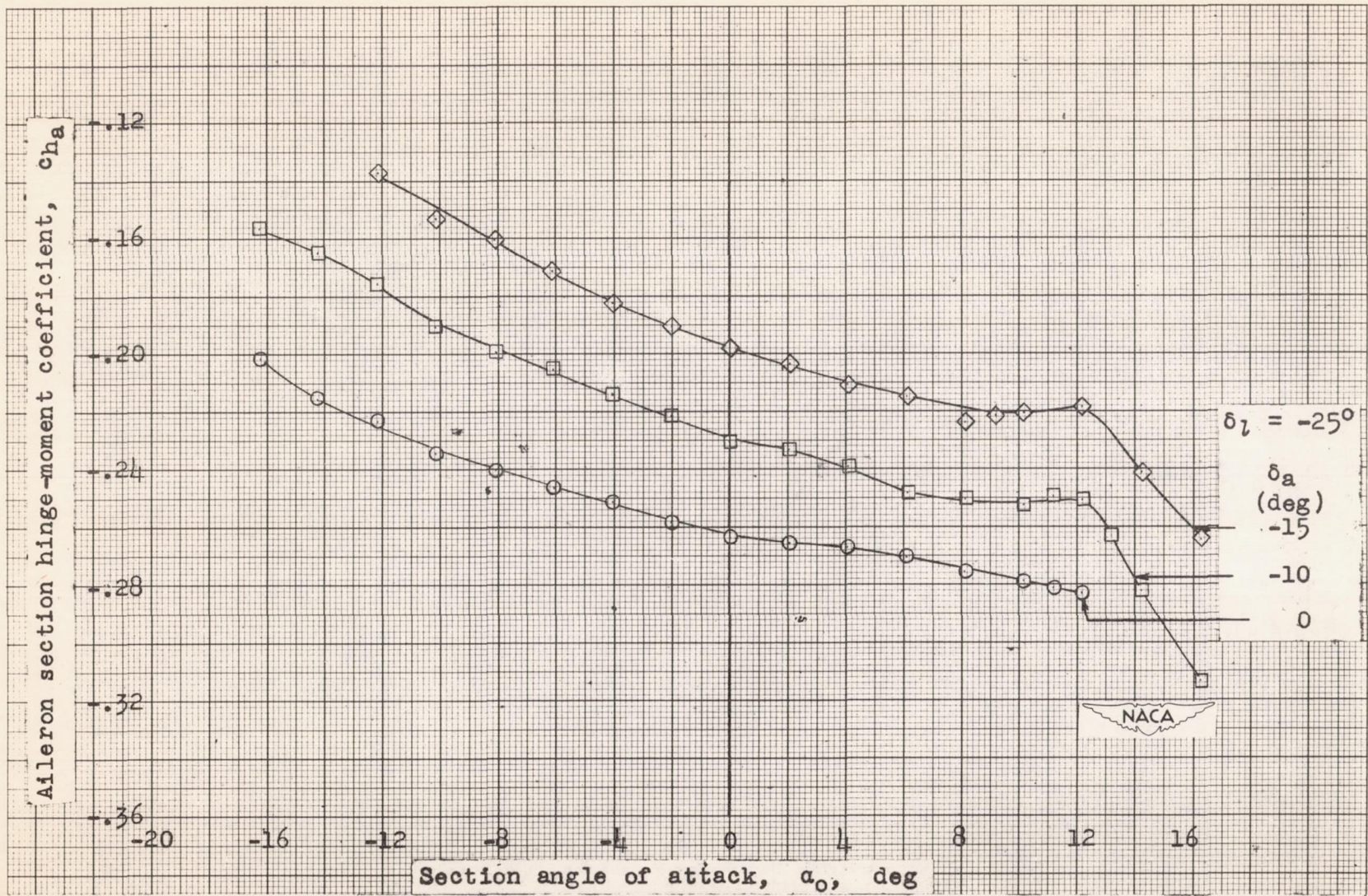


Figure 7.- Continued.



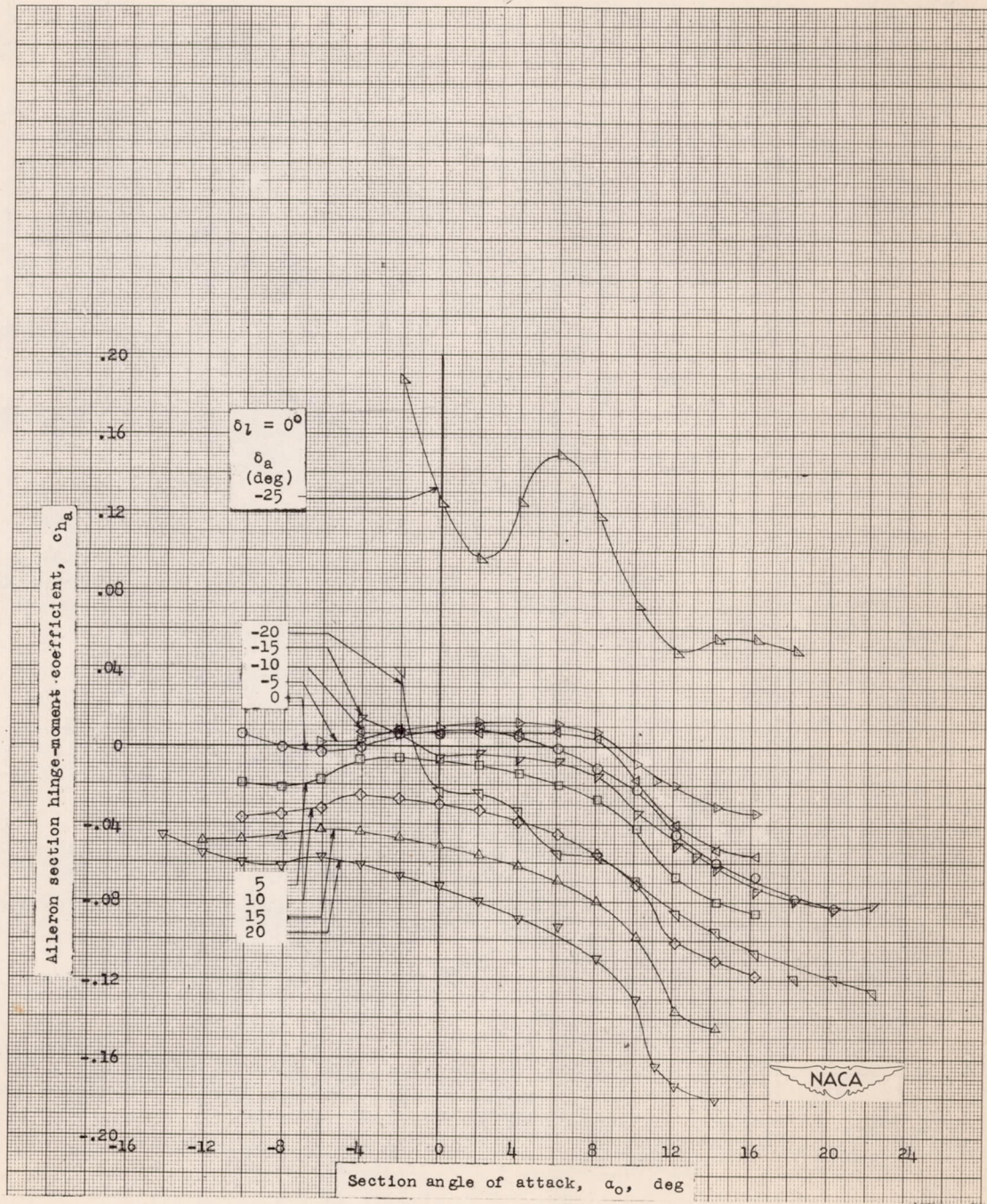
(1) $\delta_f = 40^\circ$.

Figure 7.- Continued.



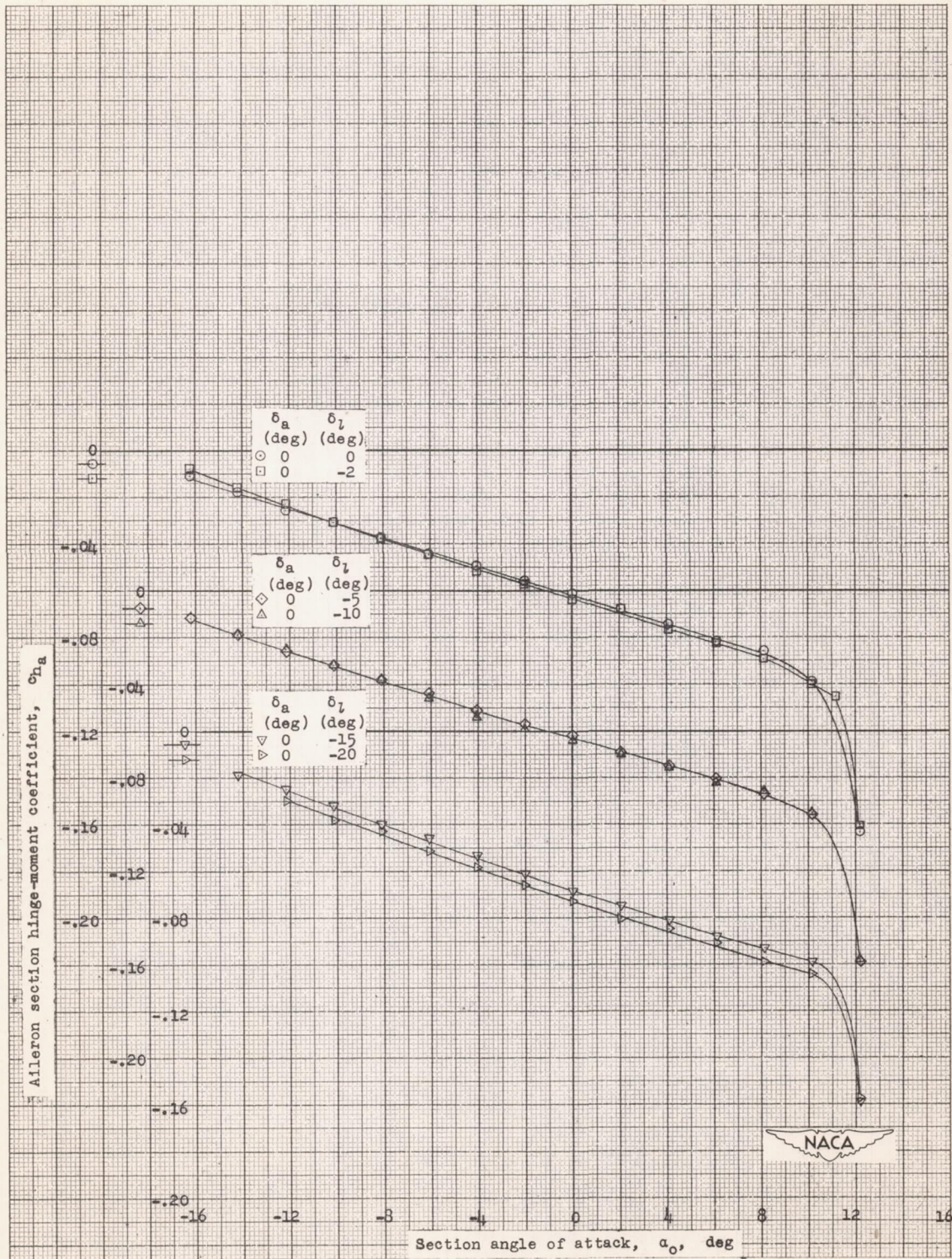
(m) $\delta_f = 40^\circ$

Figure 7.- Concluded.



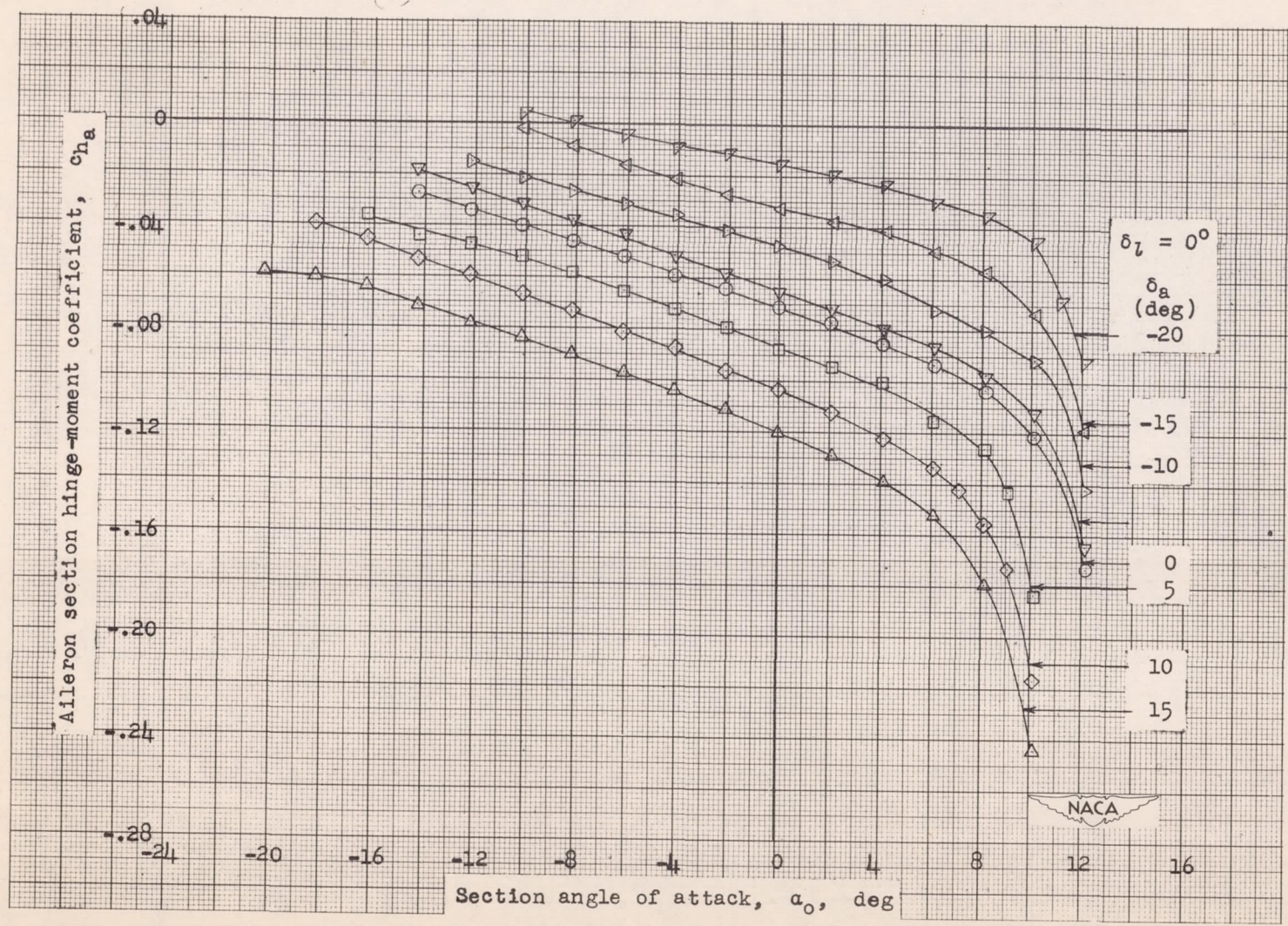
(a) $\delta_f = 0^\circ$.

Figure 8.- Hinge-moment characteristics of a straight-sided Frise aileron on the approximately 17.7-percent-chord thick NACA 7-series-type airfoil with double slotted flap and flip. Aileron balance, $0.408c_a$; $R = 6 \times 10^6$ (approx.)



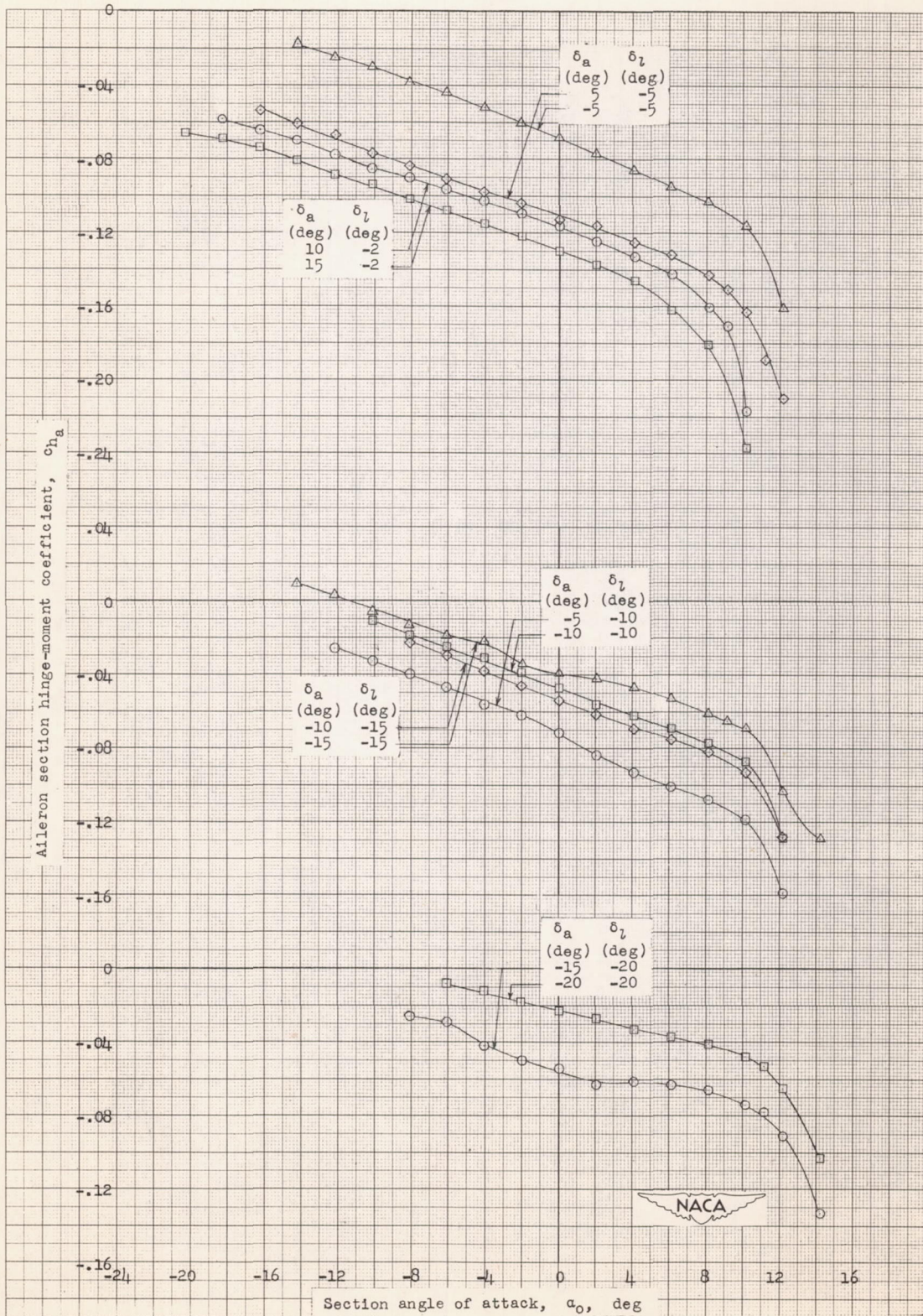
(b) $\delta_f = 20^\circ$.

Figure 8.- Continued.



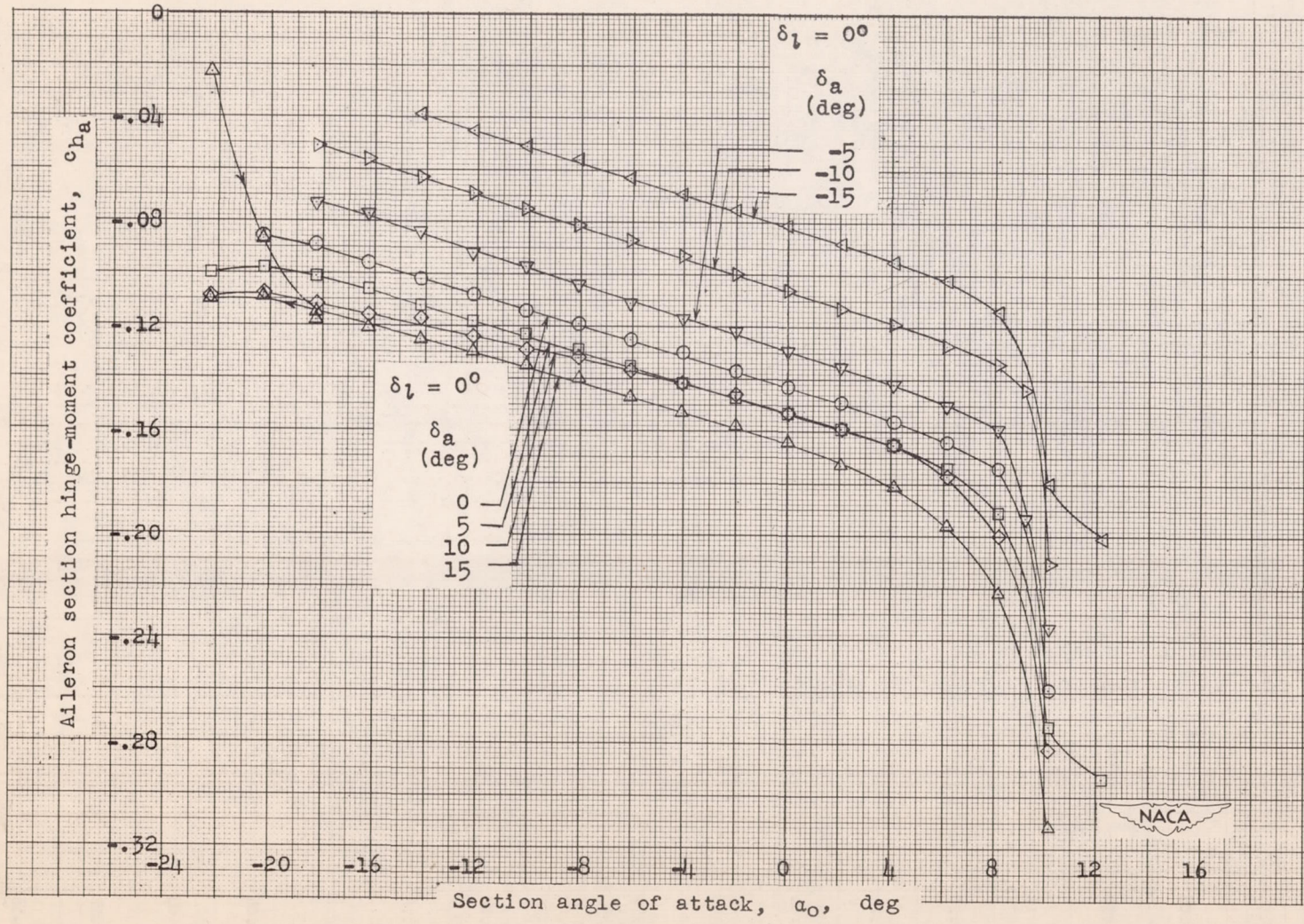
(c) $\delta_f = 25^\circ$.

Figure 8.- Continued.



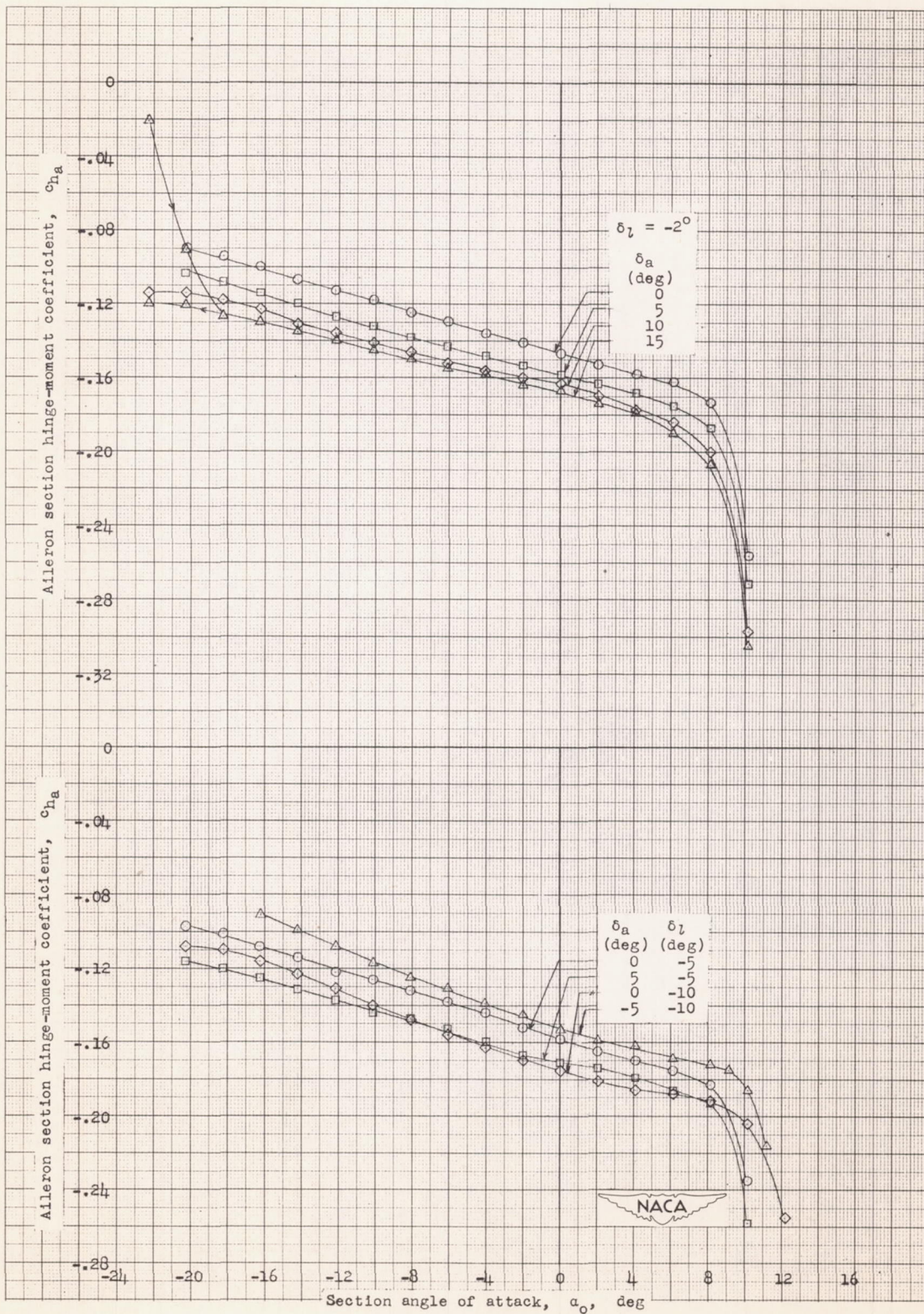
(d) $\delta_f = 25^\circ$

Figure 8.- Continued.



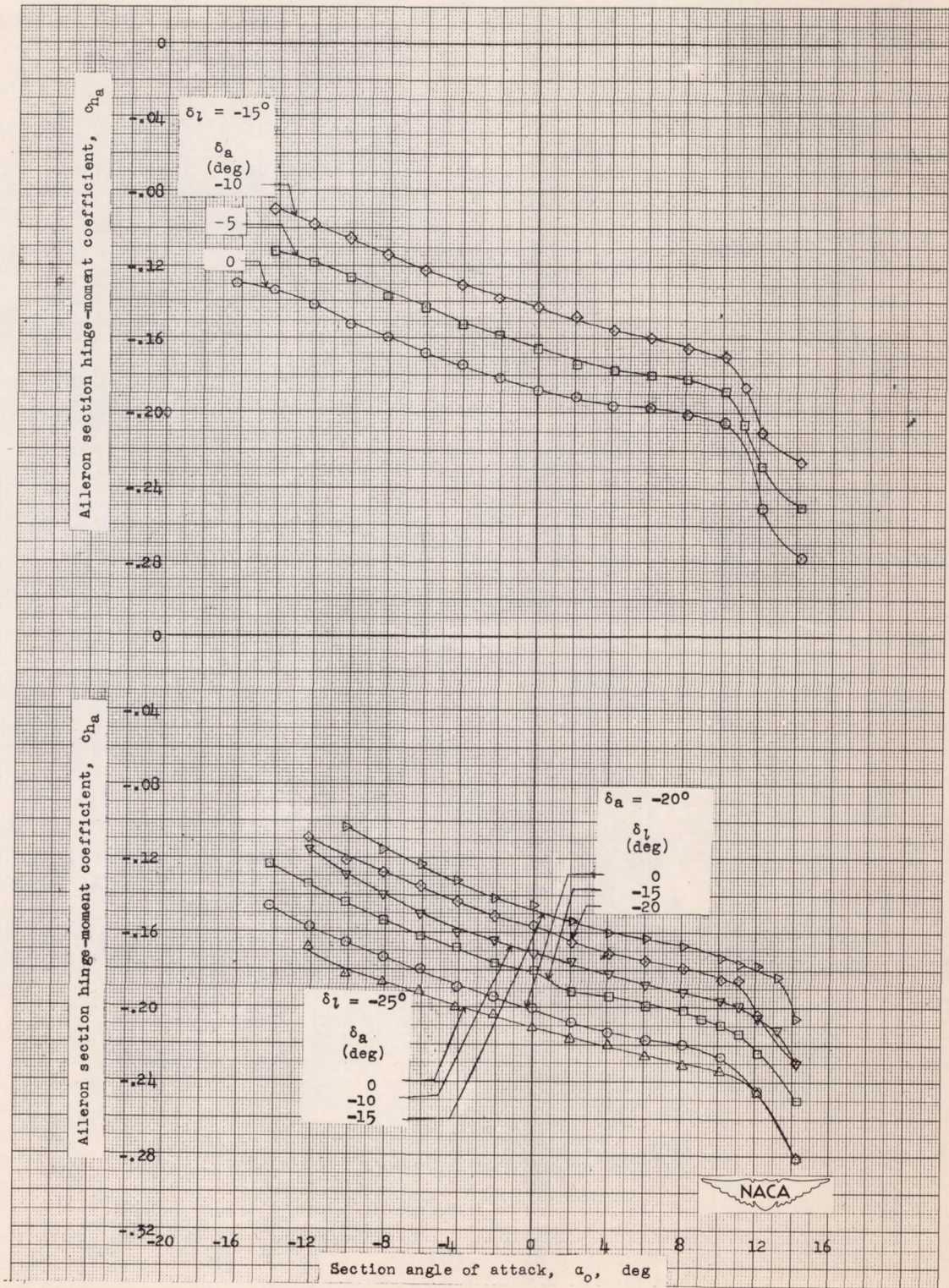
(e) $\delta_f = 40^\circ$.

Figure 8.- Continued.



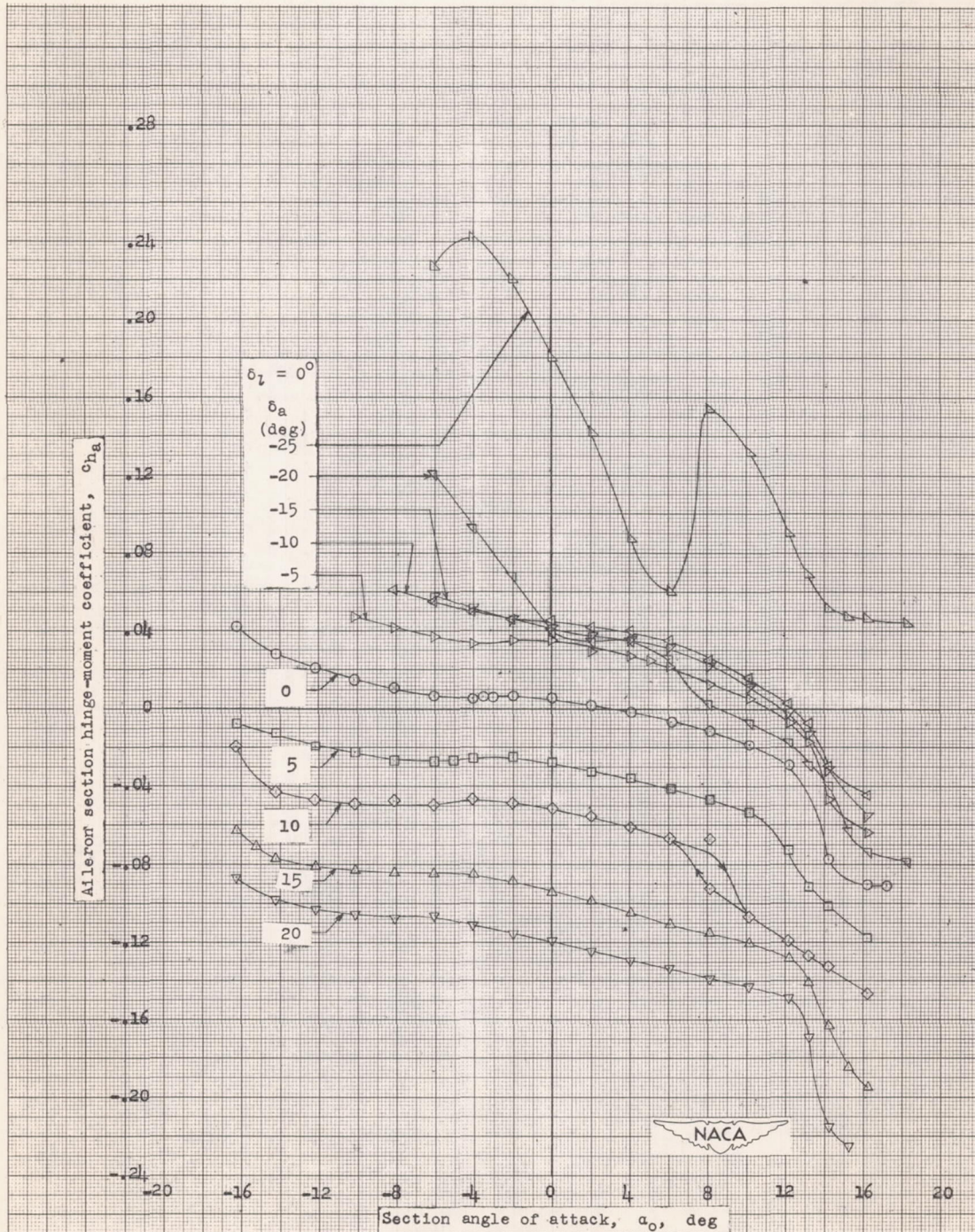
(f) $\delta_f = 40^\circ$.

Figure 8.- Continued.



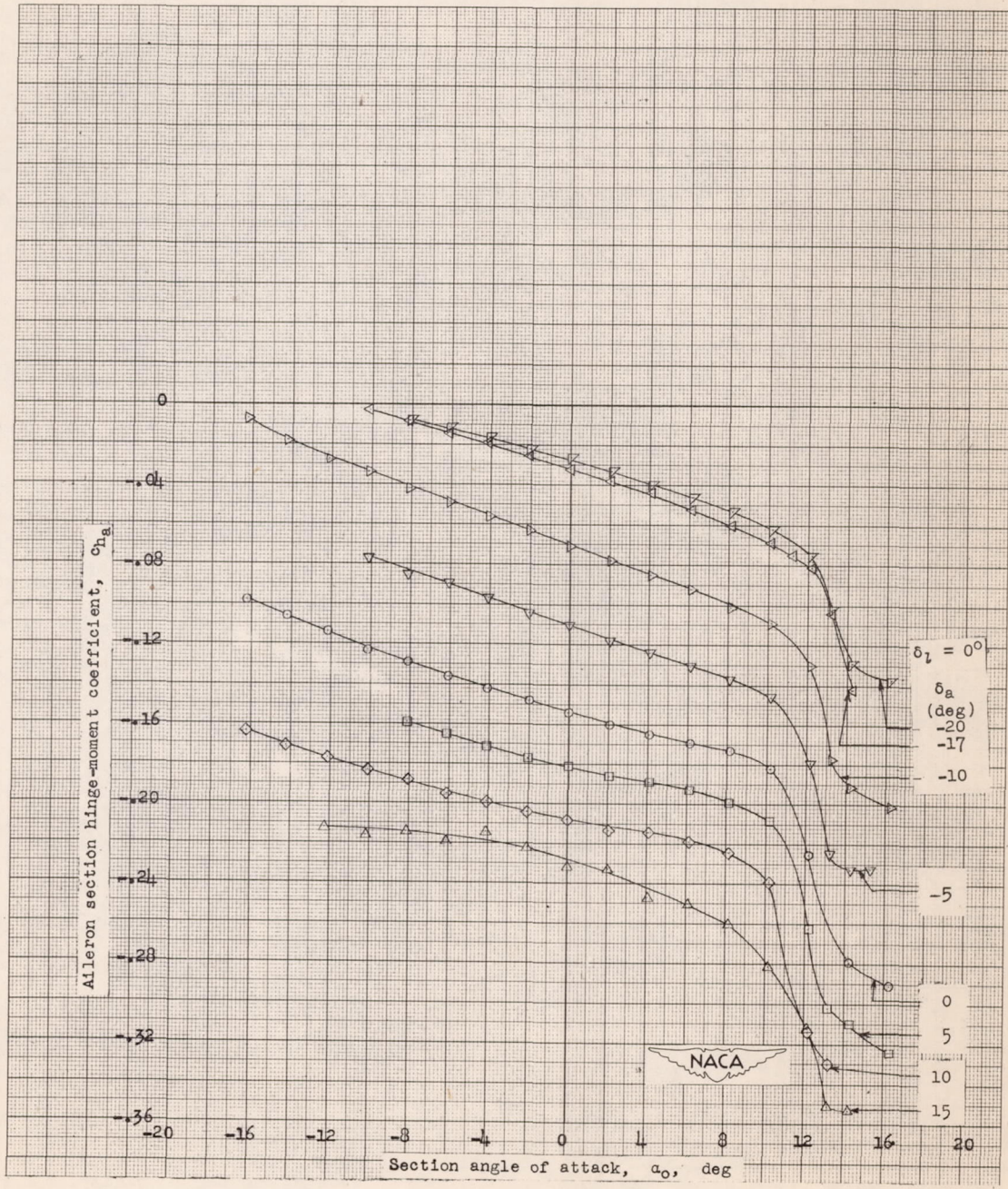
(g) $\delta_r = 40^\circ$.

Figure 8.- Concluded.



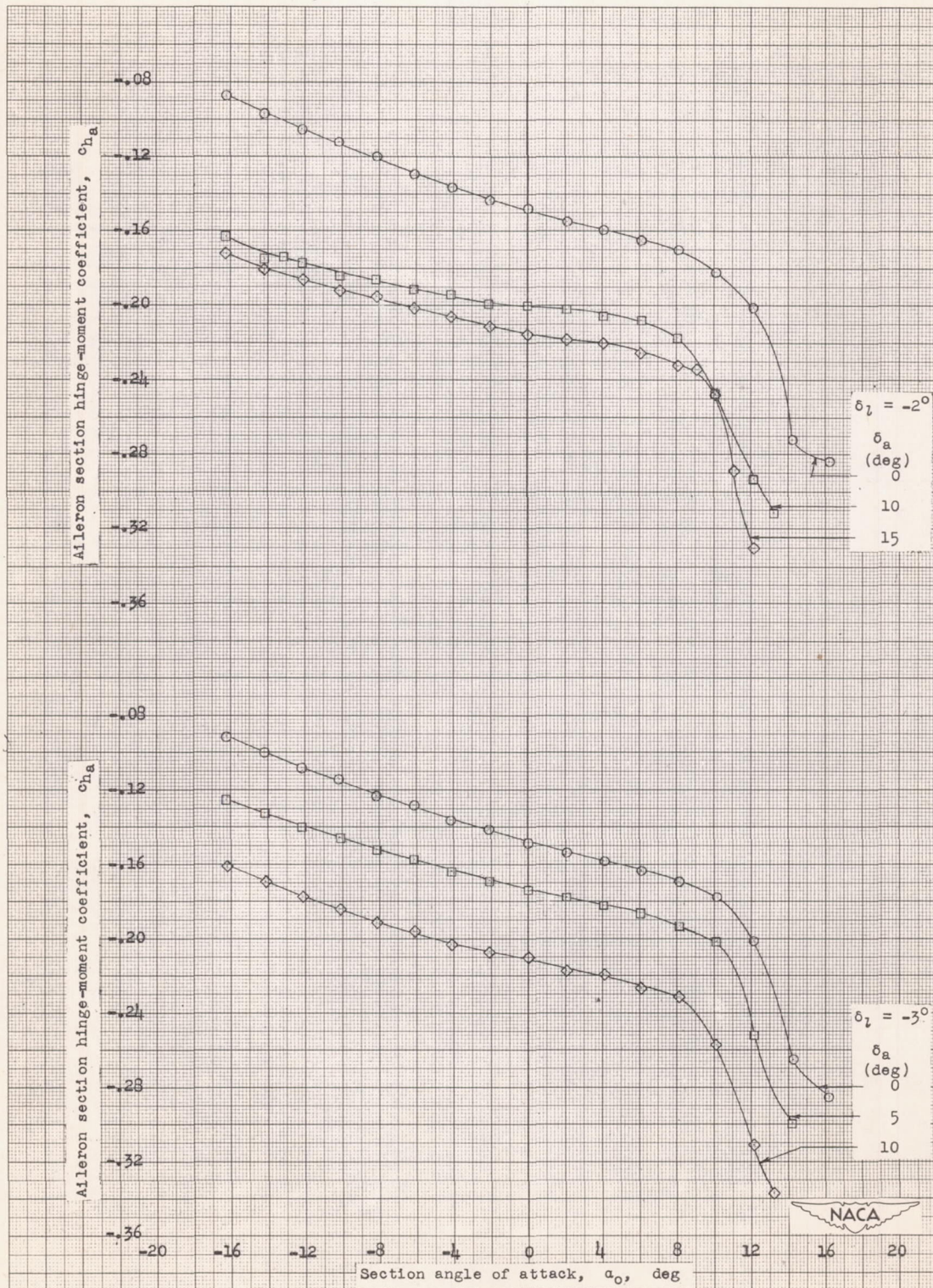
(a) $\delta_f = 0^\circ$.

Figure 9.- Hinge-moment characteristics of a straight-aided Frise aileron on the 15.4-percent-chord thick NACA 7-series-type airfoil with double slotted flap and flip. Aileron balance, $0.351c_a$; $R = 6 \times 10^6$ (approx.).



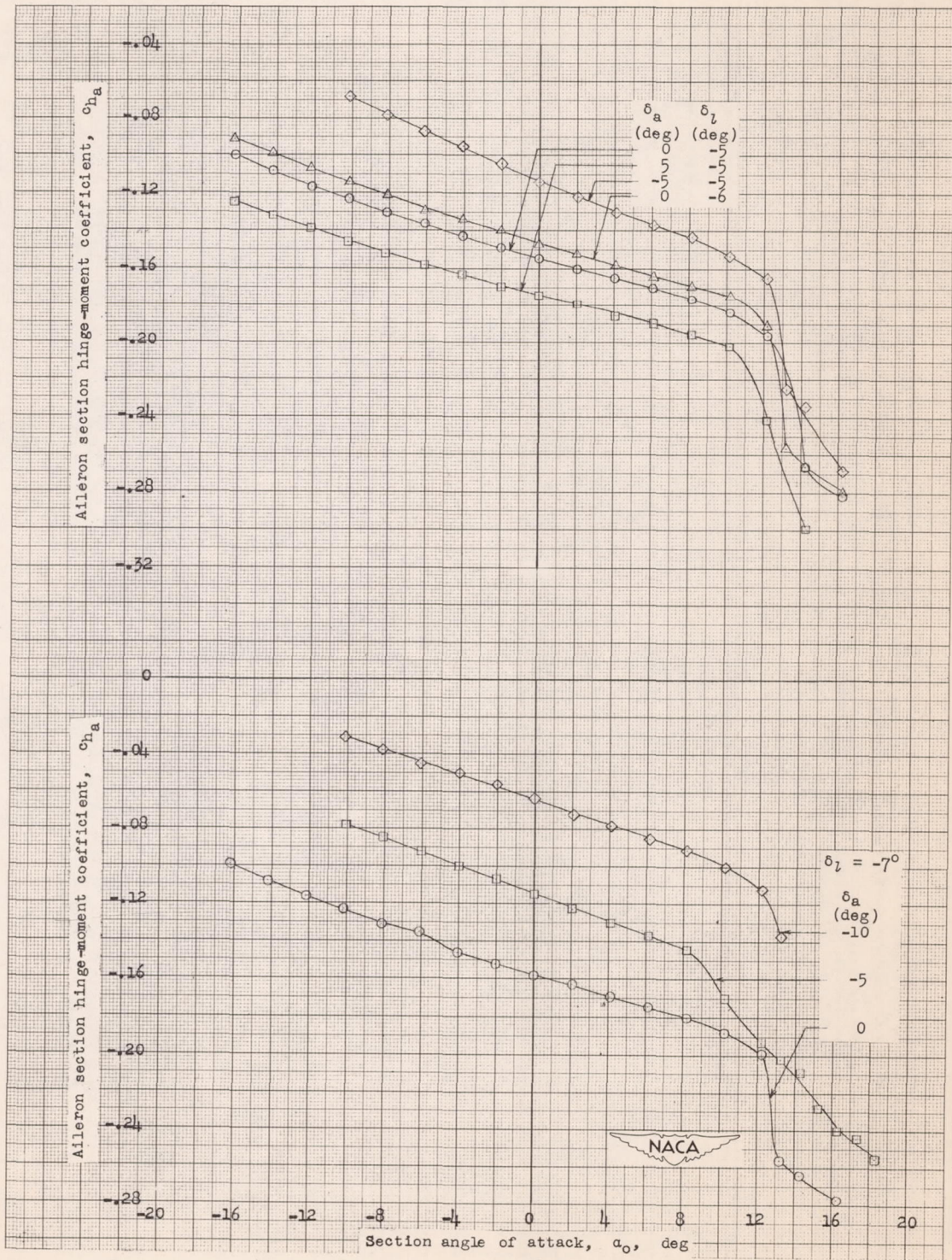
(b) $\delta_f = 25^\circ$.

Figure 9.- Continued.



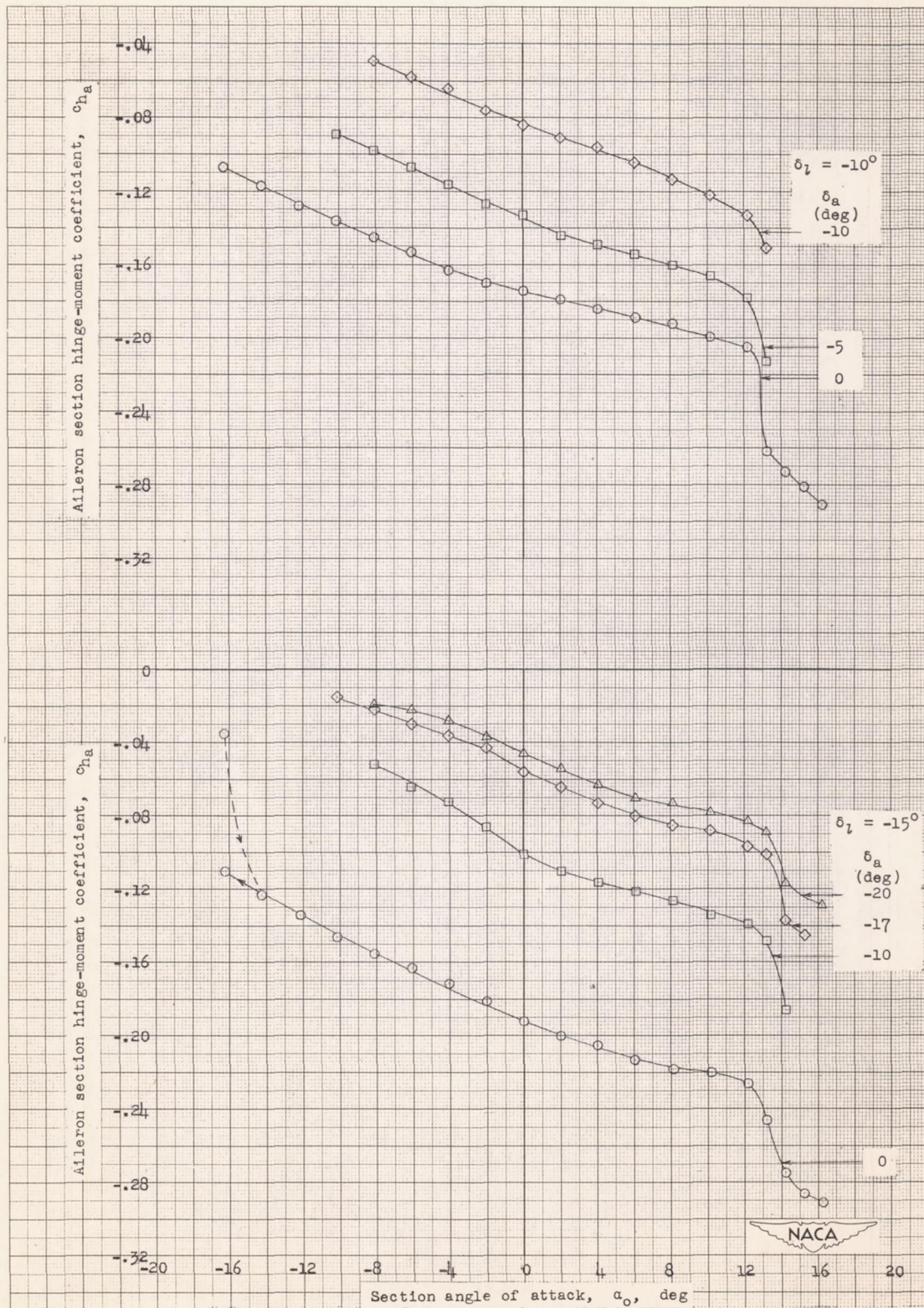
(c) $\delta_f = 25^\circ$.

Figure 9.- Continued.



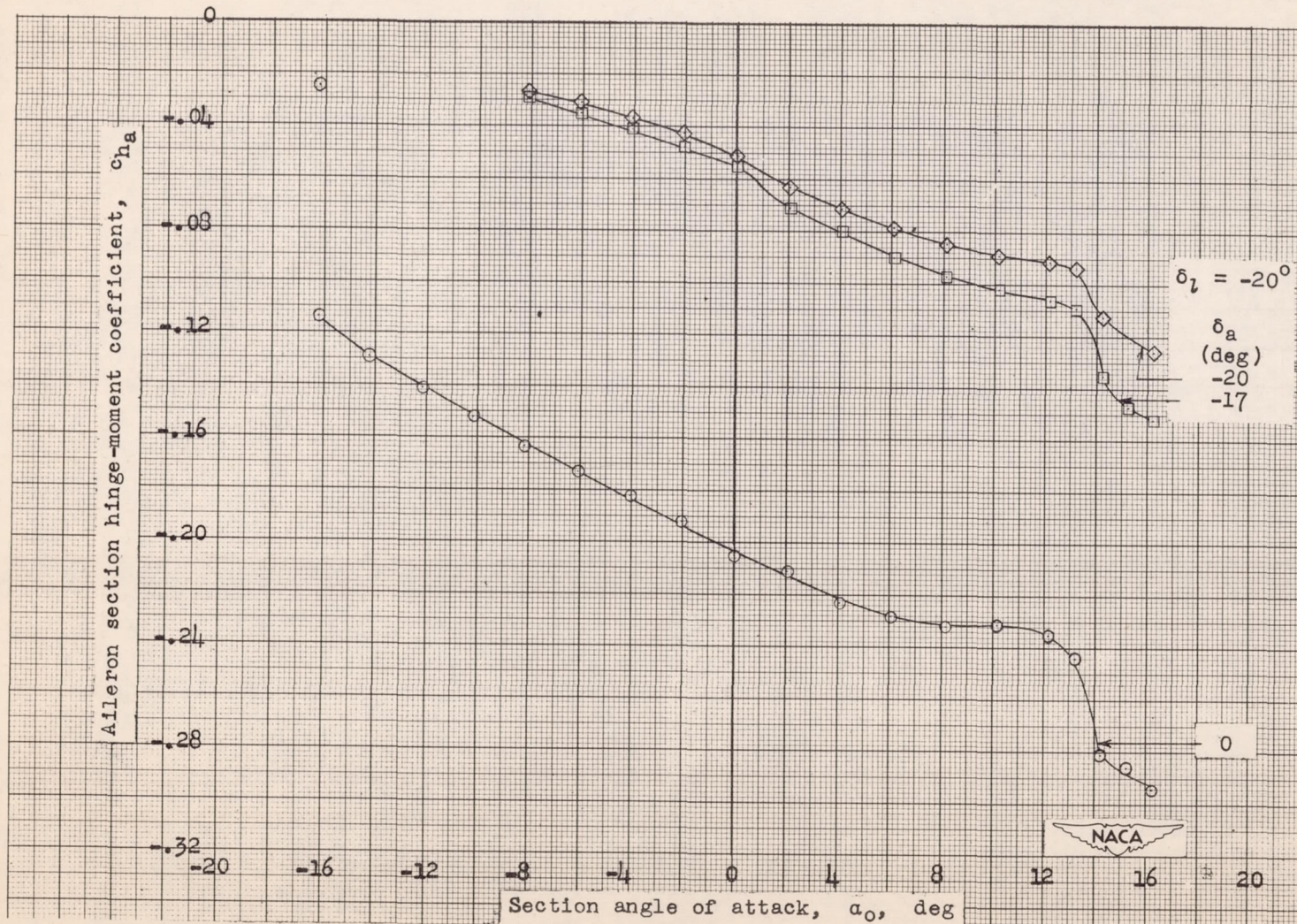
(d) $\delta_f = 25^\circ$.

Figure 9.- Continued.



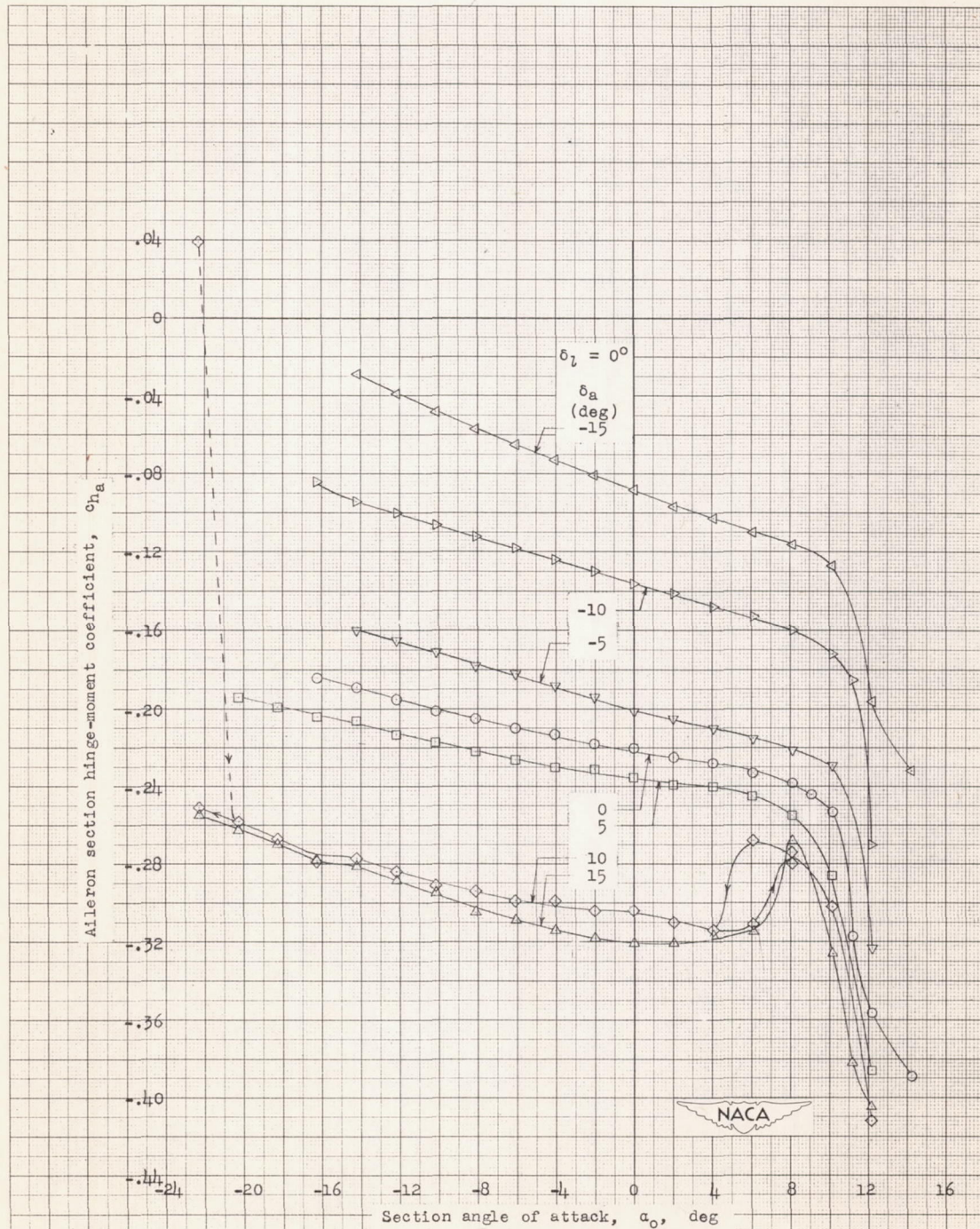
(e) $\delta_f = 25^\circ$.

Figure 9.- Continued.



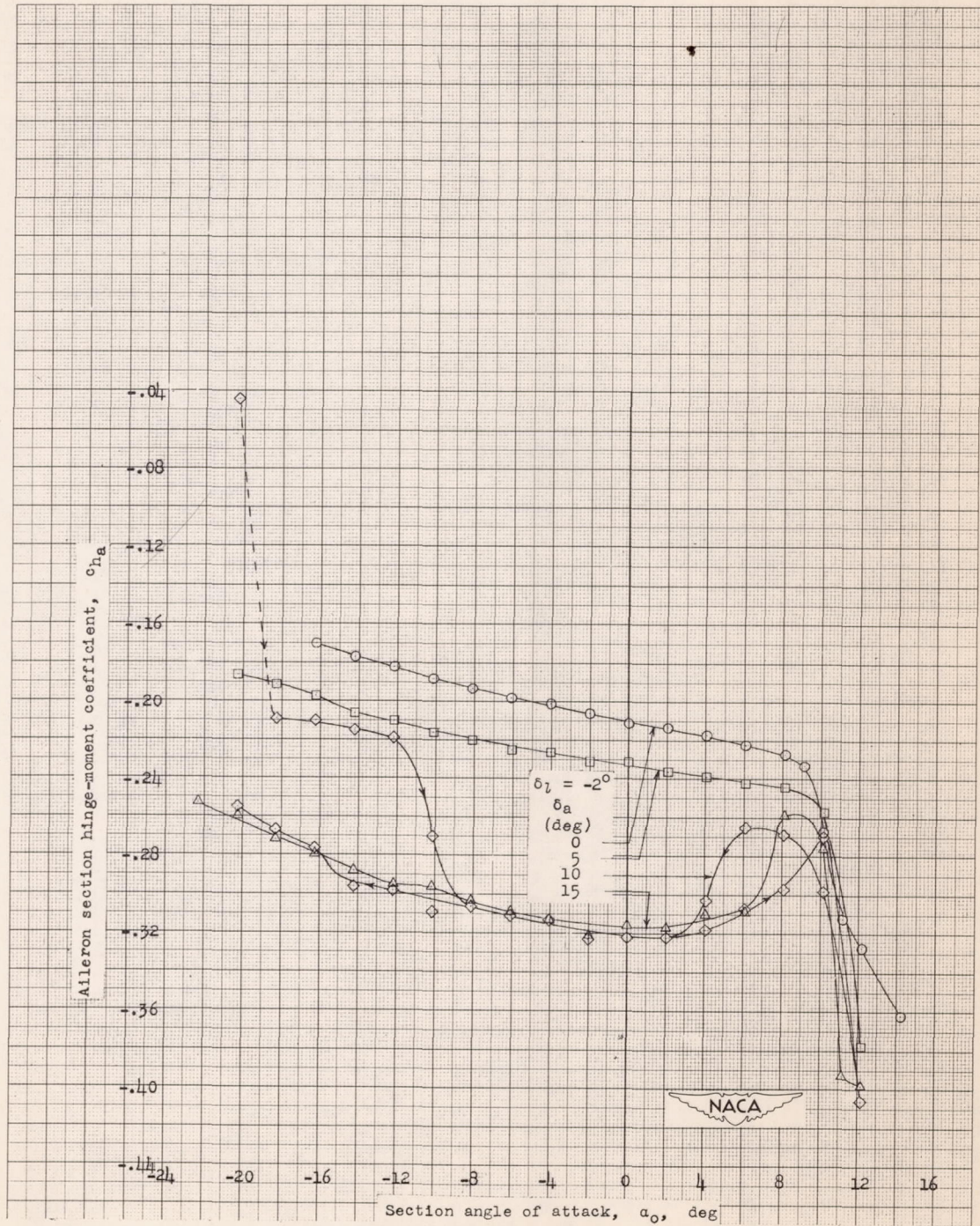
(f) $\delta_f = 25^\circ$.

Figure 9.- Continued.



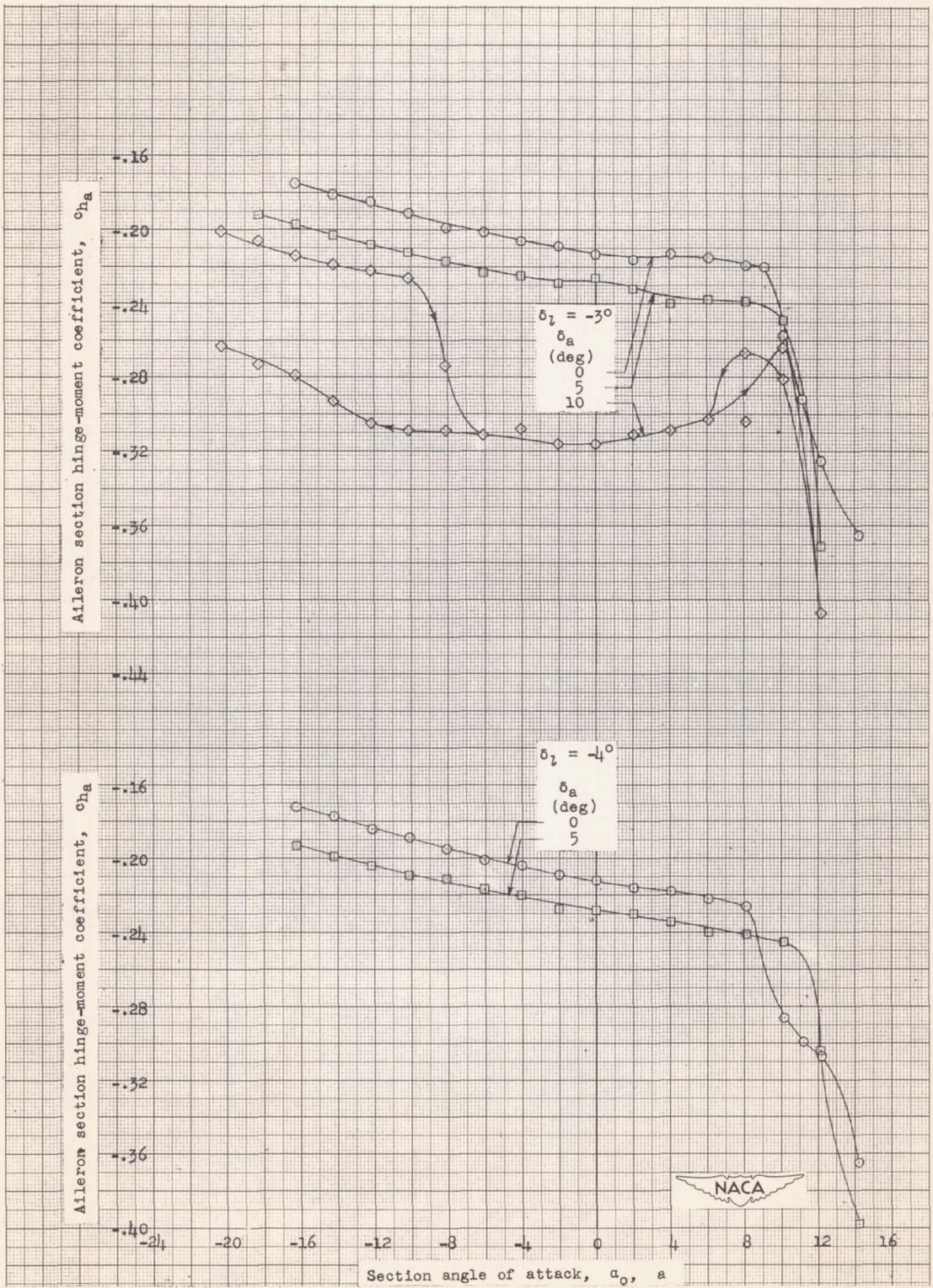
(g) $\delta_r = 40^\circ$.

Figure 9.- Continued.



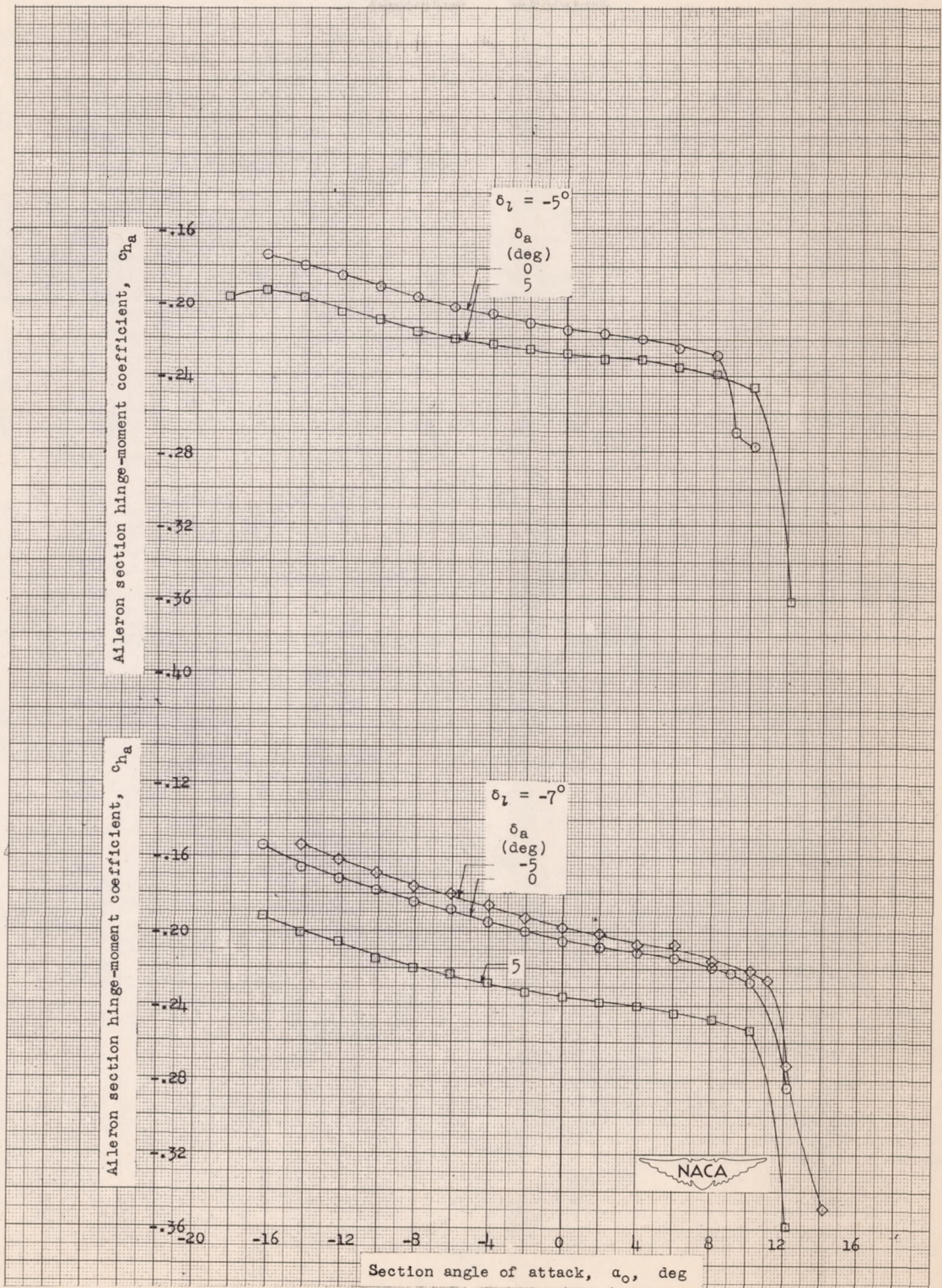
(h) $\delta_r = 40^\circ$.

Figure 9.- Continued.



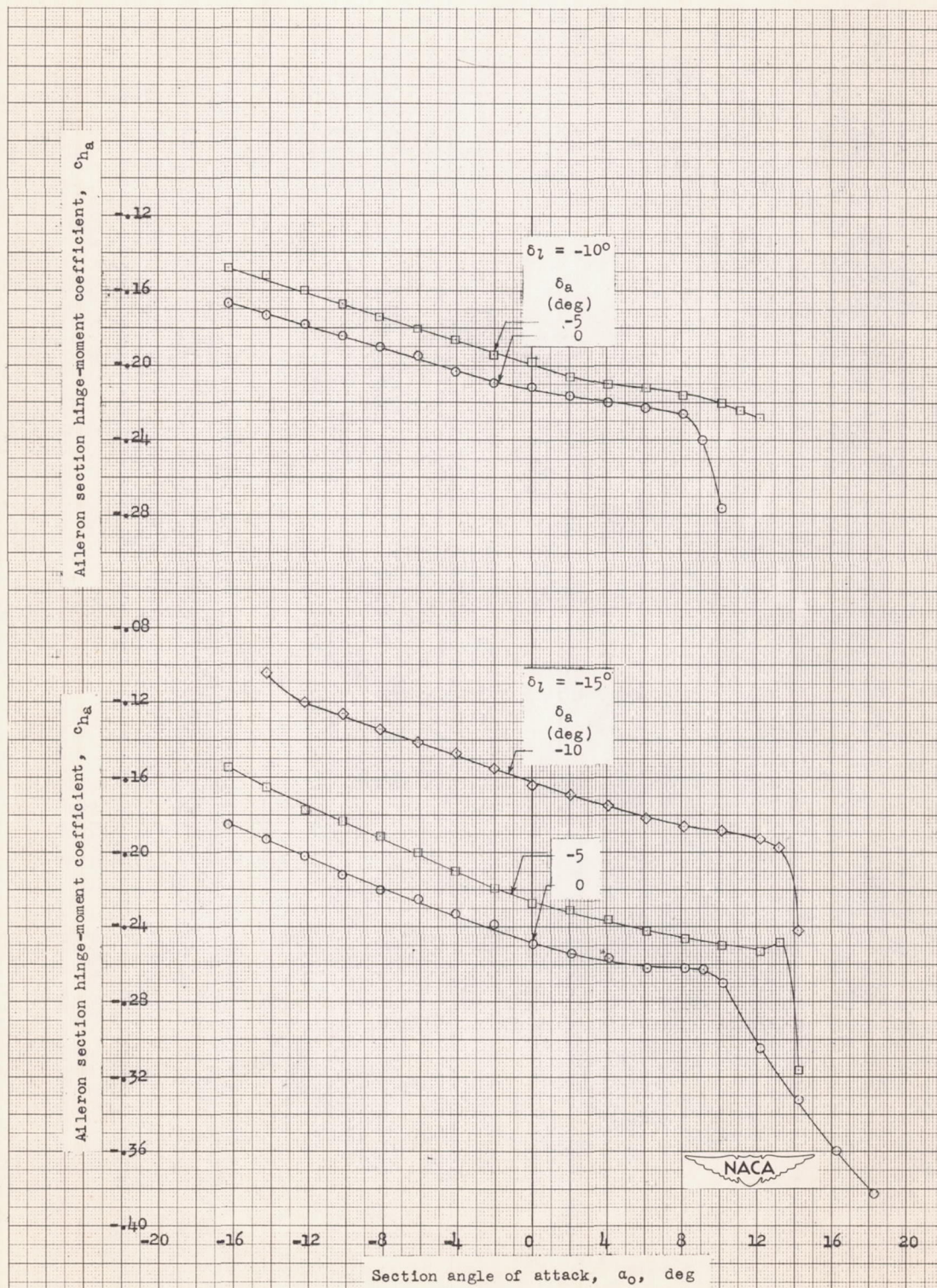
(1) $\delta_f = 40^\circ$.

Figure 9.- Continued.



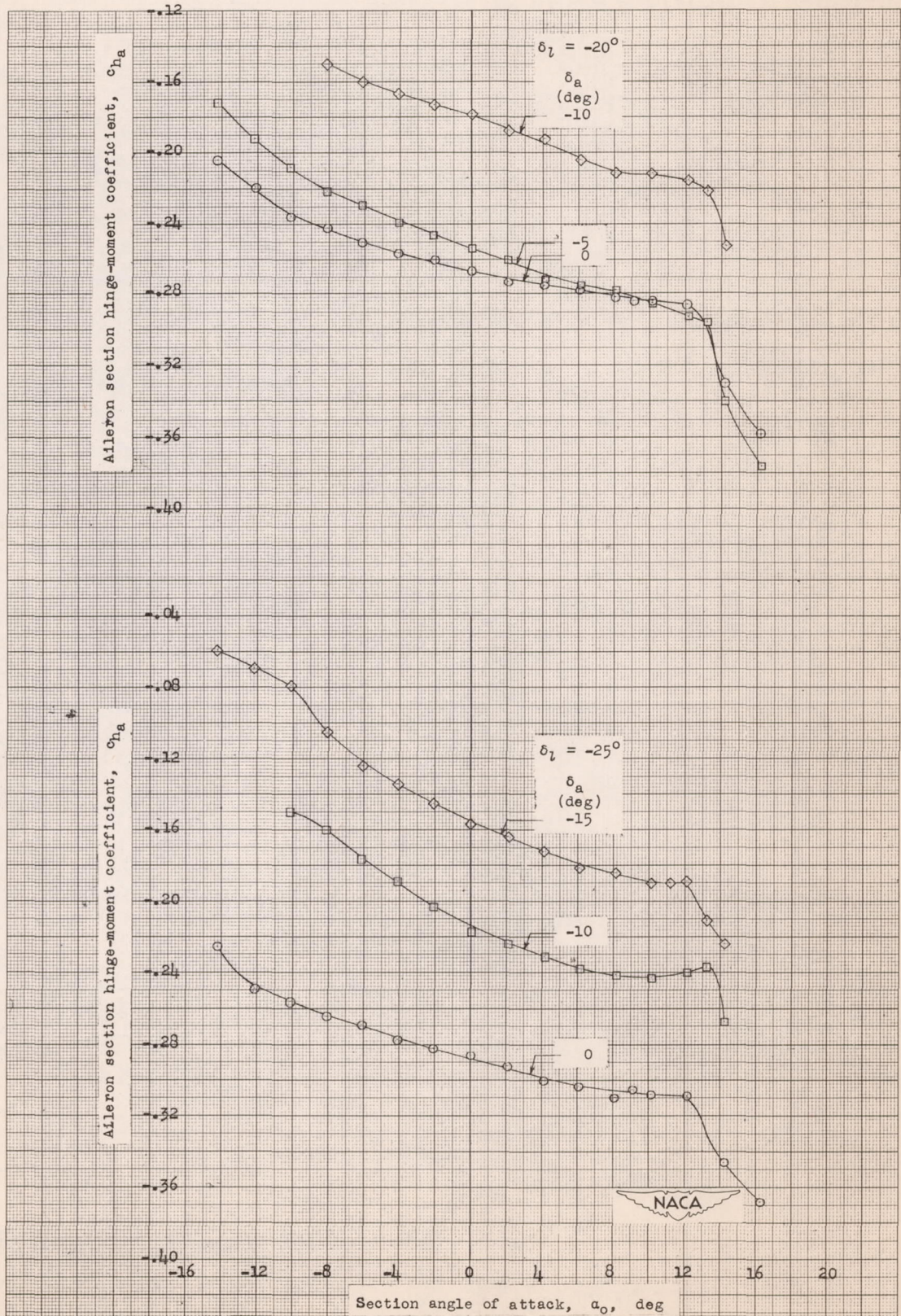
(j) $\delta_f = 40^\circ$.

Figure 9.- Continued.



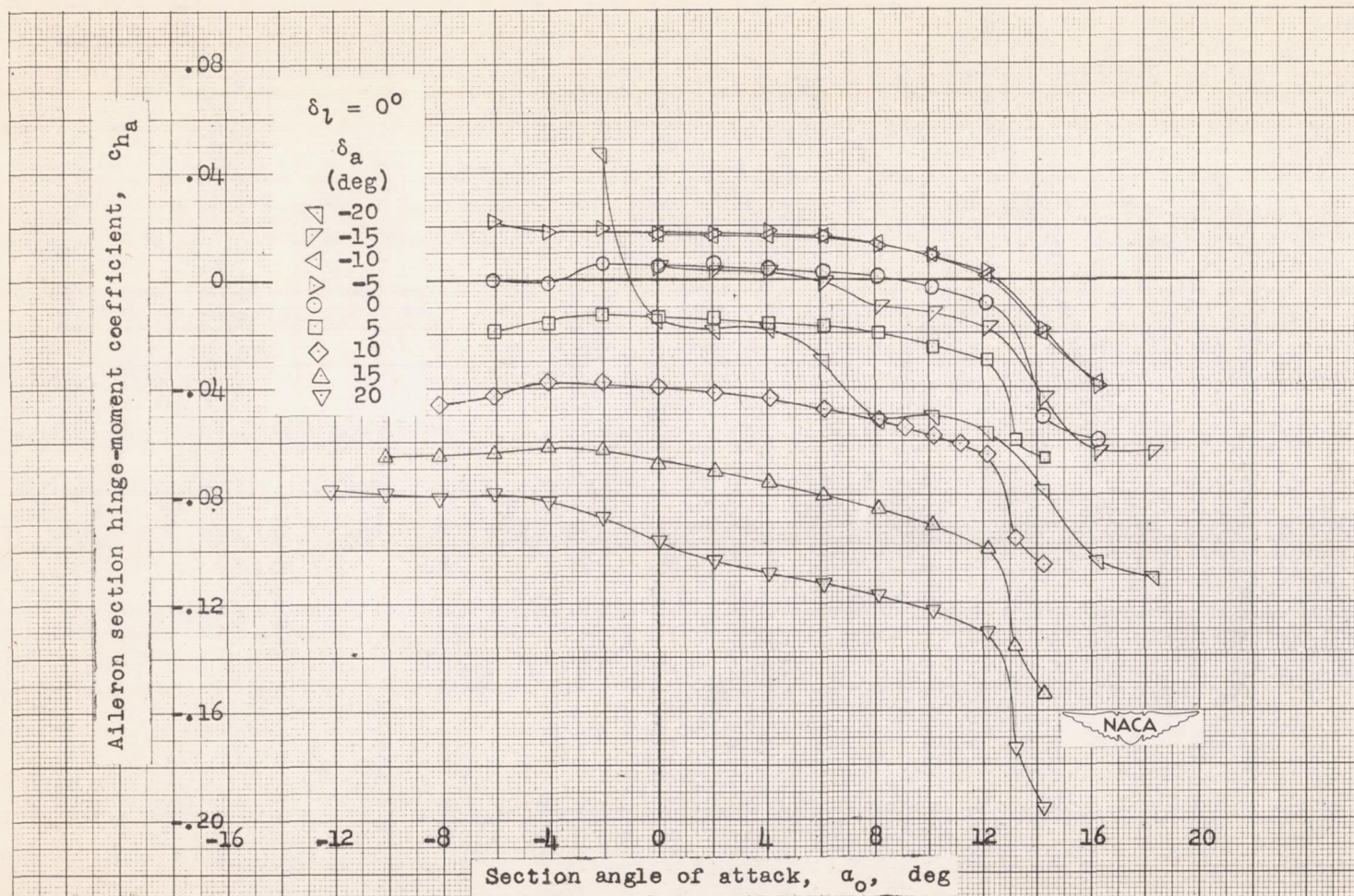
(k) $\delta_f = 40^\circ$.

Figure 9.- Continued.



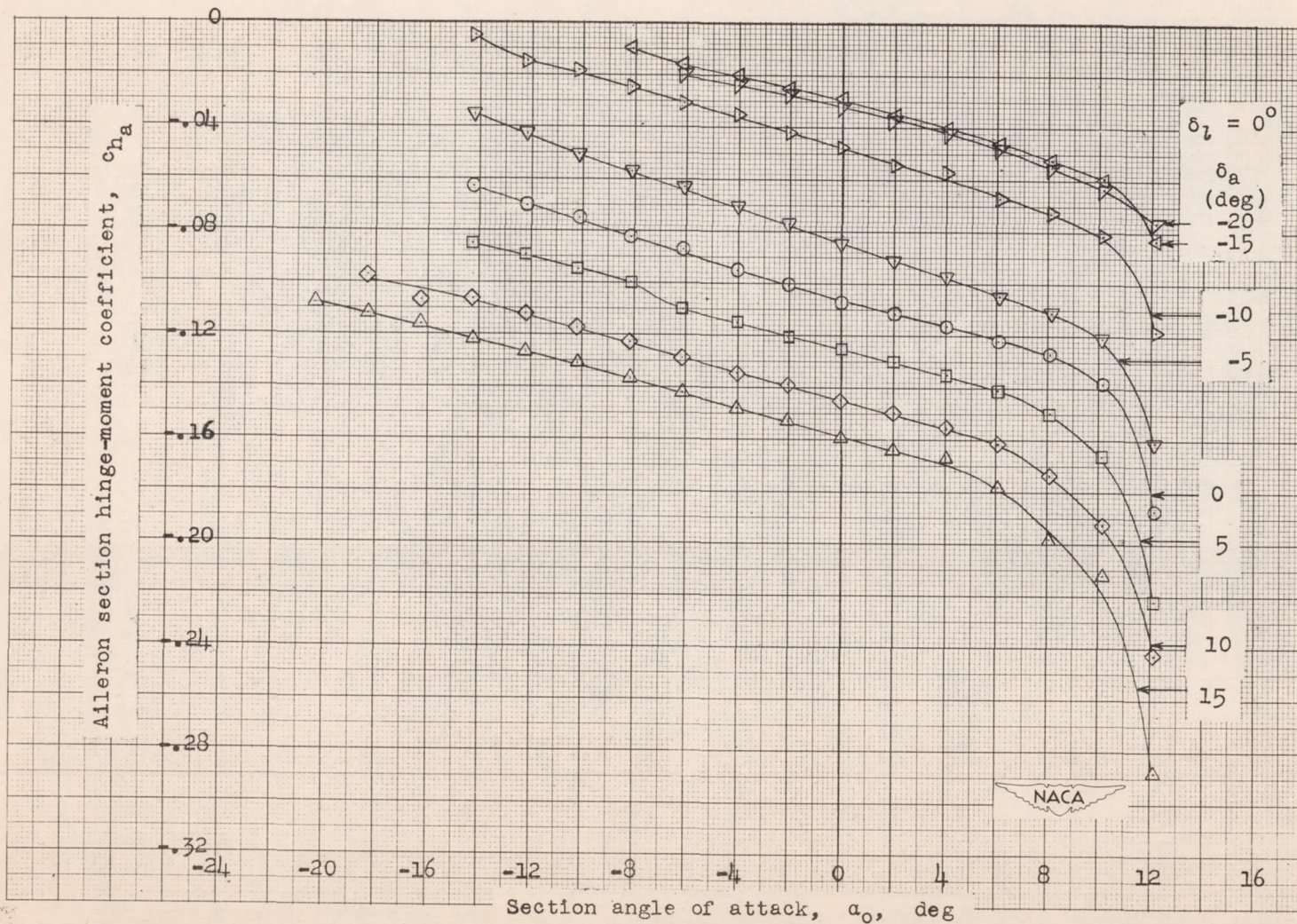
(1) $\delta_r = 40^\circ$.

Figure 9.- Concluded.



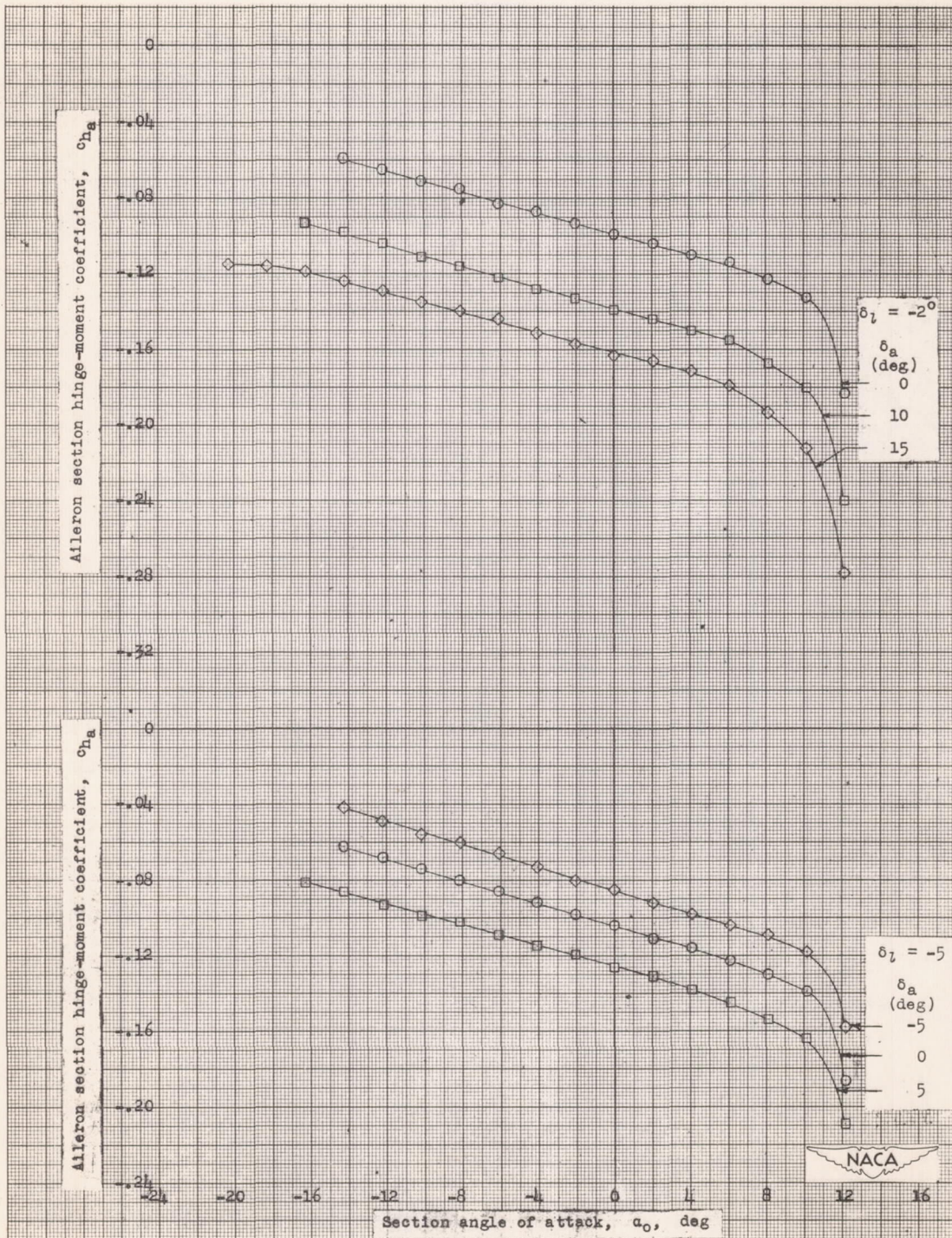
(a) $\delta_f = 0^\circ$.

Figure 10.- Hinge-moment characteristics of a straight-sided Frise aileron on the approximately 15.4-percent-chord thick NACA 7-series-type airfoil with double slotted flap and flap. Aileron balance, $0.408c_a$; $R = 6 \times 10^6$ (approx.)



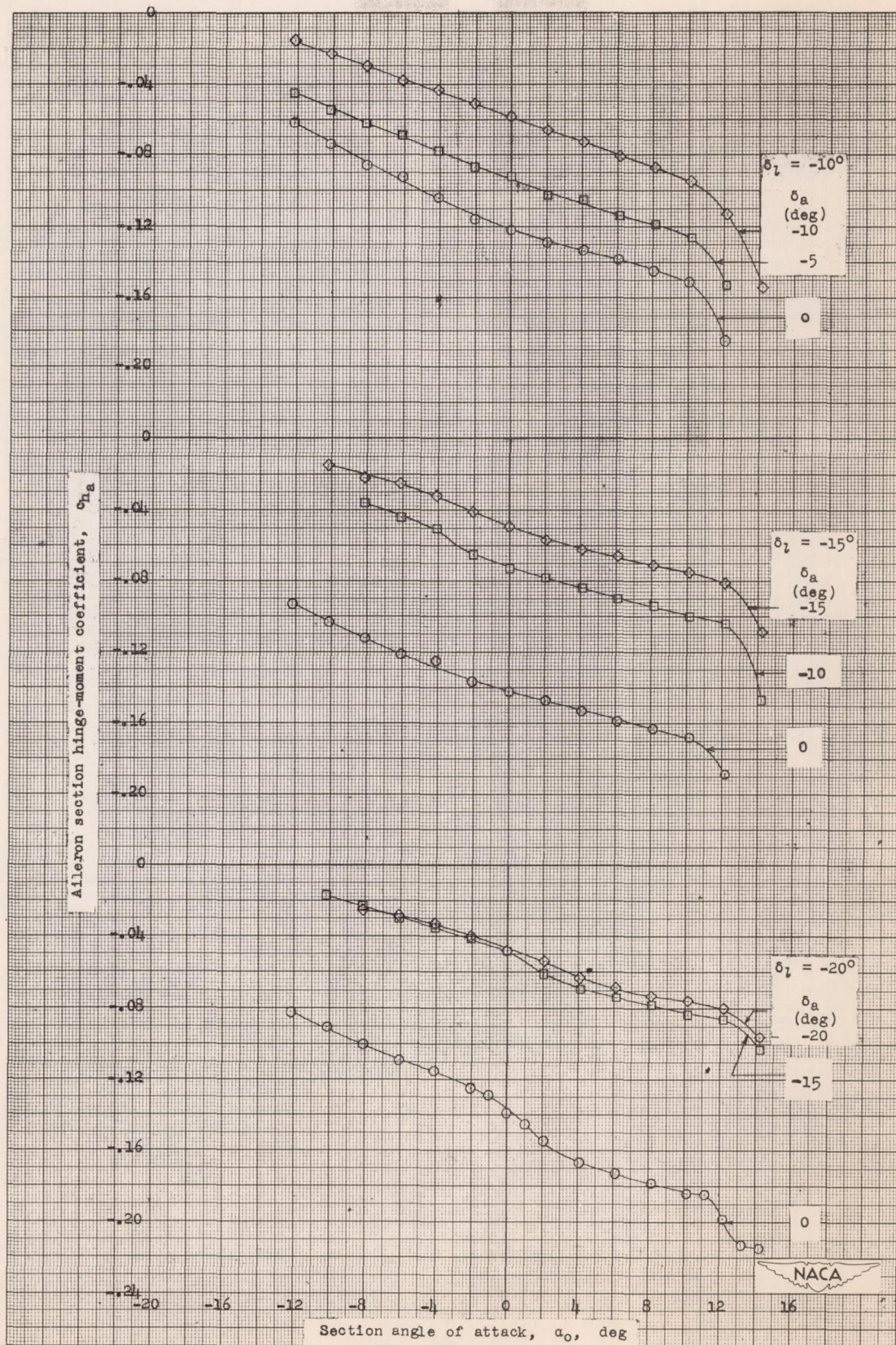
(b) $\delta_f = 25^\circ$.

Figure 10.- Continued.



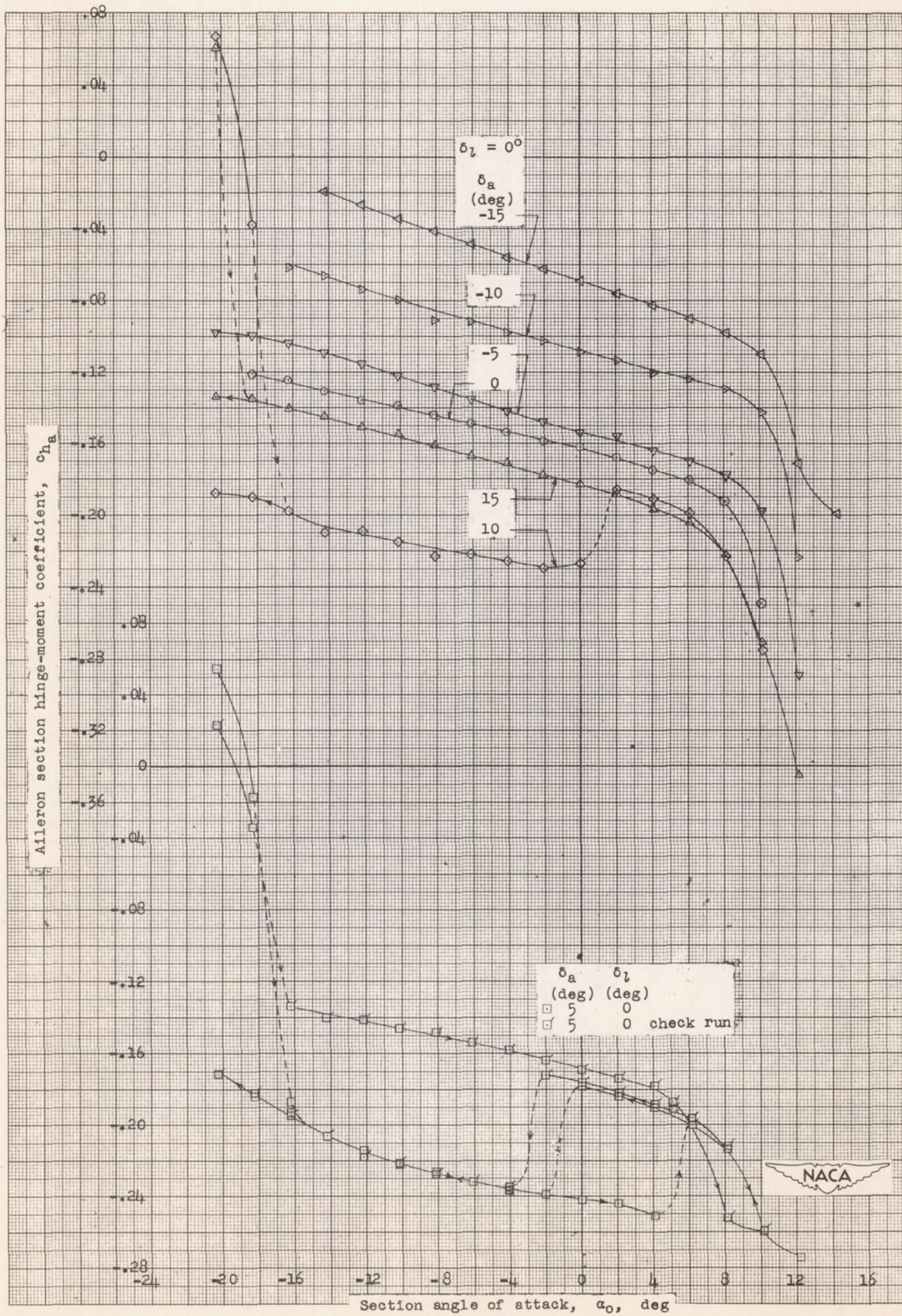
(c) $\delta_r = 25^\circ$.

Figure 10.- Continued.



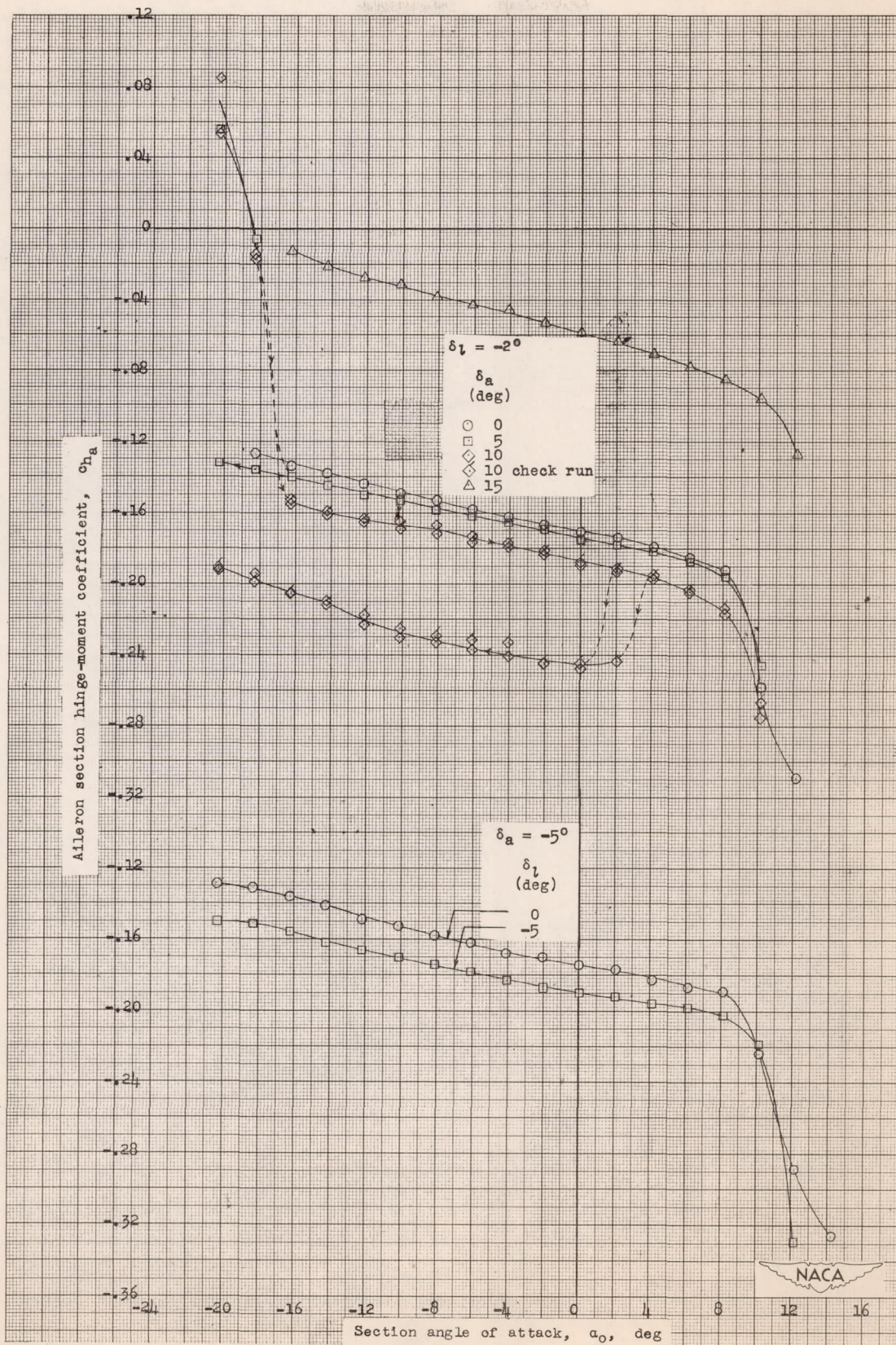
(d) $\delta_f = 25^\circ$.

Figure 10.- Continued.



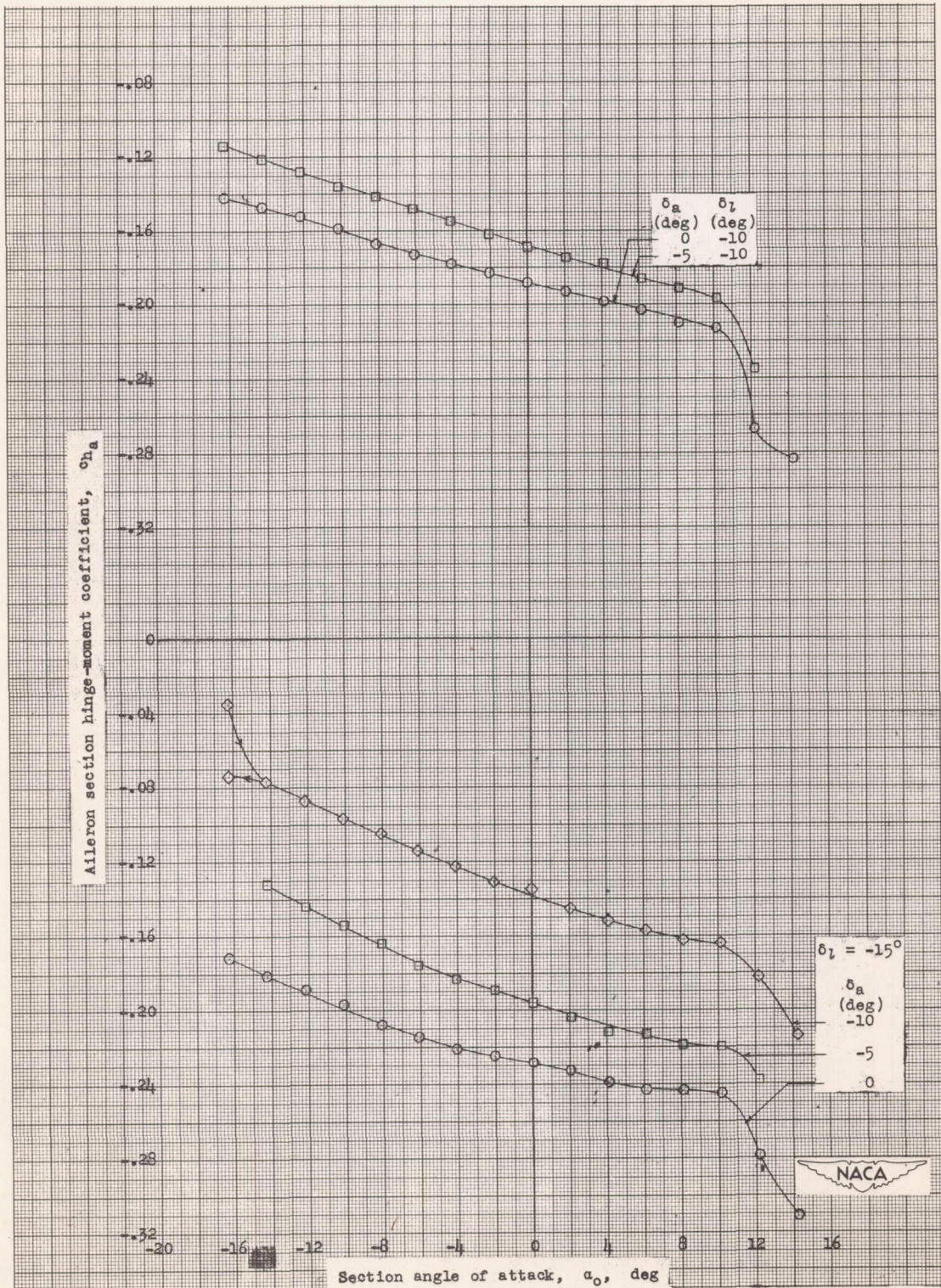
(e) $\delta_f = 40^\circ$.

Figure 10.- Continued.



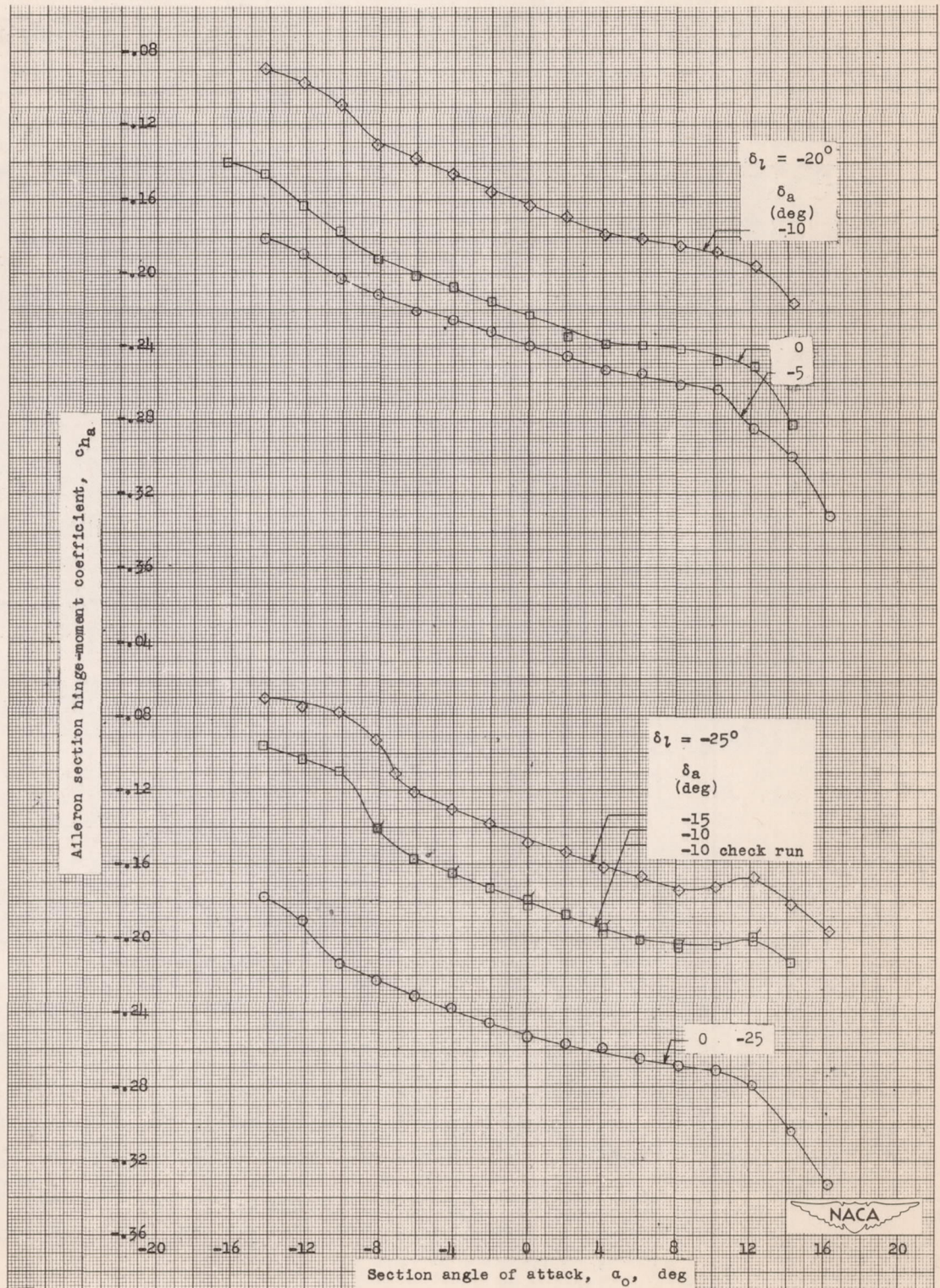
(f) $\delta_f = 40^\circ$.

Figure 10.- Continued.



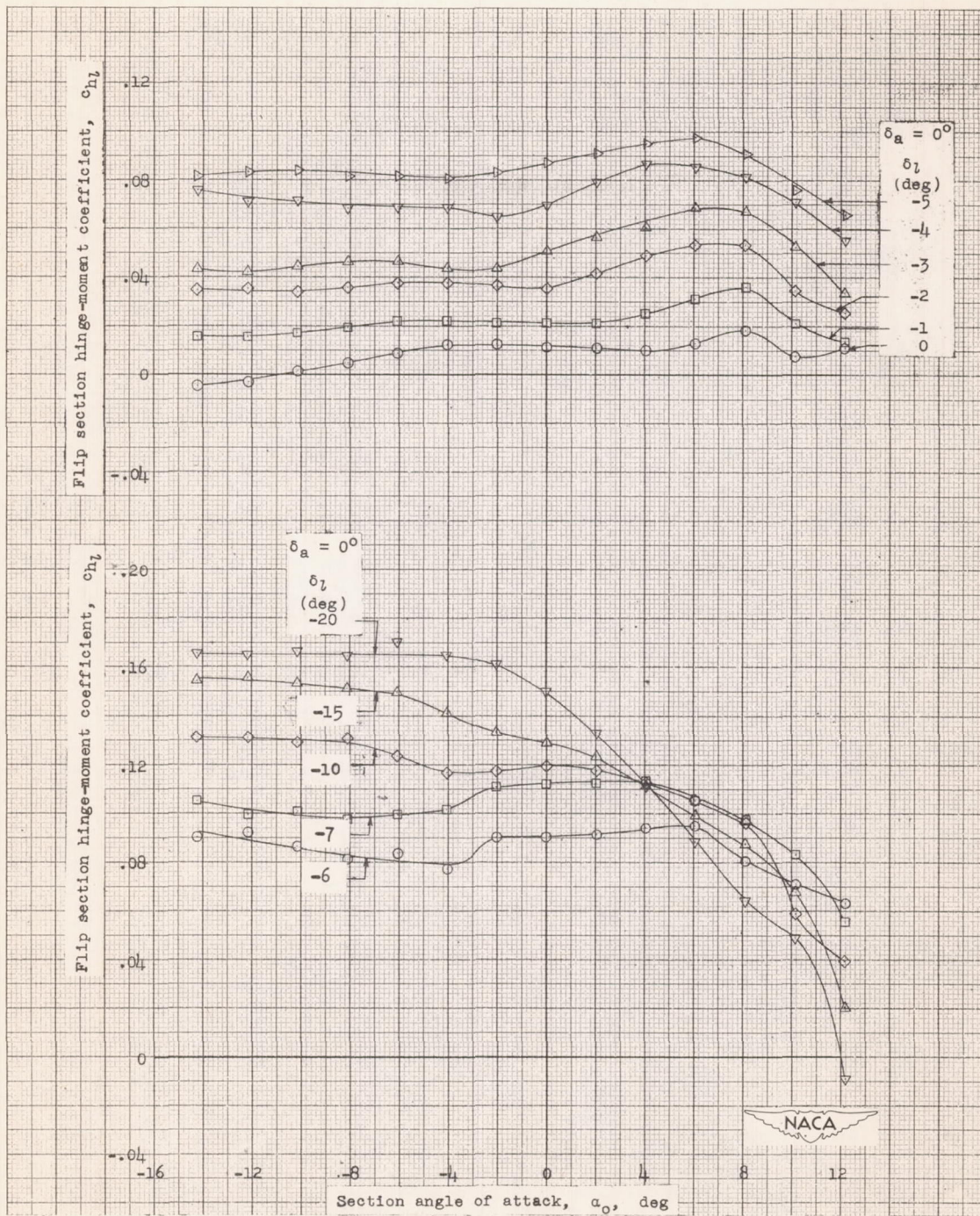
(g) $\delta_l = 40^\circ$.

Figure 10.- Continued.



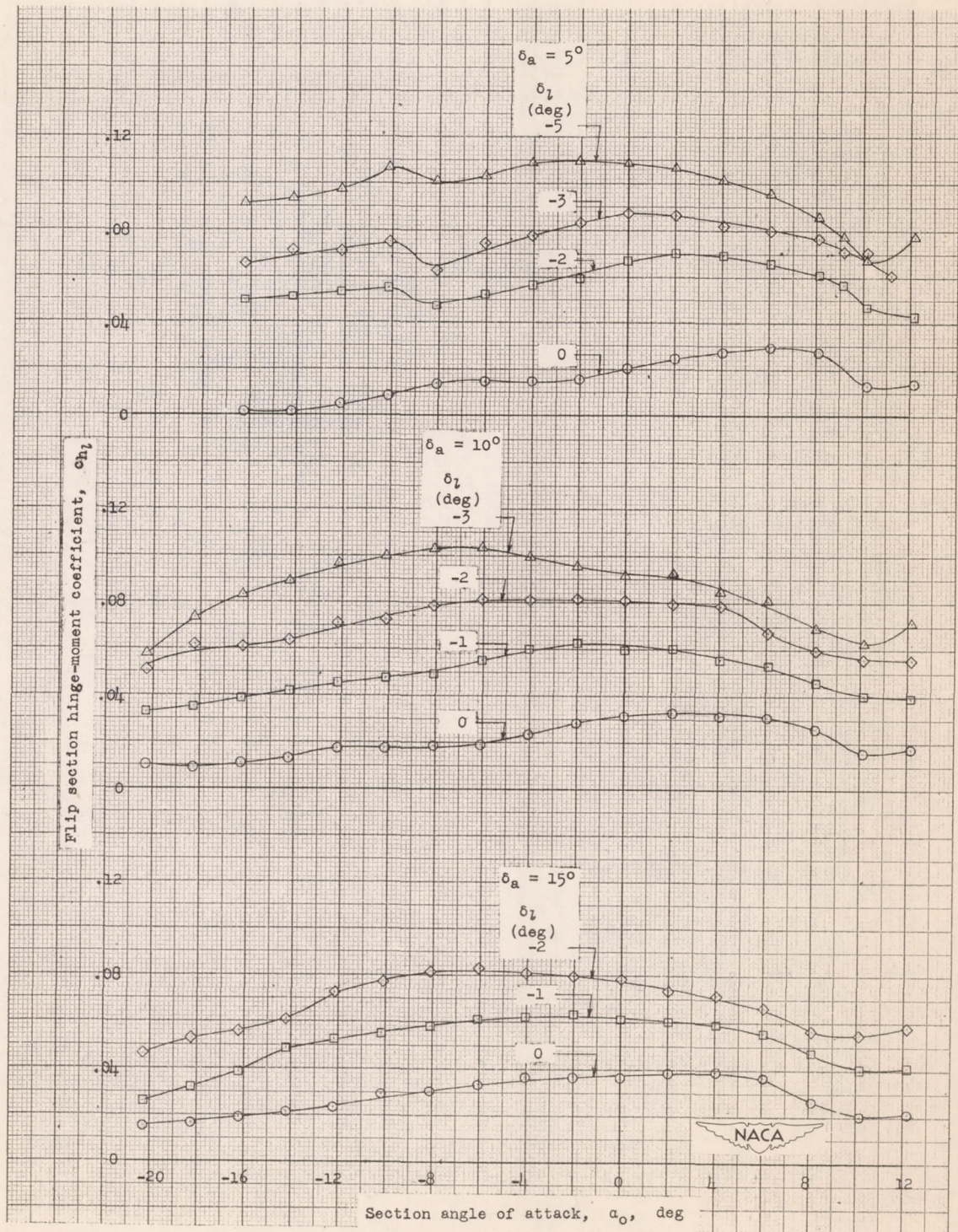
(h) $\delta_f = 40^\circ$.

Figure 10.- Concluded.



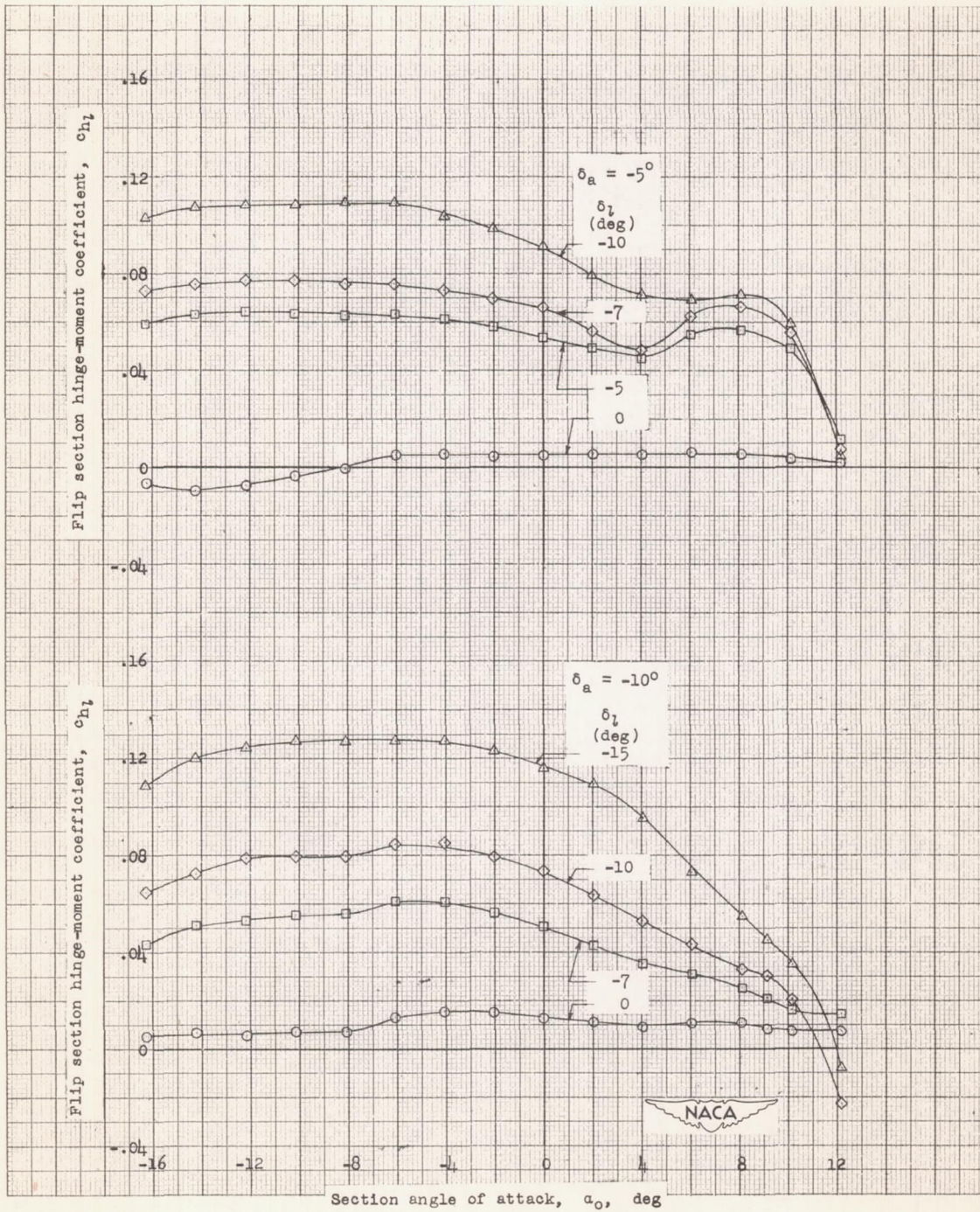
(a) $\delta_f = 25^\circ$.

Figure 11.- Hinge-moment characteristics of a flap on the approximately 17.7-percent-chord thick NACA 7-series-type airfoil with double slotted flap and straight-sided Frise aileron. Aileron balance, $0.351c_a$; $R = 6.0 \times 10^6$ (approx.)



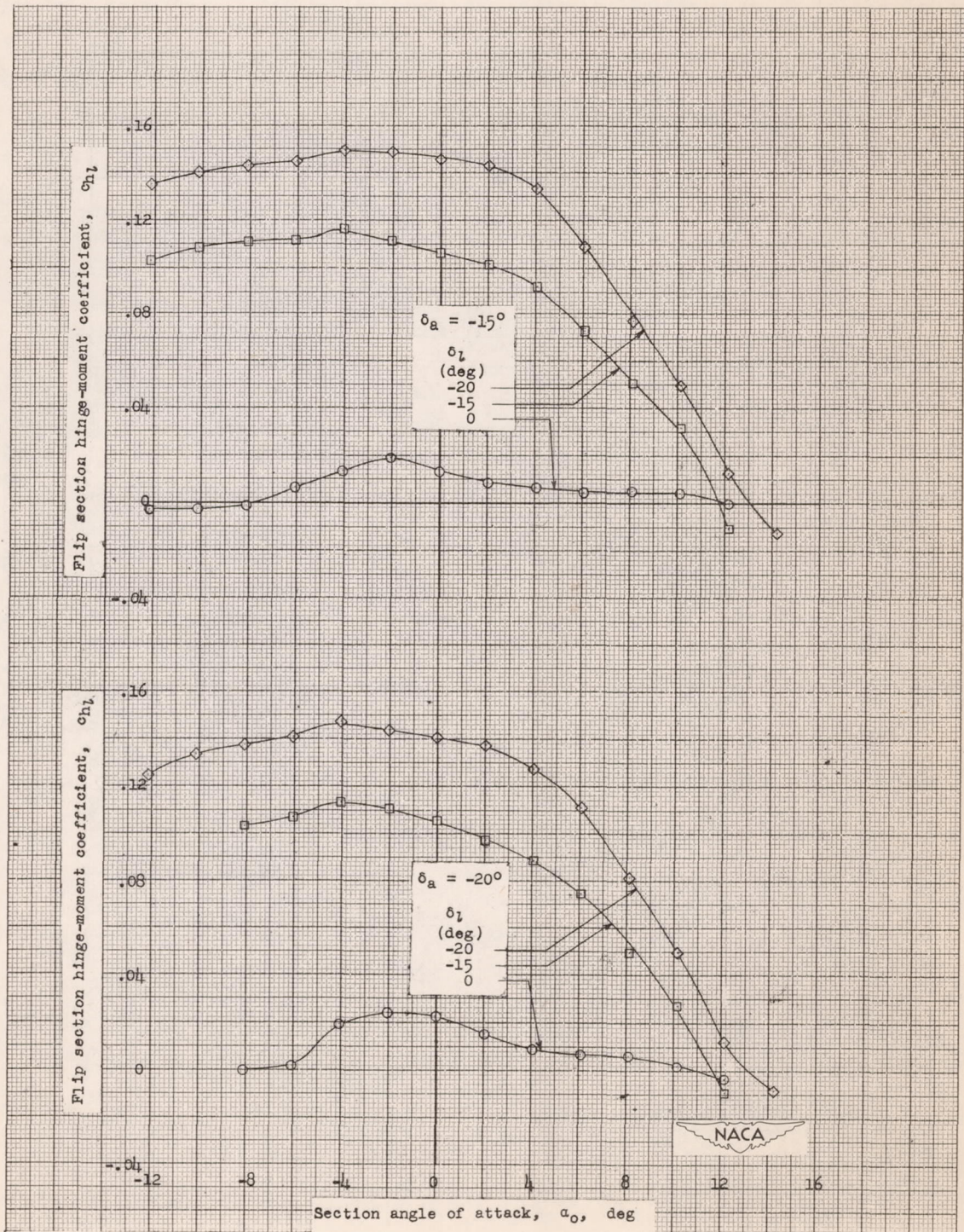
(b) $\delta_f = 25^\circ$.

Figure 11.- Continued.



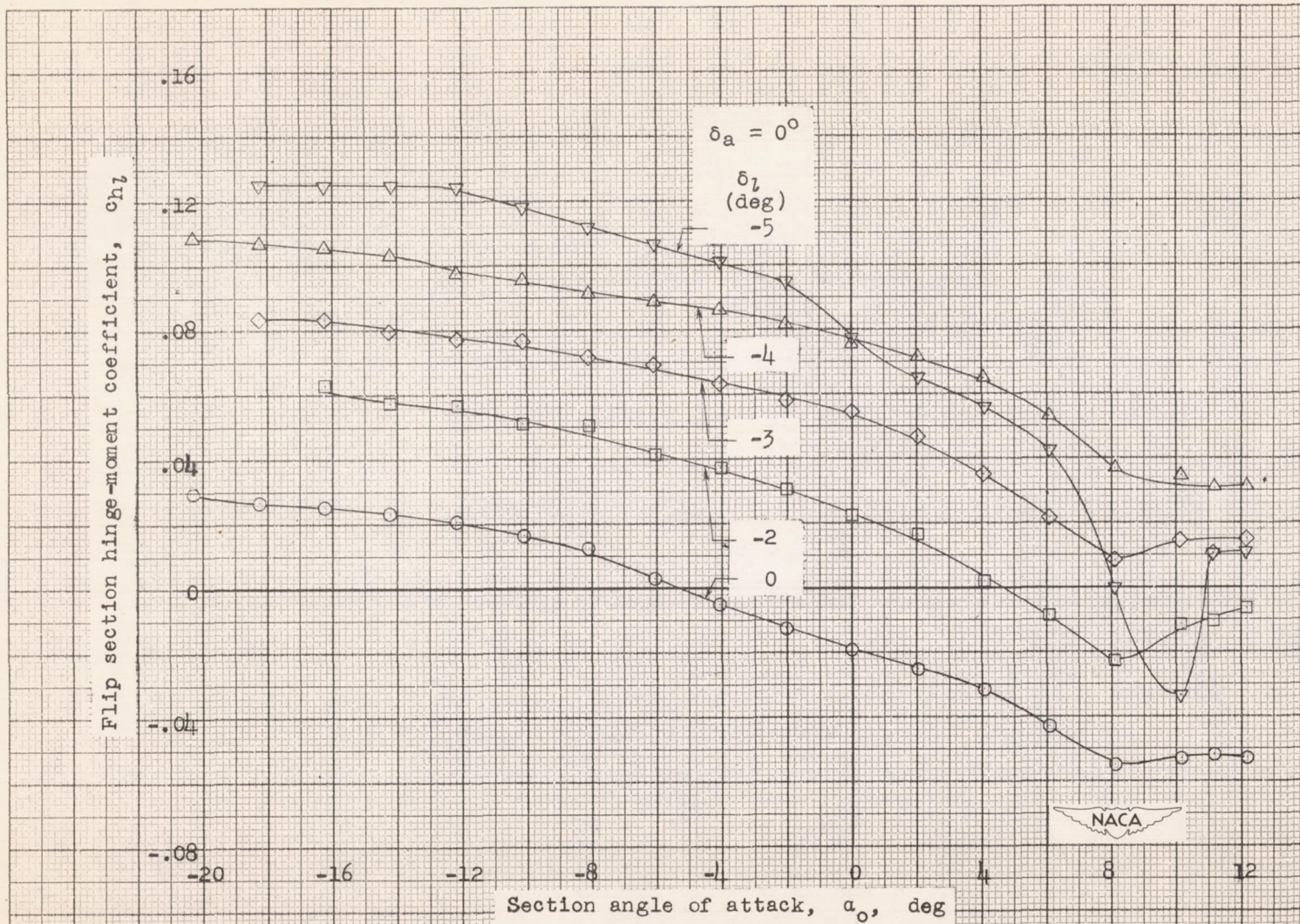
(c) $\delta_f = 25^\circ$.

Figure 11.- Continued.



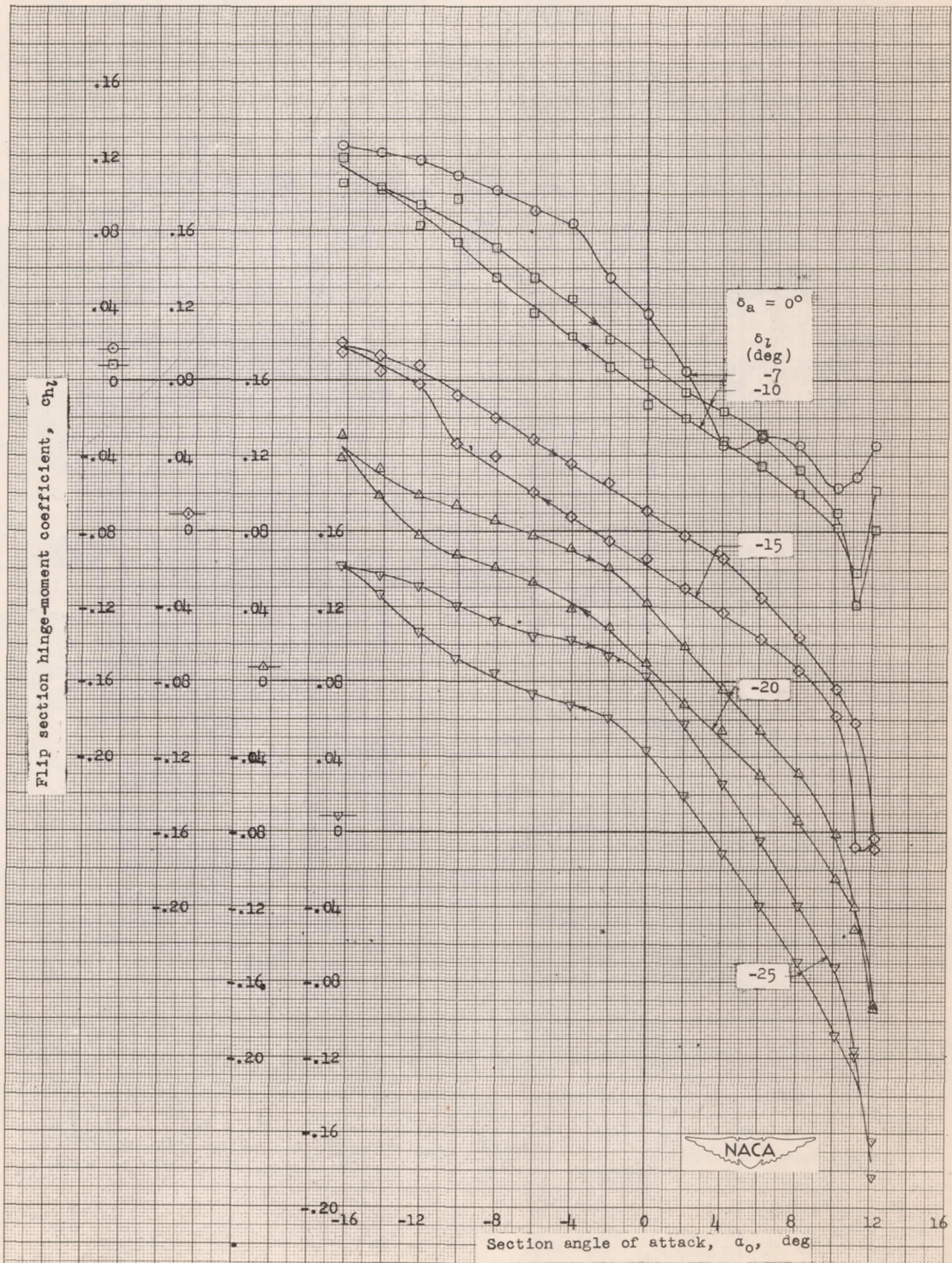
(d) $\delta_r = 25^\circ$.

Figure 11.- Continued.



(e) $\delta_f = 40^\circ$.

Figure 11.- Continued.



(f) $\delta_f = 40^\circ$.

Figure 11.- Continued.

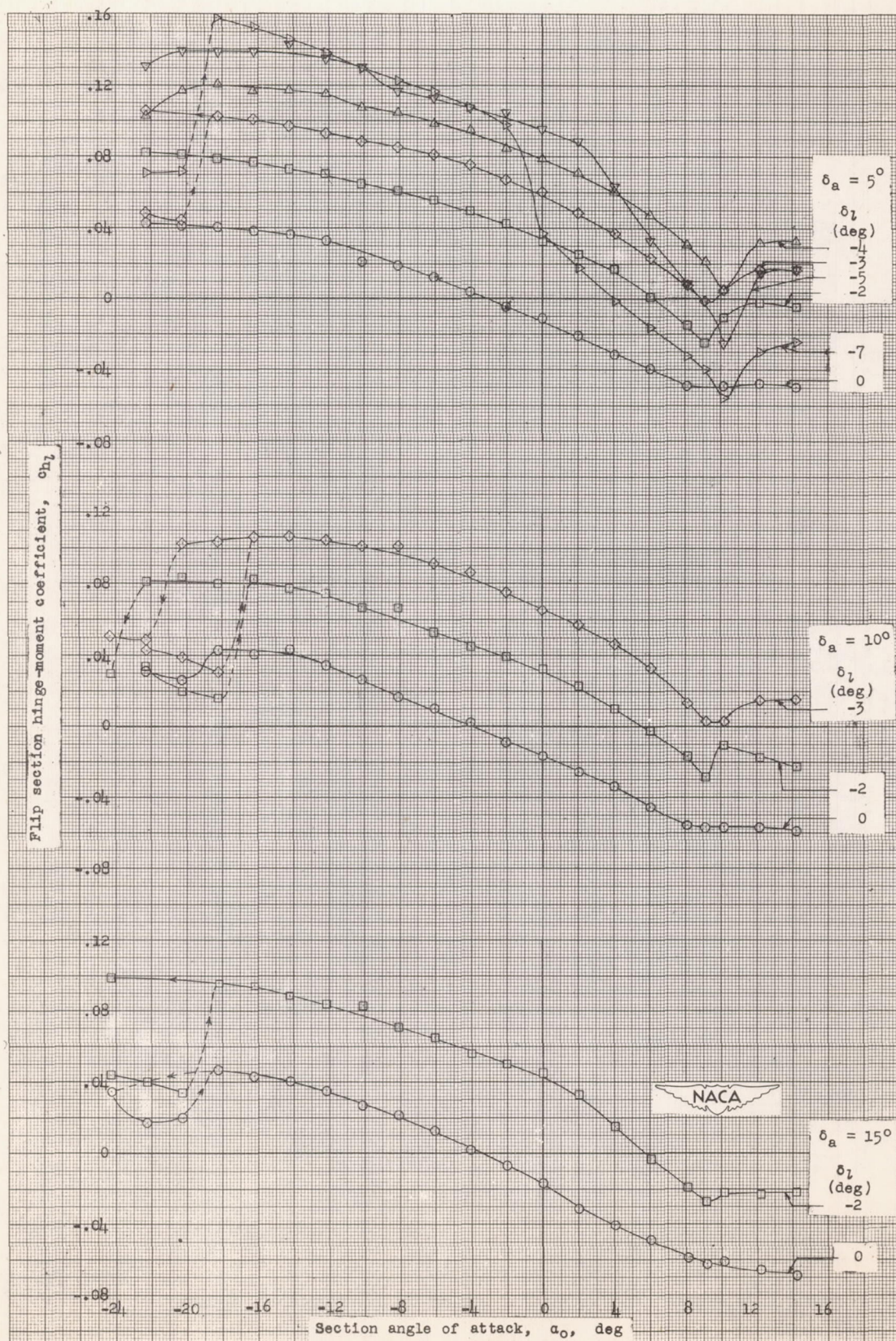
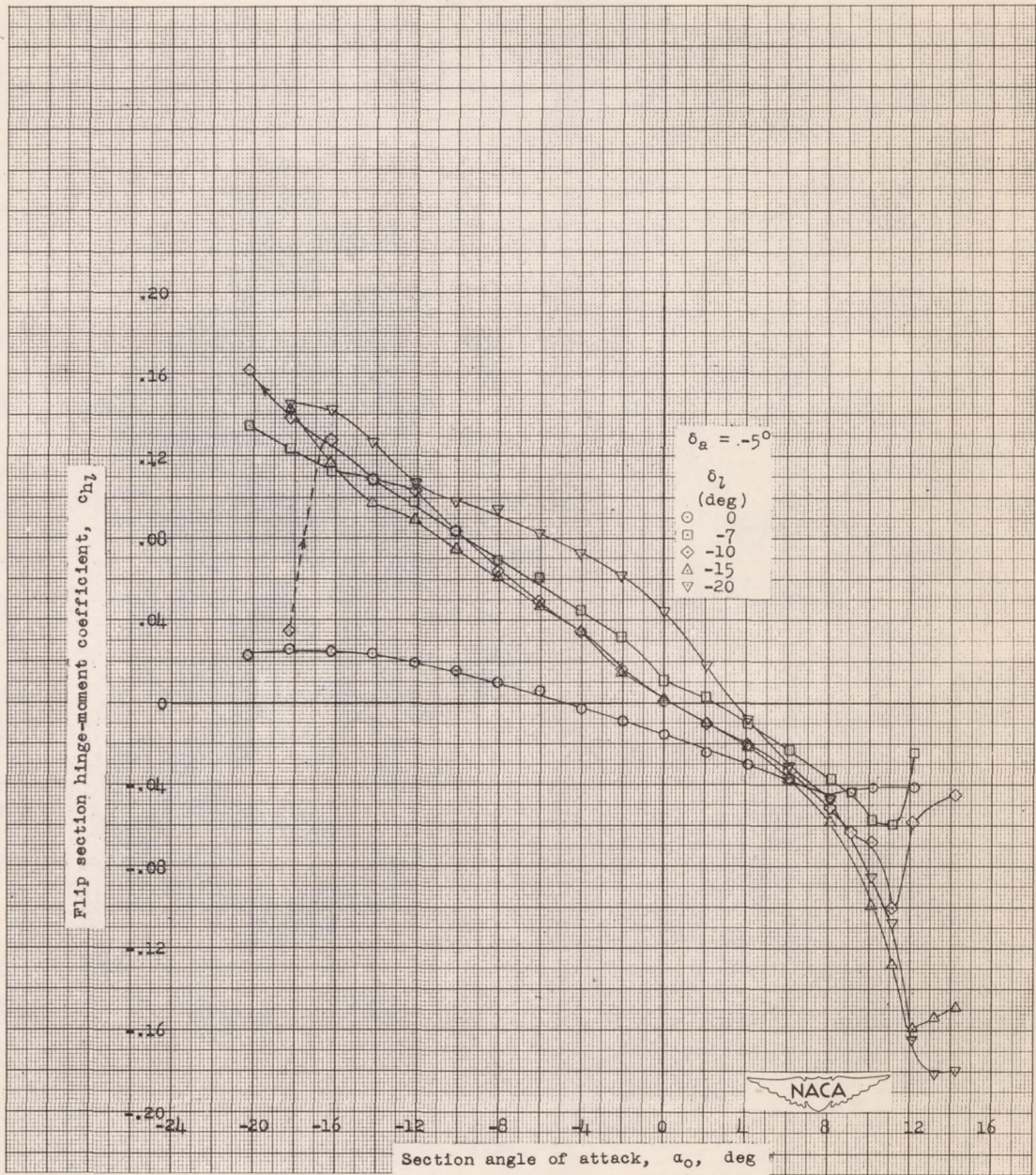
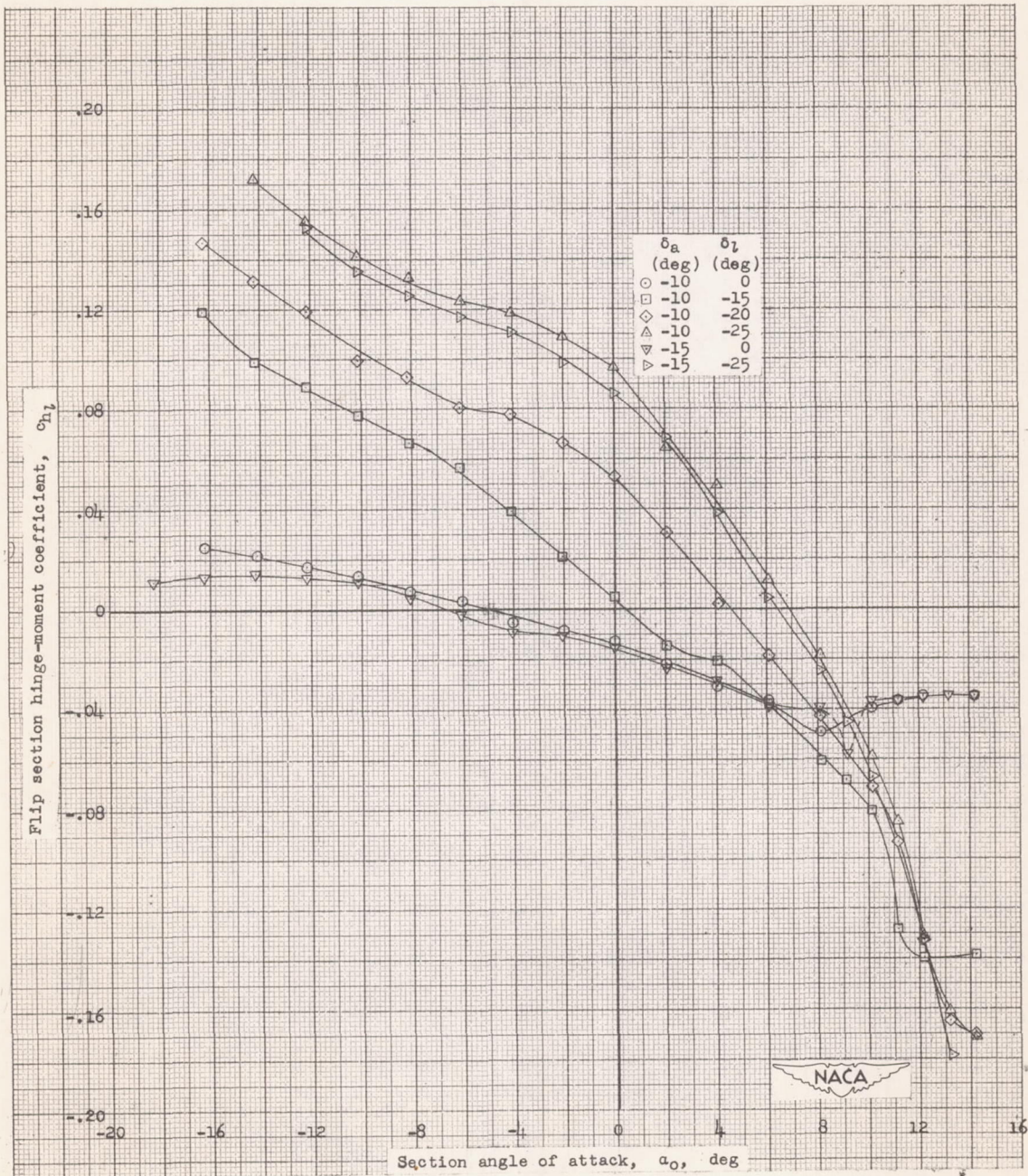


Figure 11.- Continued.



(h) $\delta_f = 40^\circ$.

Figure 11.- Continued.



(1) $\delta_f = 40^\circ$.

Figure 11.- Concluded.

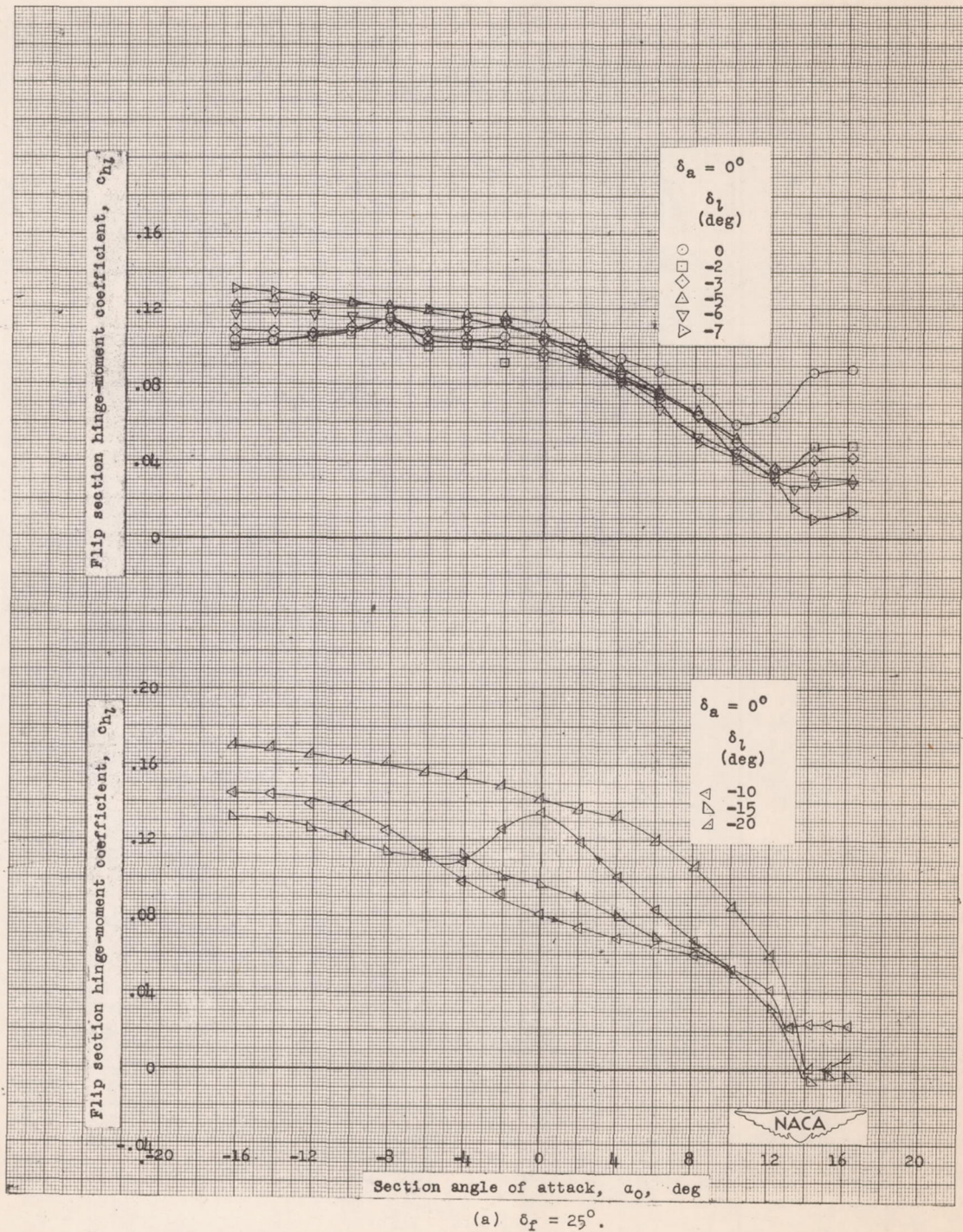
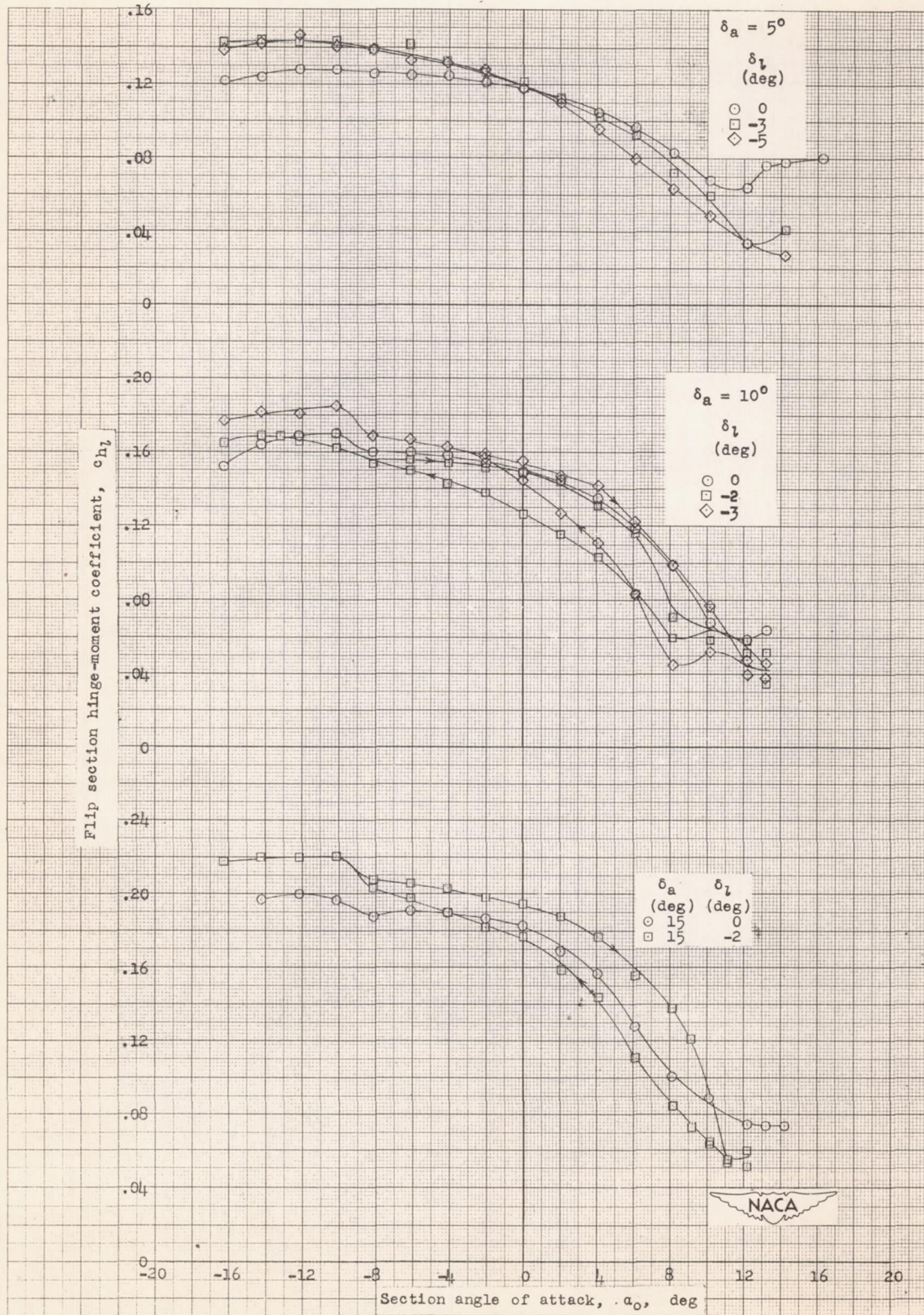
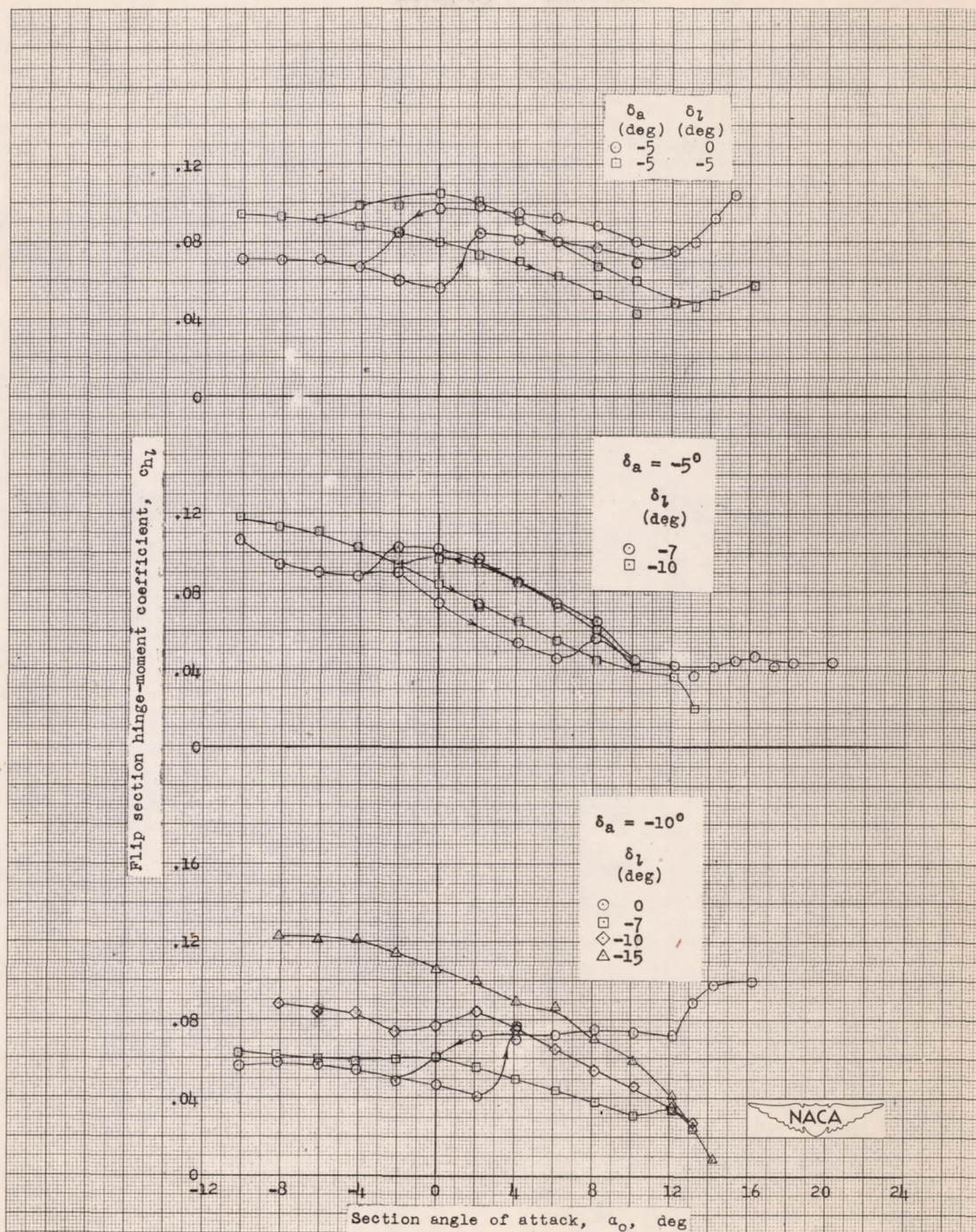


Figure 12.- Hinge-moment characteristics of a flip on the approximately 15.4-percent-chord thick NACA 7-series-type airfoil with double slotted flap and straight-sided Frise aileron. Aileron balance, $0.351c_a$; $R = 6 \times 10^6$ (approx.)



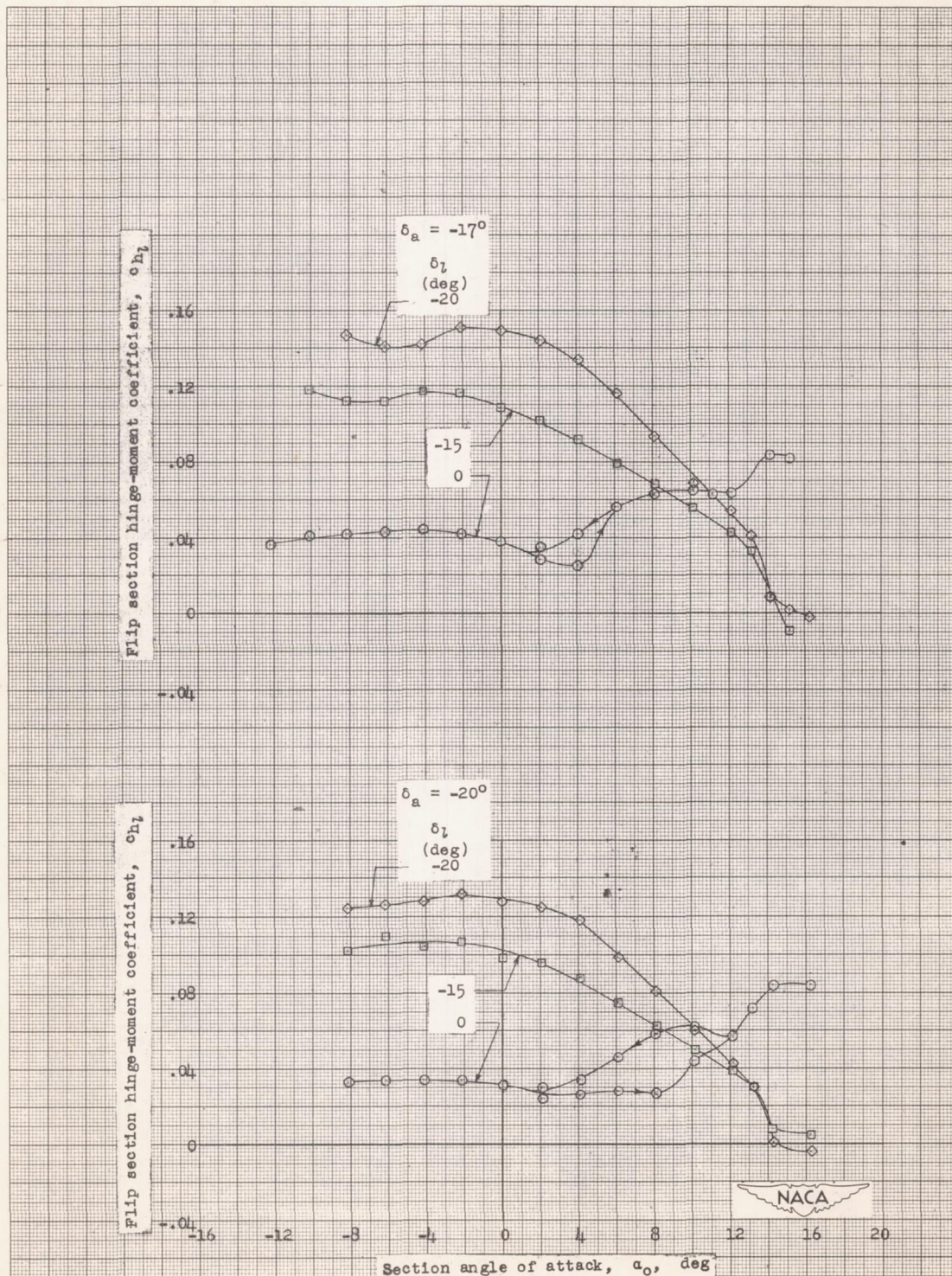
(b) $\delta_f = 25^\circ$.

Figure 12.- Continued.



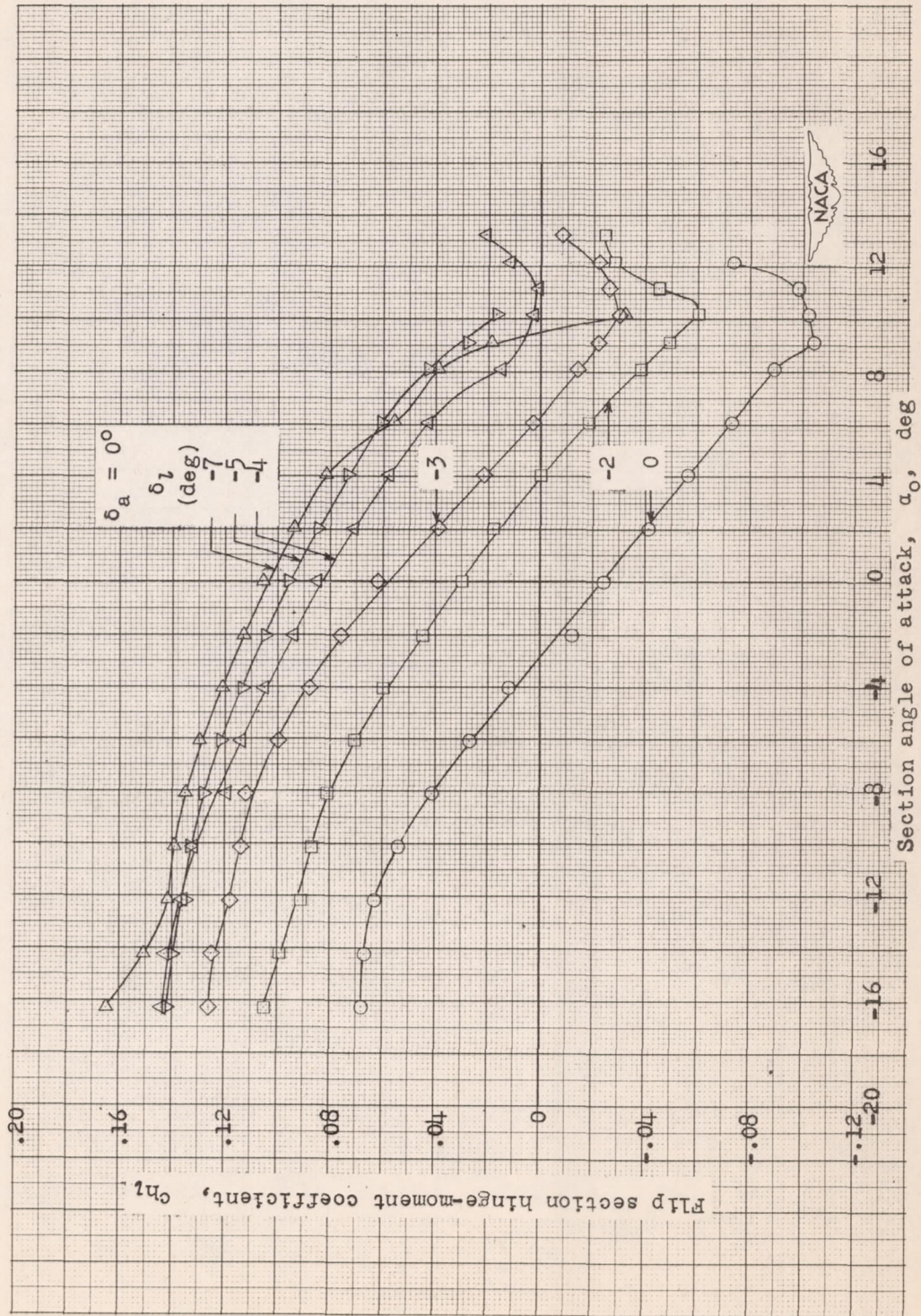
(c) $\delta_r = 25^\circ$.

Figure 12.- Continued.



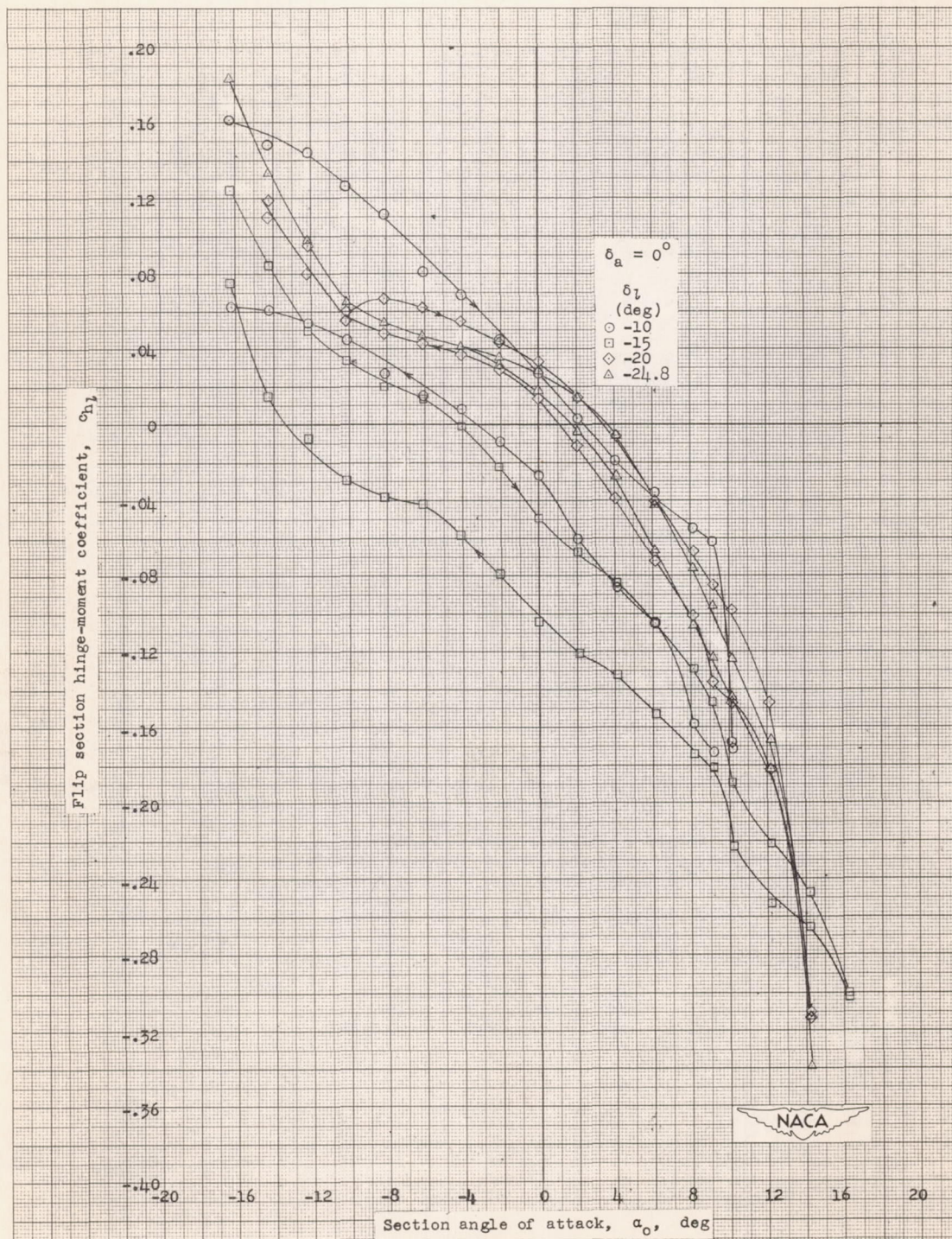
(d) $\delta_f = 25^\circ$.

Figure 12.- Continued.



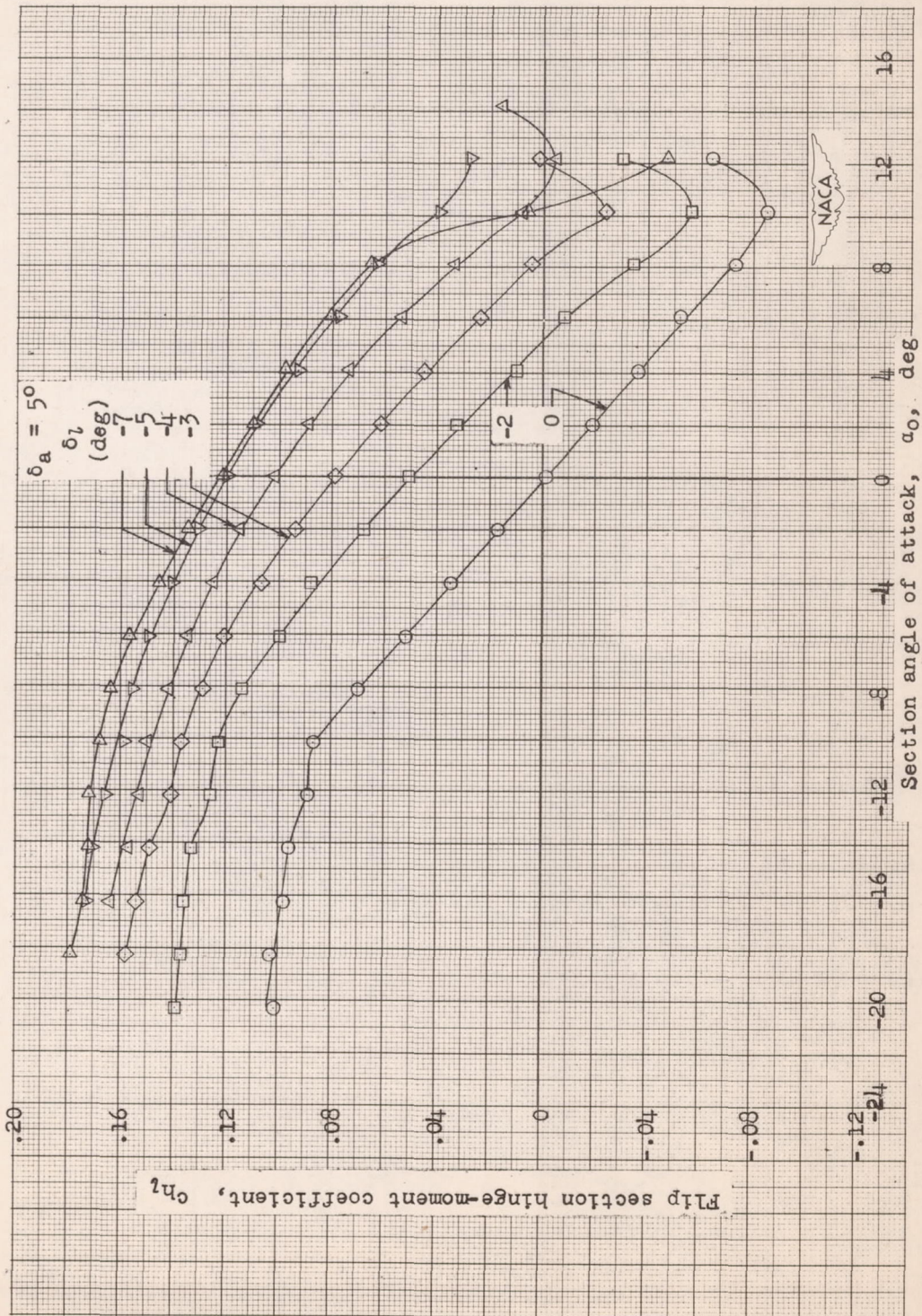
(e) $\delta_f = 40^\circ$.

Figure 12.- Continued.

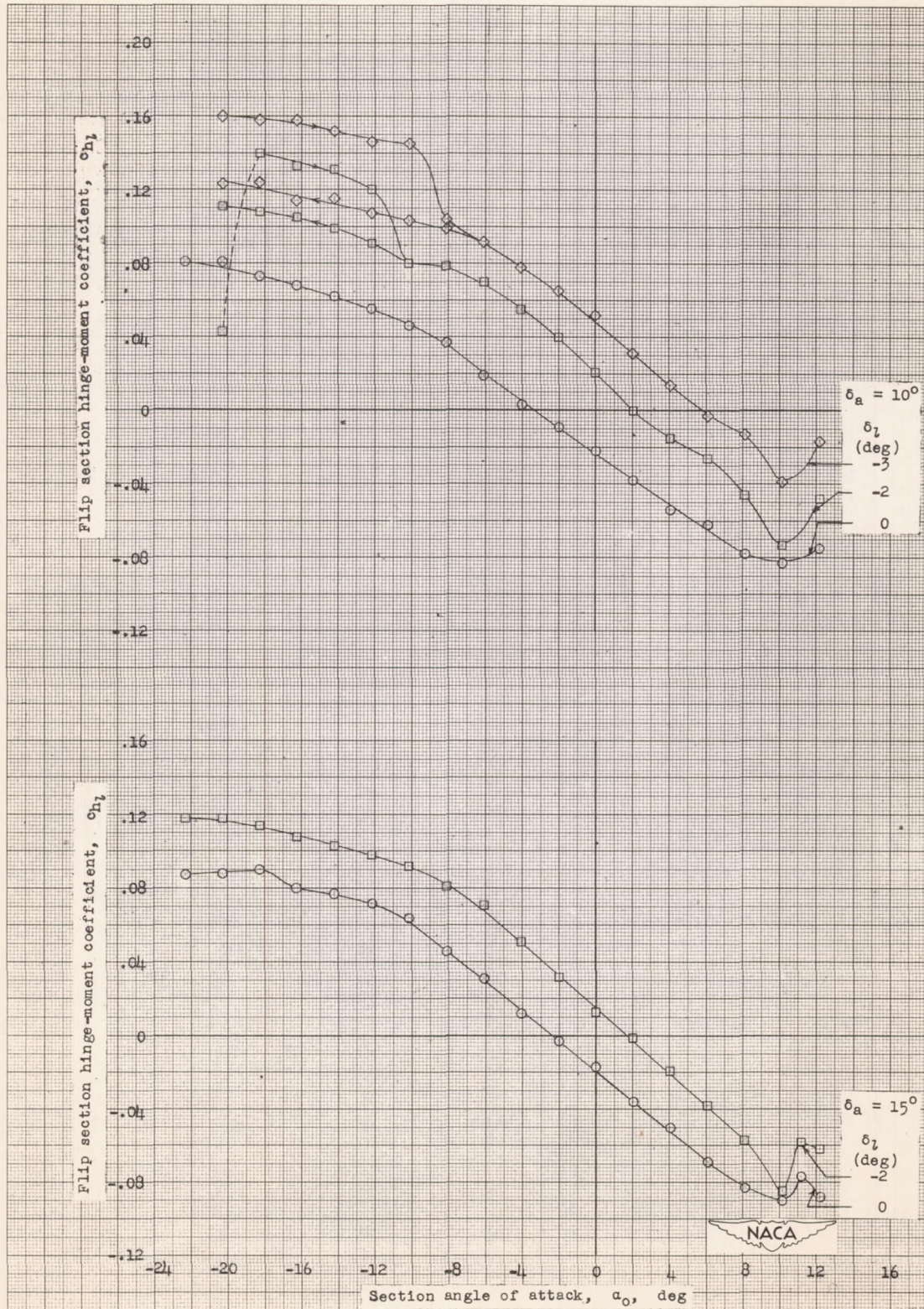


(f) $\delta_f = 40^\circ$.

Figure 12.- Continued.

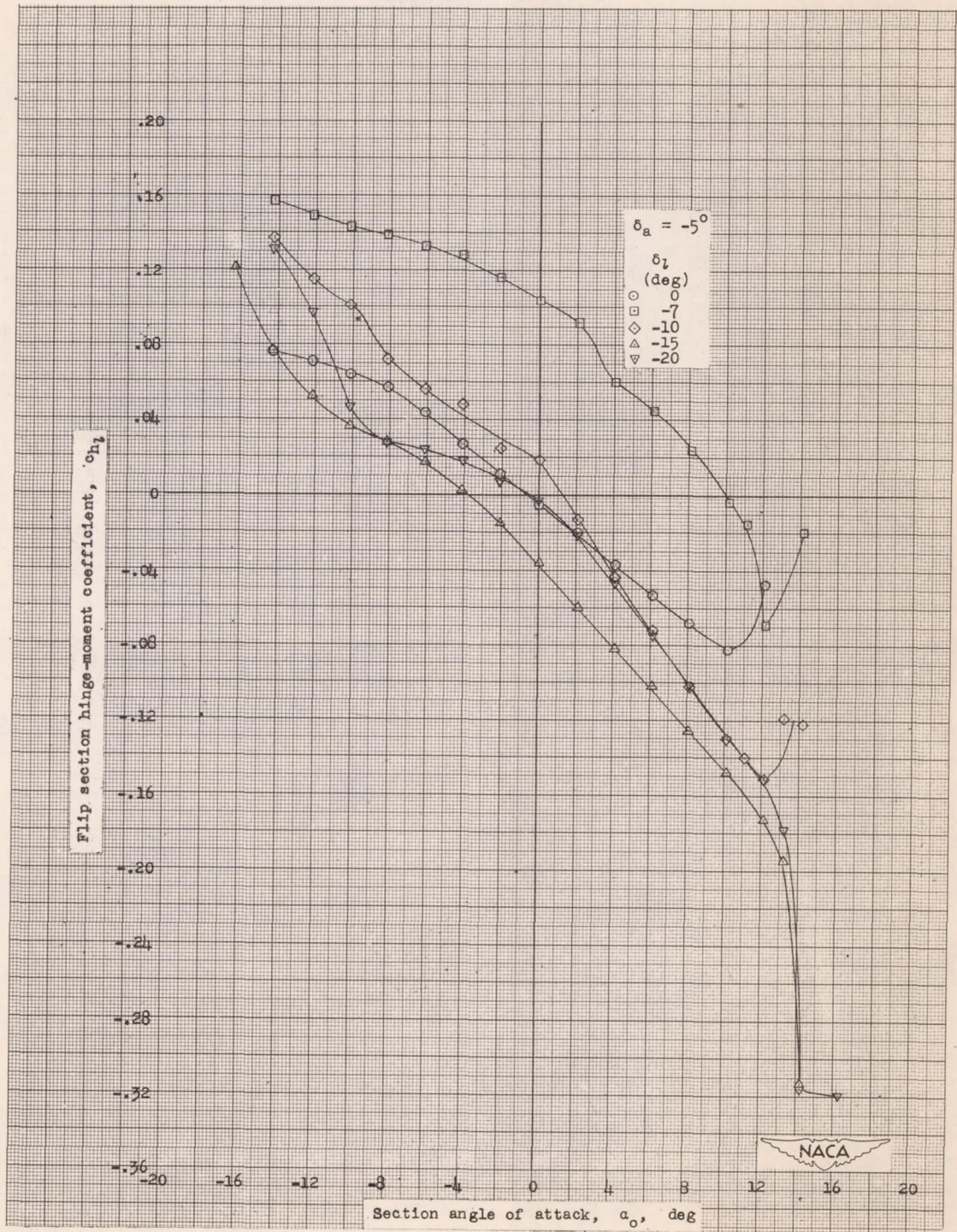


(g) $\delta_f = 40^\circ$
 Figure 12.- Continued.



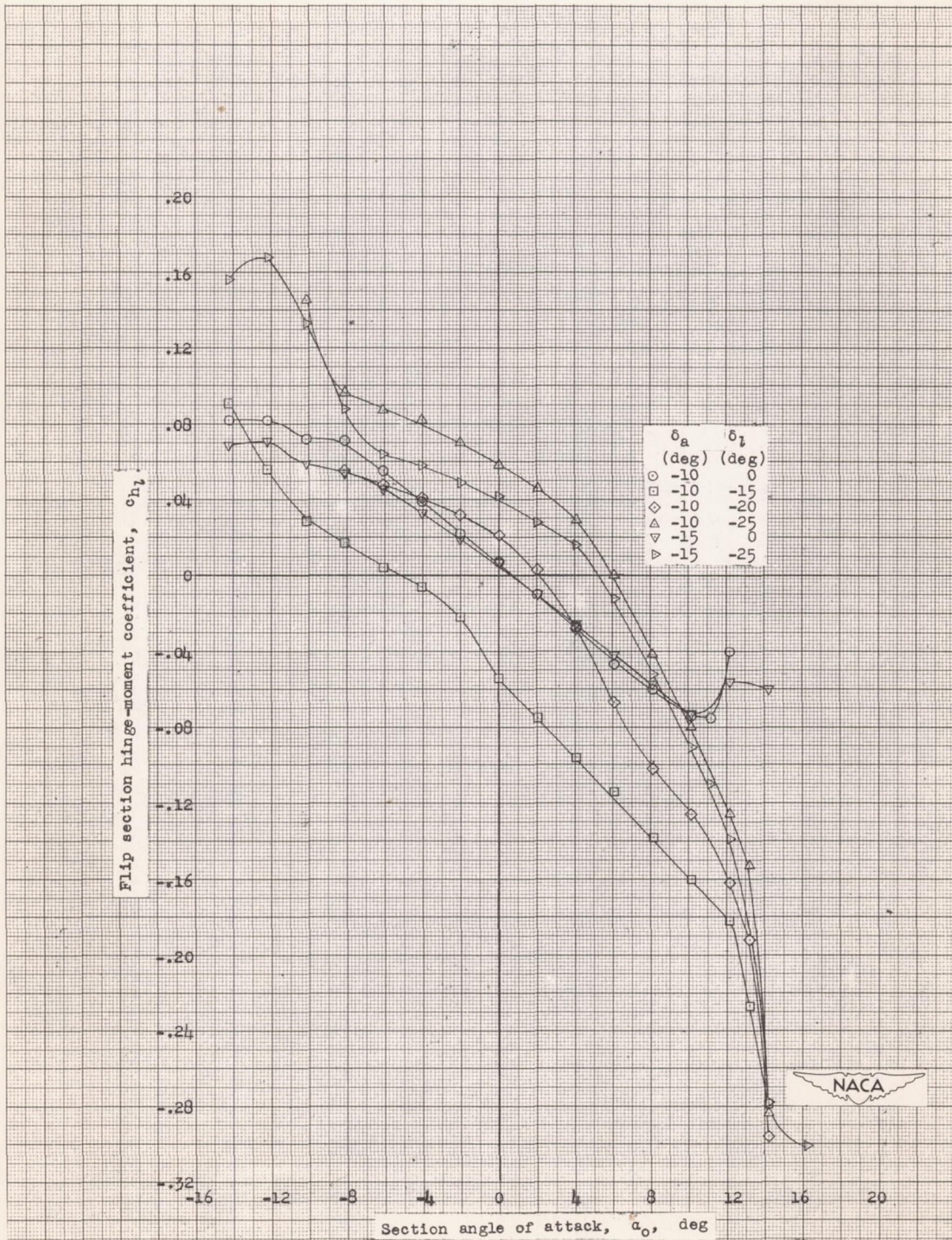
(h) $\delta_f = 40^\circ$.

Figure 12.- Continued.



(1) $\delta_f = 40^\circ$.

Figure 12.- Continued.



(j) $\delta_r = 40^\circ$

Figure 12.- Concluded.

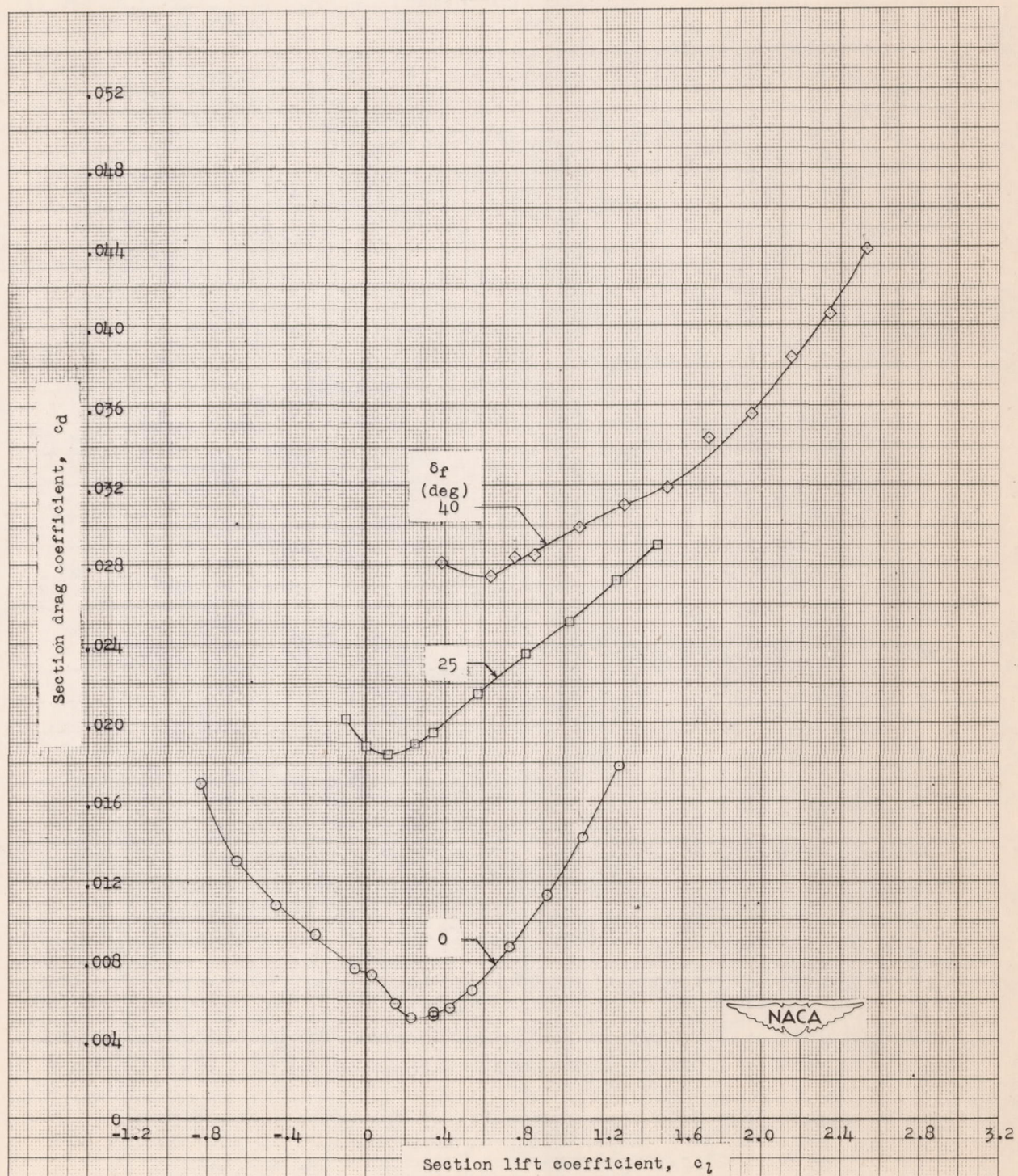


Figure 13.- Drag characteristics of the approximately 17.7 percent-chord thick NACA 7-series-type airfoil with double slotted flap, straight-sided Frise alleron, and flap. $R = 6 \times 10^6$ (approx.); $\delta_a = 0^\circ$, $\delta_l = 0^\circ$.

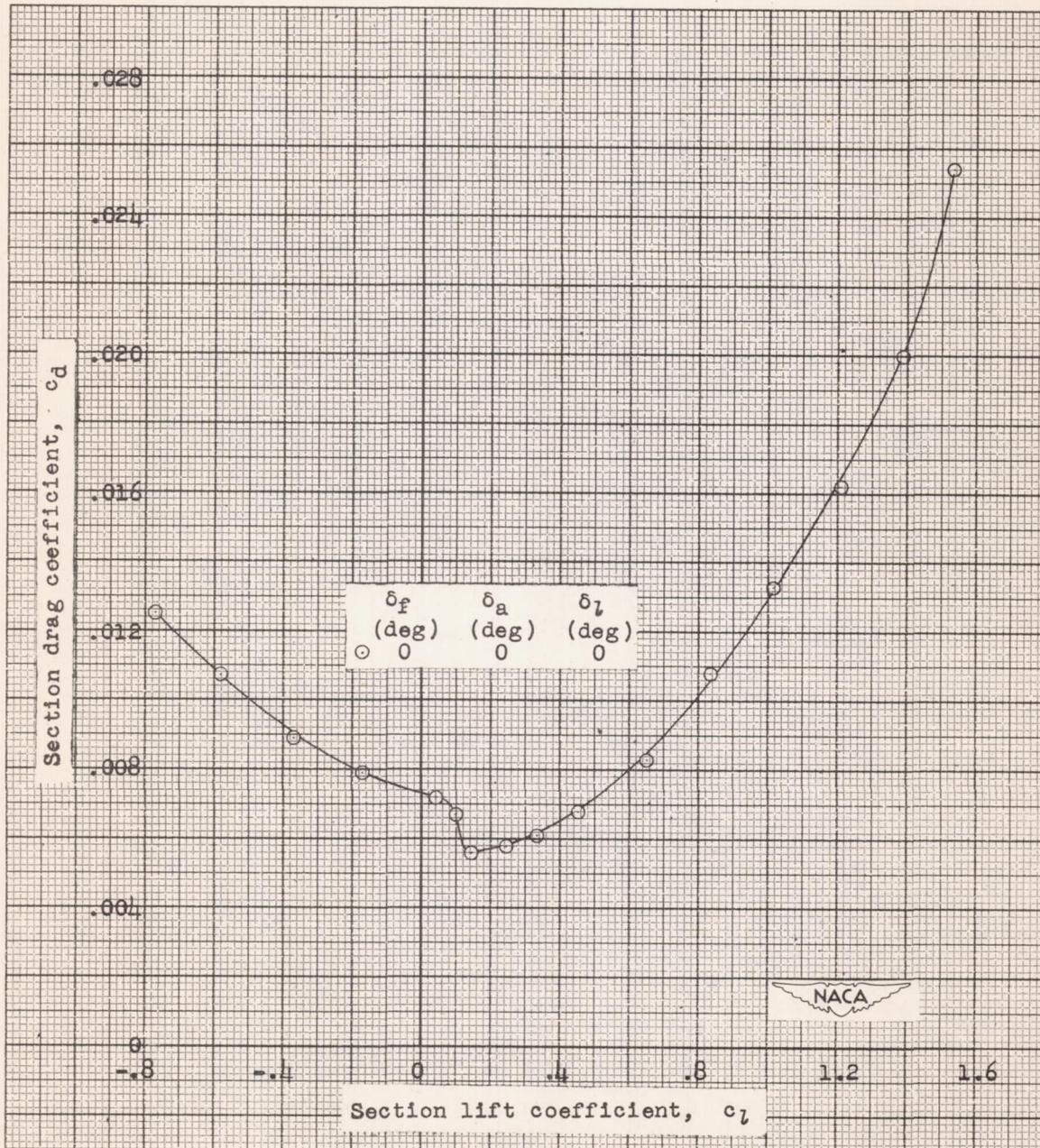


Figure 14.- Drag characteristics of the approximately 15.4-percent-chord thick NACA 7-series-type airfoil with double slotted flap, straight-sided Frise aileron, and flap.

$R = 6 \times 10^6$ (approx.).

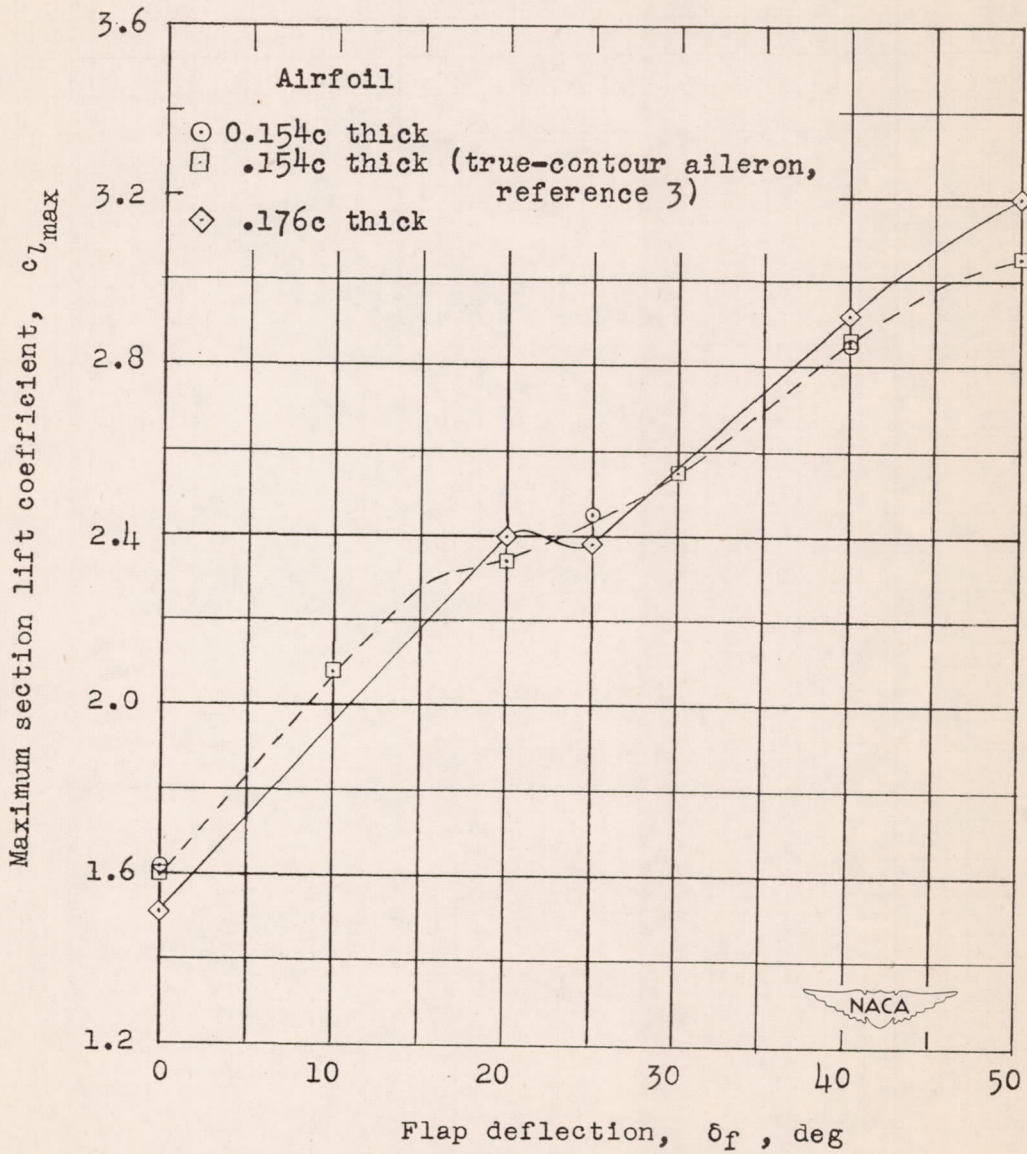
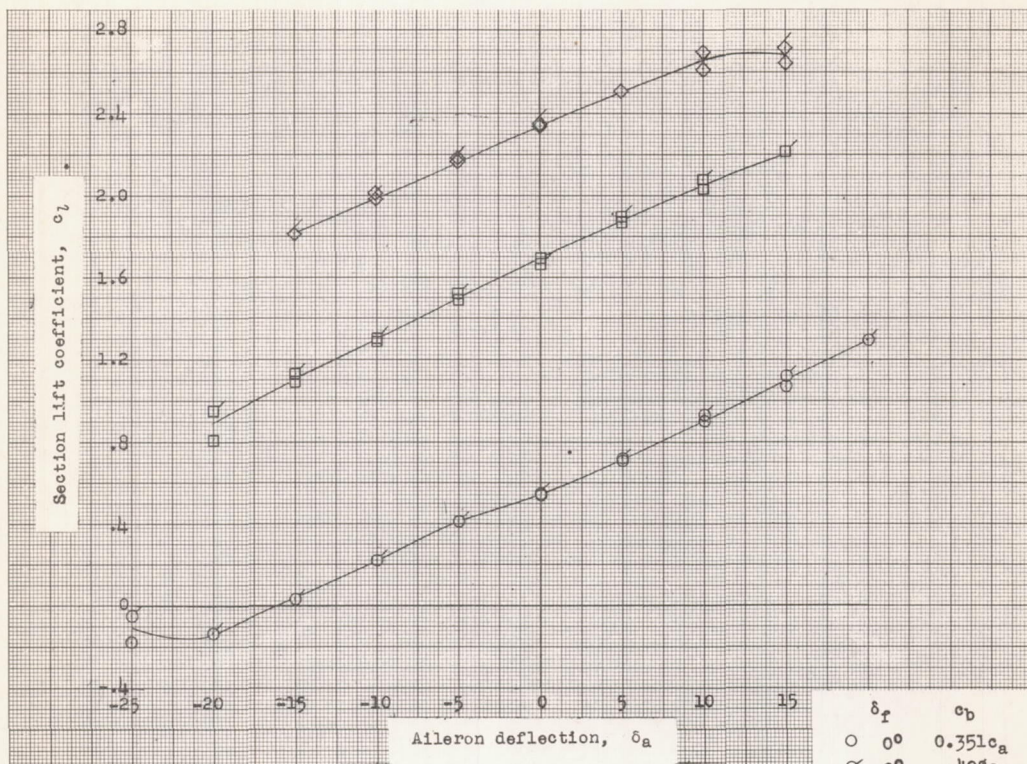
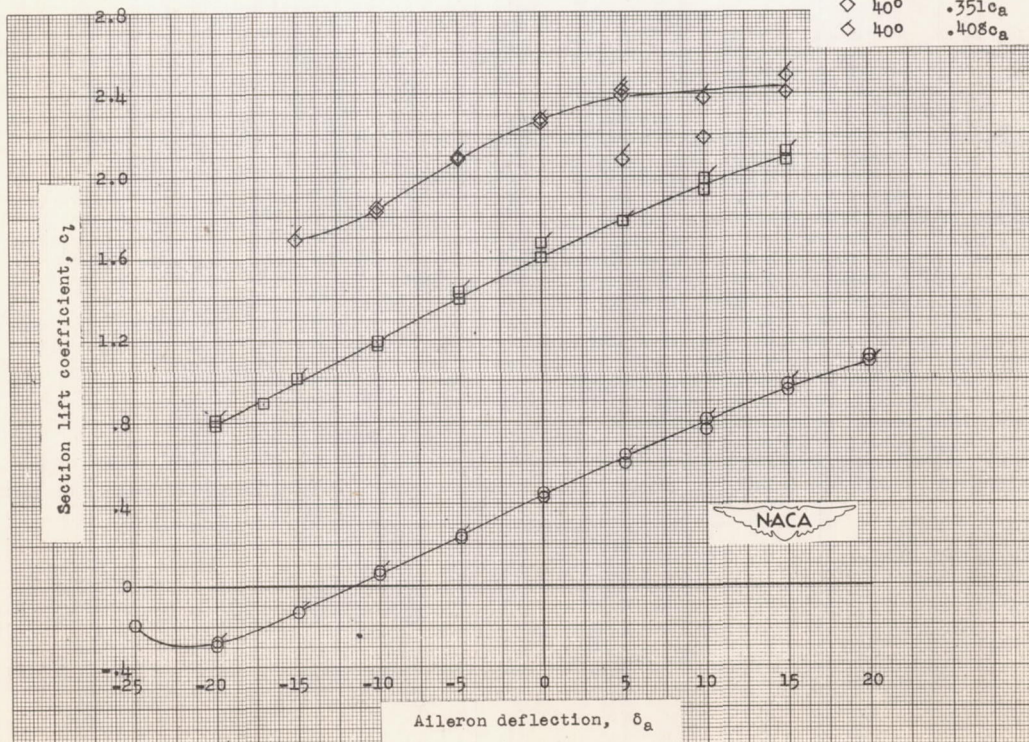


Figure 15.- Maximum lift characteristics of the NACA 7-series-type airfoils with double slotted flap, straight-sided Frise aileron, and flap. $R = 6 \times 10^6$ (approx.); $\delta_a = 0^\circ$; $\delta_l = 0^\circ$; $c_b = 0.408c_a$.



(a) 0.177c thick airfoil.



(b) 0.154c thick airfoil.

Figure 16.- Variation of section lift characteristics with deflection of straight-sided Frise aileron on two NACA 7-series-type airfoils with double slotted flap and flap. $\alpha_0 = 0^\circ$; $\delta_1 = 0^\circ$; $R = 6.0 \times 10^6$ (approx.).

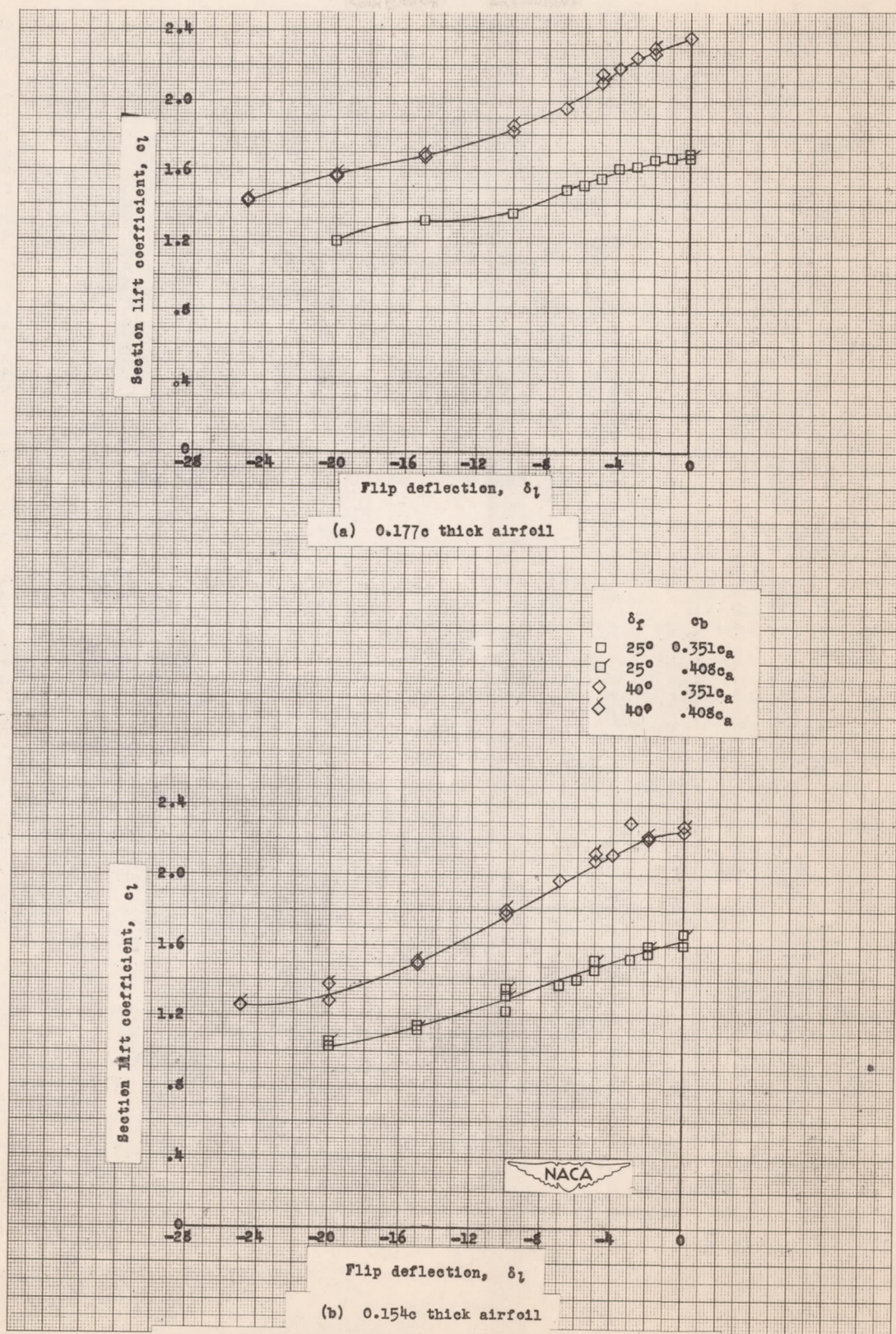
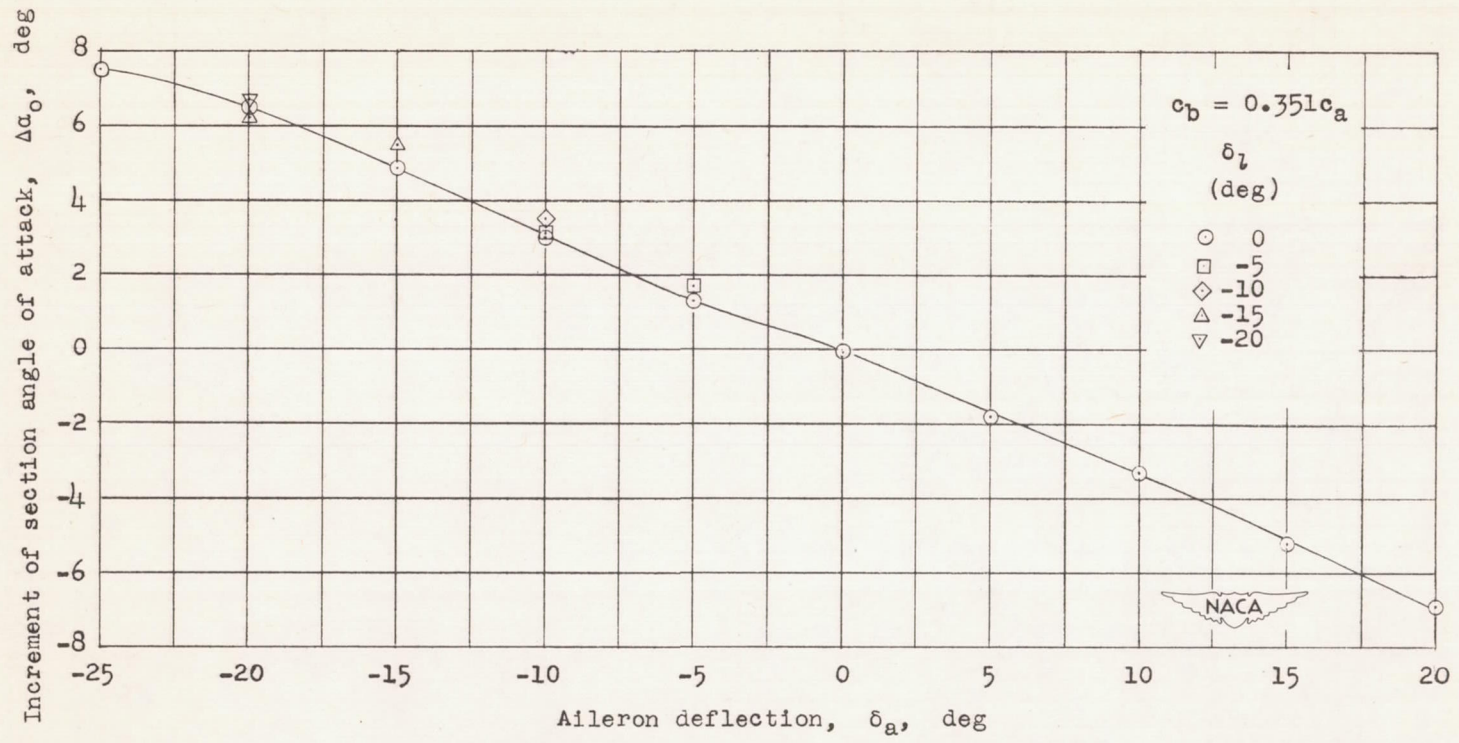


Figure 17.- Variation of section lift characteristics with flip deflection on two NACA 7-series-type airfoils with double slotted flap and straight-slided Frise aileron.
 $\alpha_0 = 0^\circ$; $\delta_a = 0^\circ$; $R = 6.0 \times 10^6$ (approx.)



(a) 0.177c thick airfoil; $\delta_f = 0^\circ$; $c_l = 0.4$.

Figure 18.- Lift effectiveness of the straight-sided Frise ailerons and flaps on the NACA 7-series-type airfoils with double slotted flaps. $R = 6 \times 10^6$ (approx.).

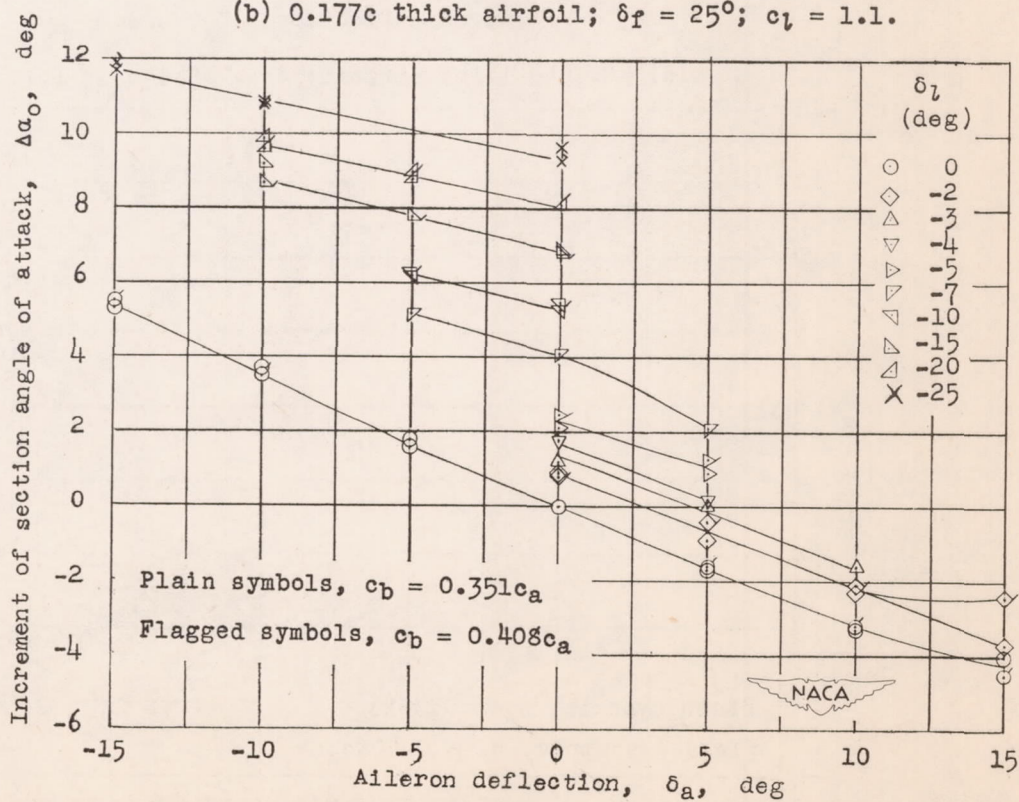
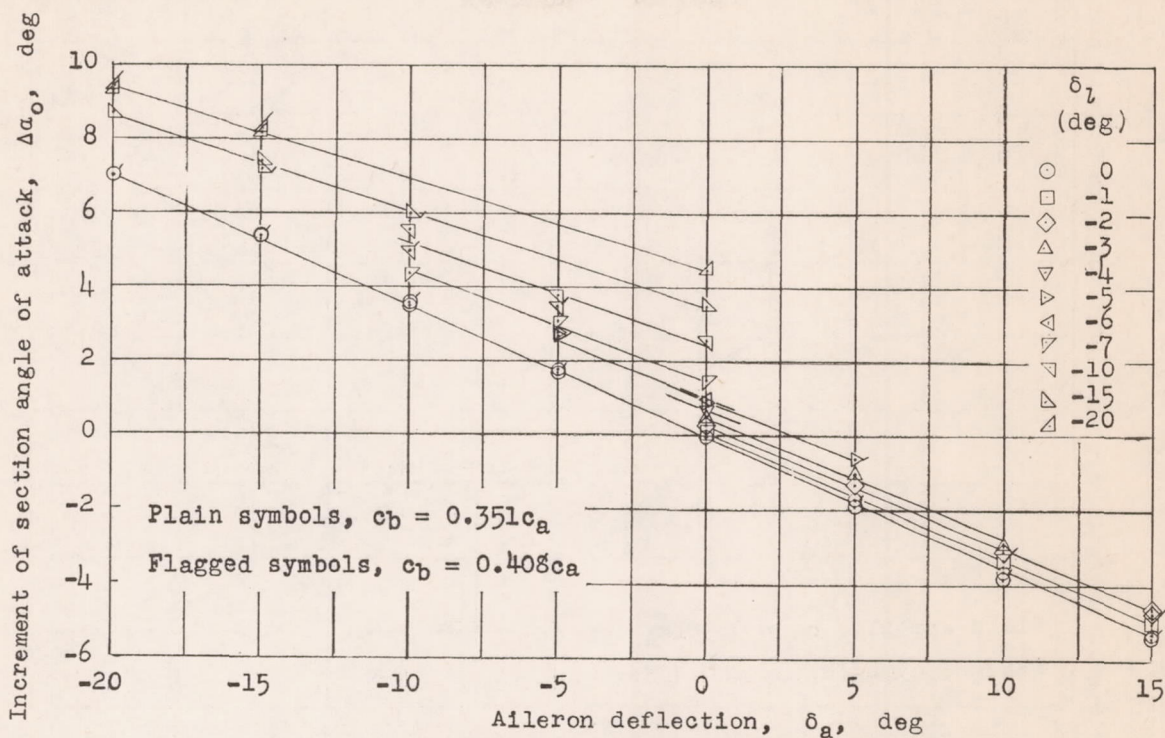
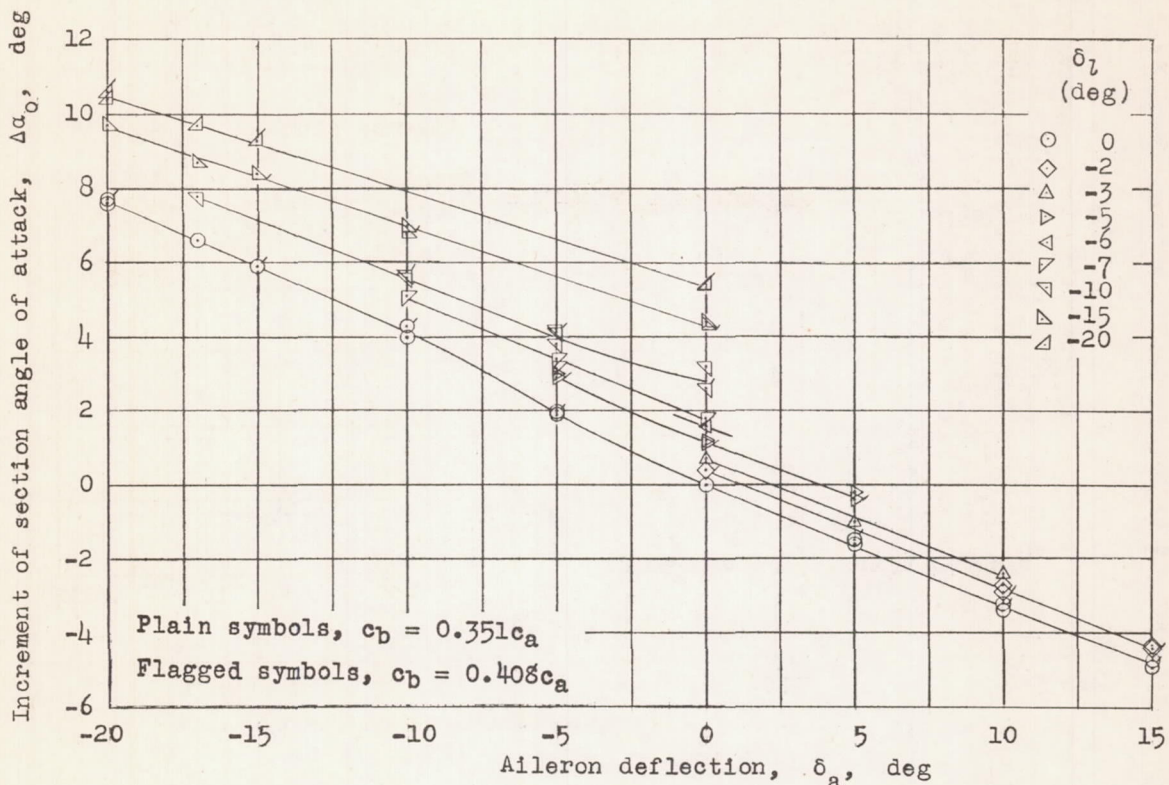
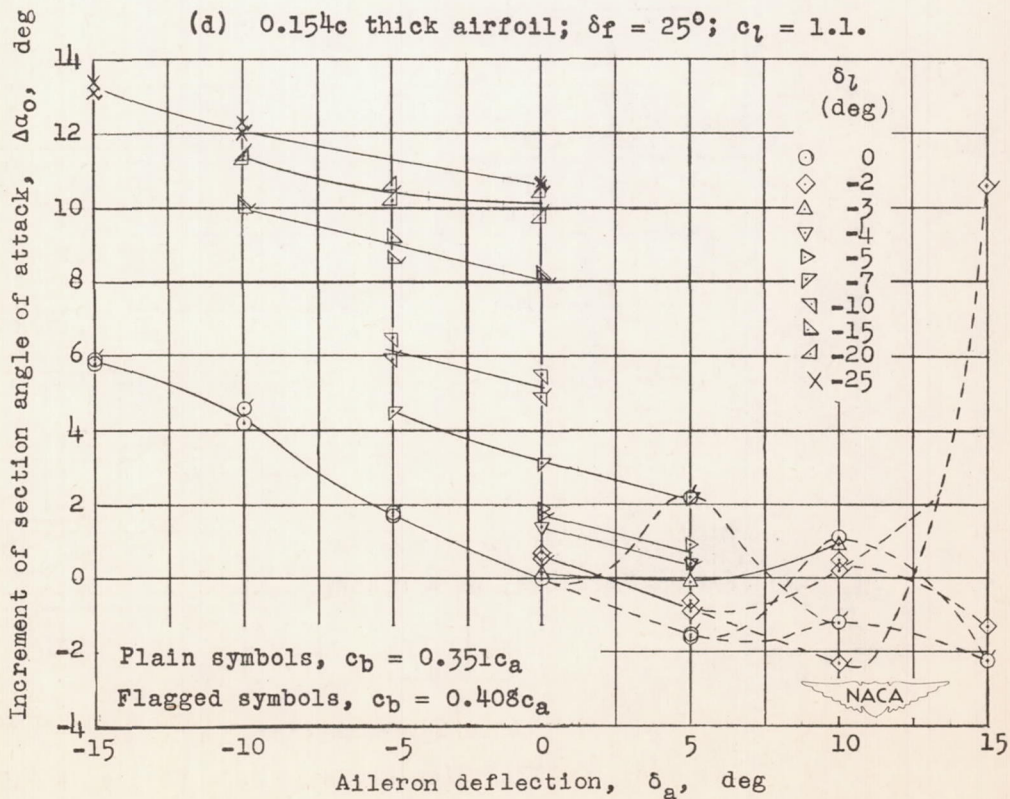


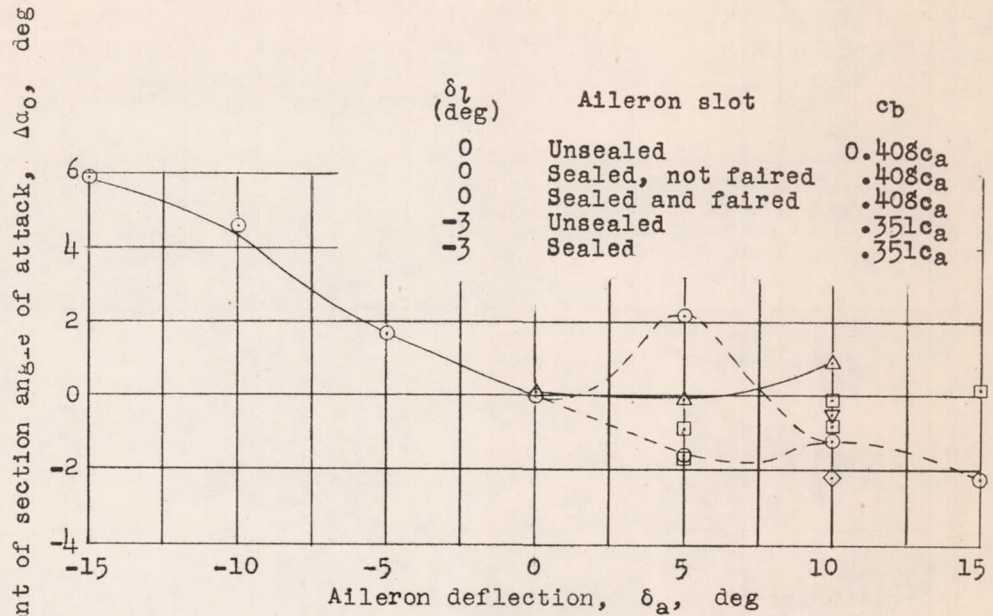
Figure 18.- Continued.



(d) 0.154c thick airfoil; $\delta_f = 25^\circ$; $c_l = 1.1$.



(e) 0.154c thick airfoil; $\delta_f = 40^\circ$; $c_l = 2.0$.



(f) 0.154c thick airfoil; $\delta_f = 40^\circ$; $c_l = 2.0$.

Figure 18.- Concluded.

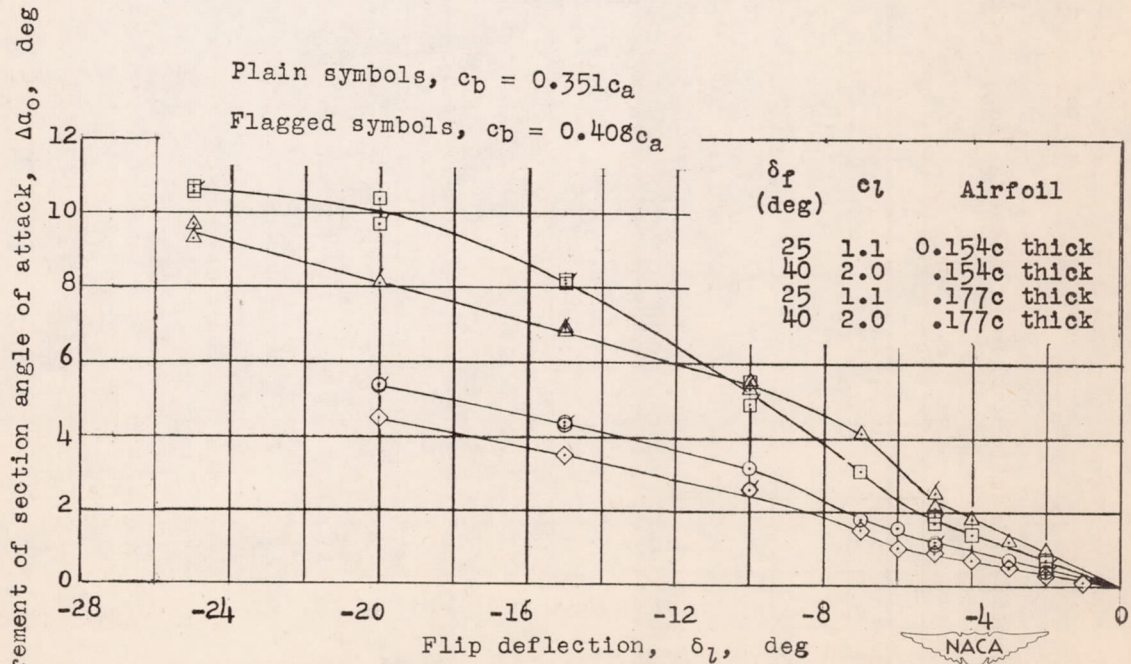
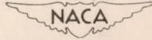
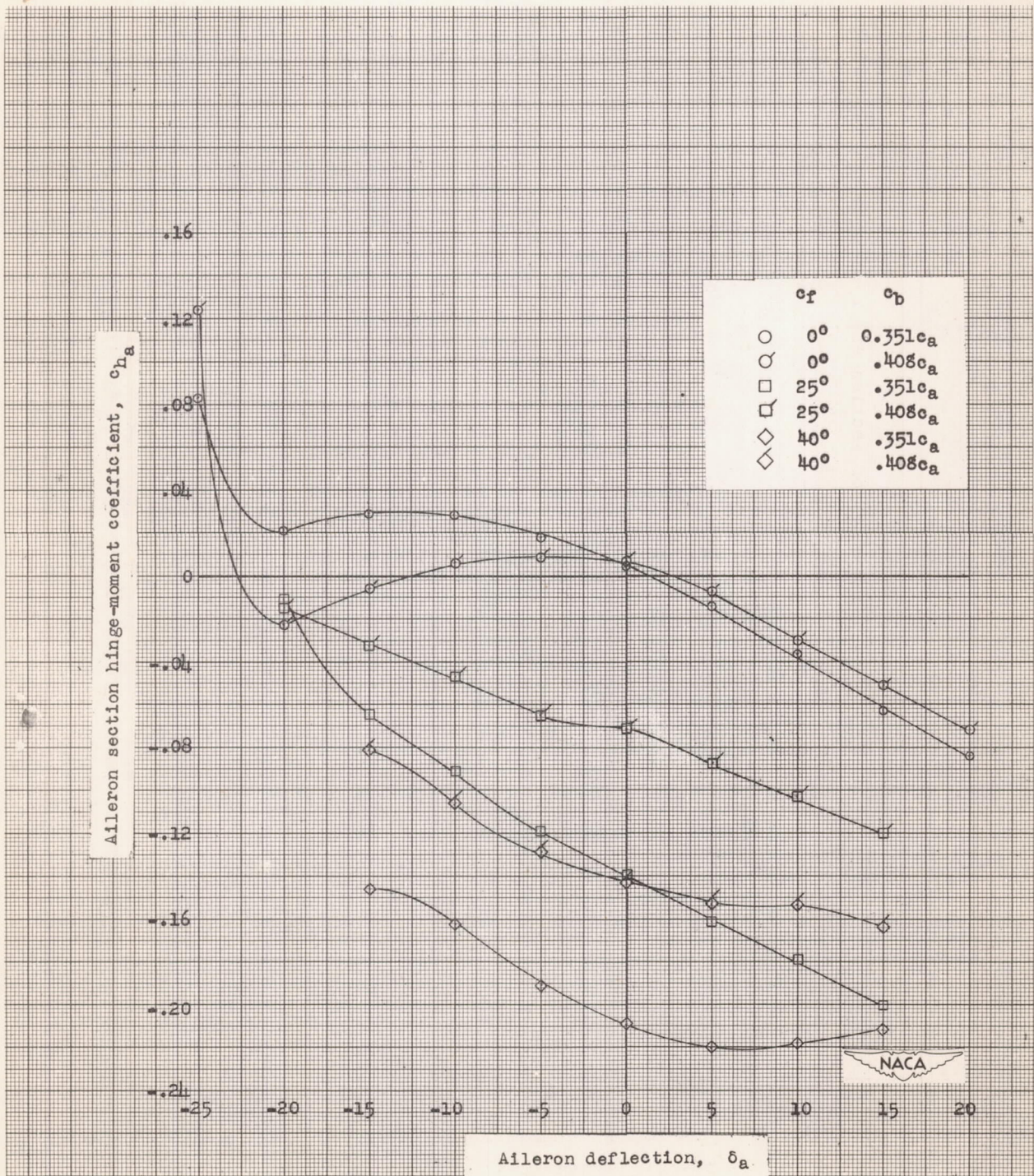


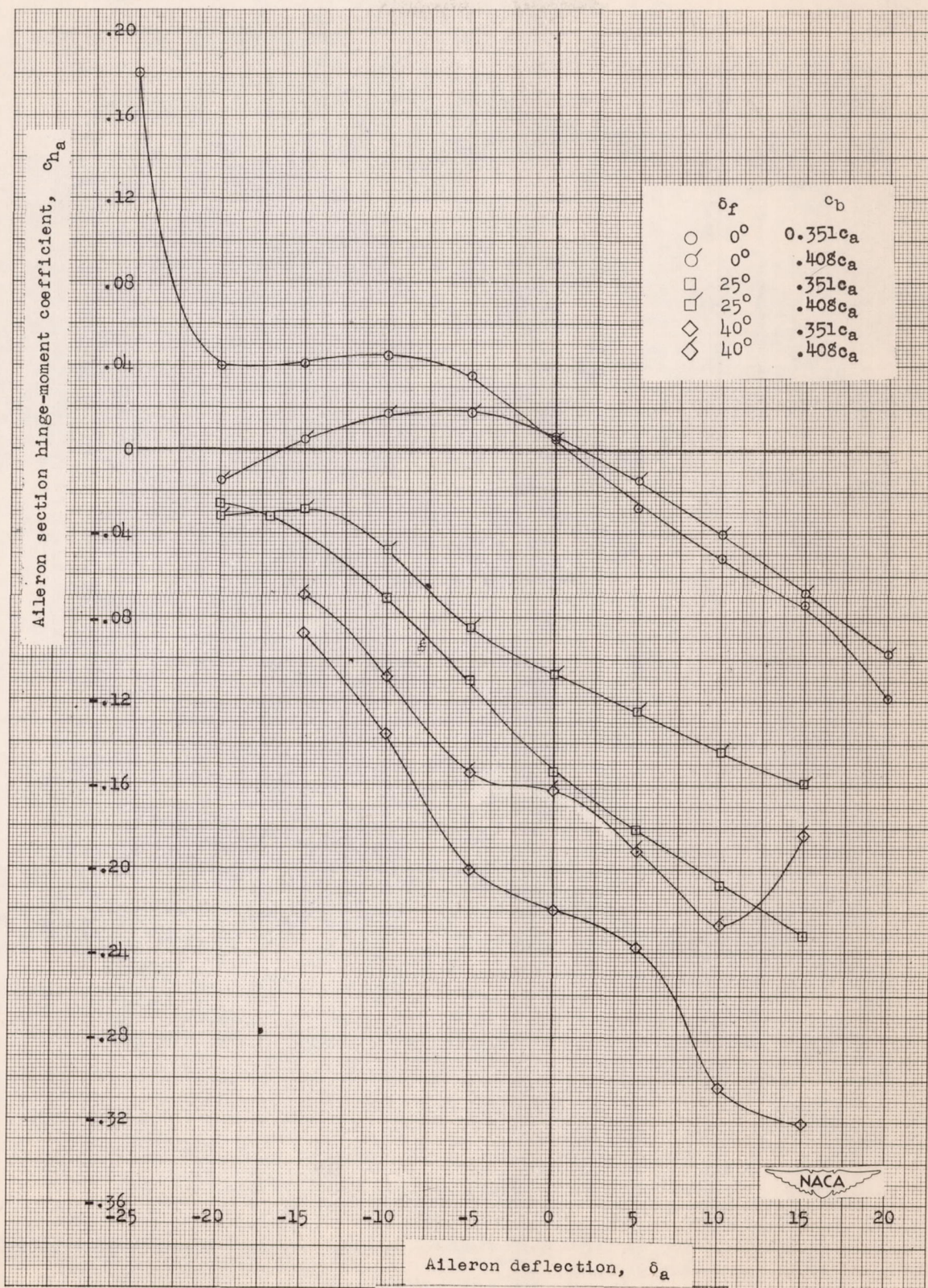
Figure 19.- Lift effectiveness of the flip on the NACA 7-series-type airfoils with straight-sided Frise aileron and double slotted flap. $R = 6 \times 10^6$ (approx.); $\delta_a = 0^\circ$.





(a) 0.17c thick airfoil.

Figure 20.- Aileron hinge-moment characteristics of a straight-sided Frise aileron on two NACA 7-series-type airfoils with double slotted flap and flip. $\alpha_0 = 0^\circ$; $\delta_f = 0^\circ$; $R = 6.0 \times 10^6$ (approx.).



(b) 0.154c thick airfoil.

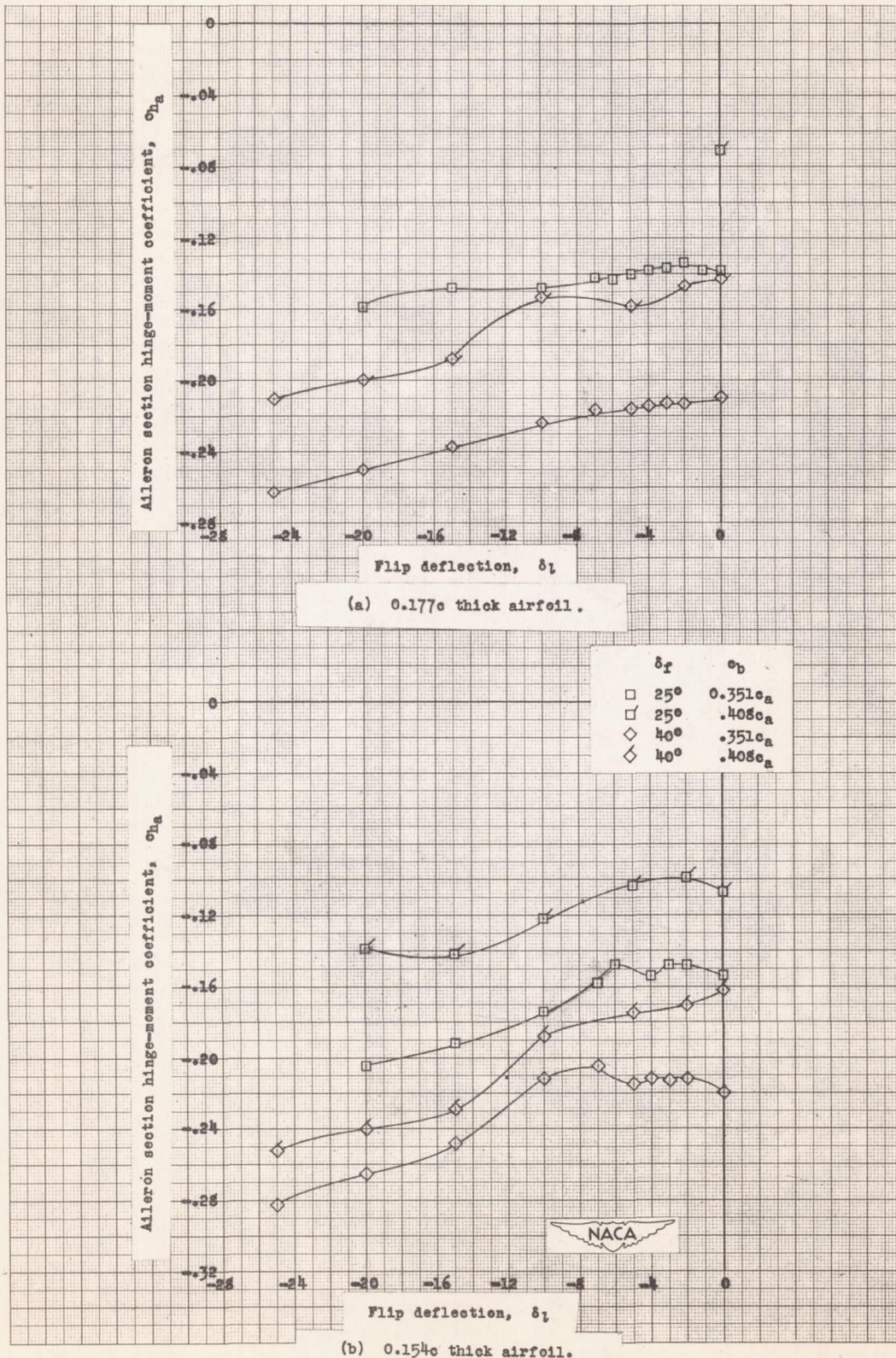
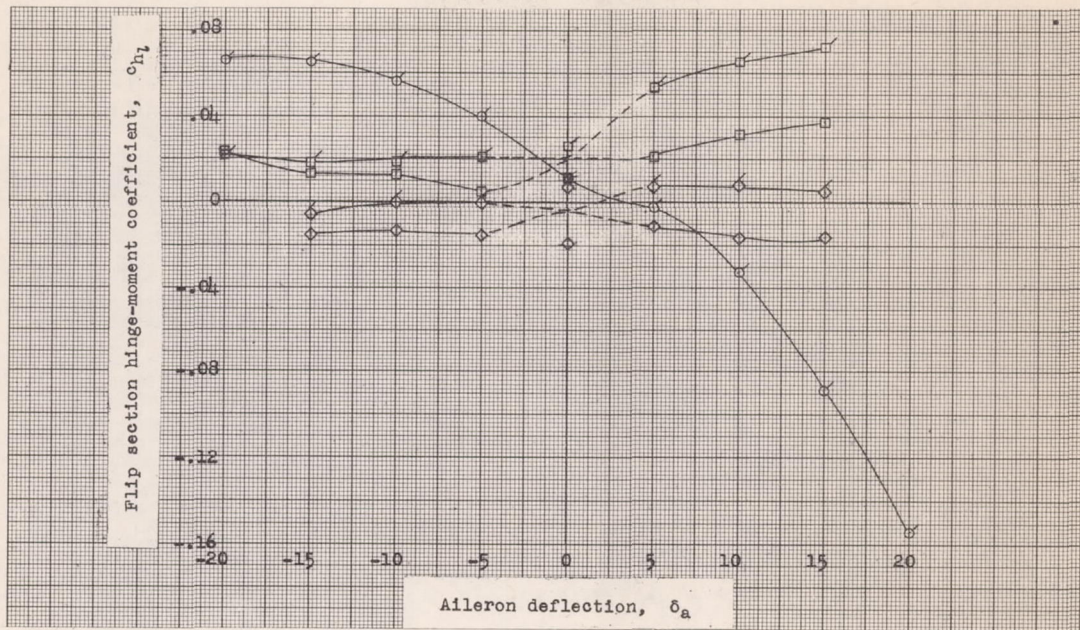
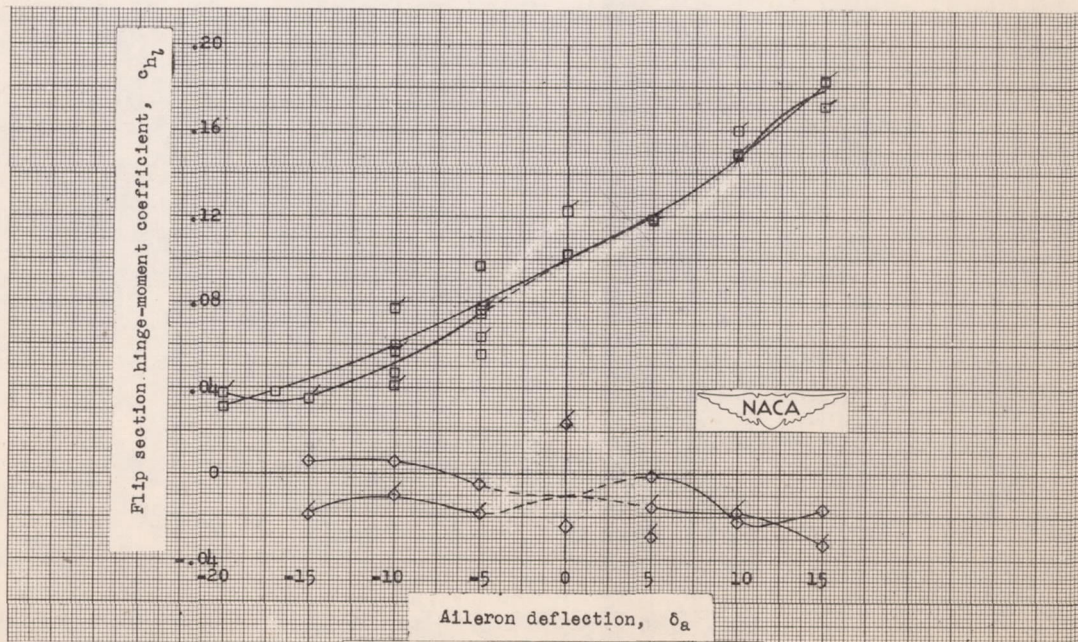


Figure 21.- Variation of straight-sided Frise aileron hinge-moment characteristics with flip deflection on two NACA 7-series-type airfoils with flip and double slotted flap. $\alpha_0 = 0^\circ$; $\delta_a = 0^\circ$; $R = 6.0 \times 10^6$ (approx.).



(a) 0.177c thick airfoil.

δ_f	c_b
\circ	$0.408c_a$
\square	$0.351c_a$
\square	$0.408c_a$
\diamond	$0.351c_a$
\diamond	$0.408c_a$



(b) 0.154c thick airfoil.

Figure 22.- Effect of aileron deflection on flip hinge-moment characteristics on two NACA 7-series-type airfoils with double slotted flap and straight-sided Frise aileron. $\alpha_0 = 0^\circ$; $\delta_f = 0^\circ$; $R = 6.0 \times 10^6$ (approx.).

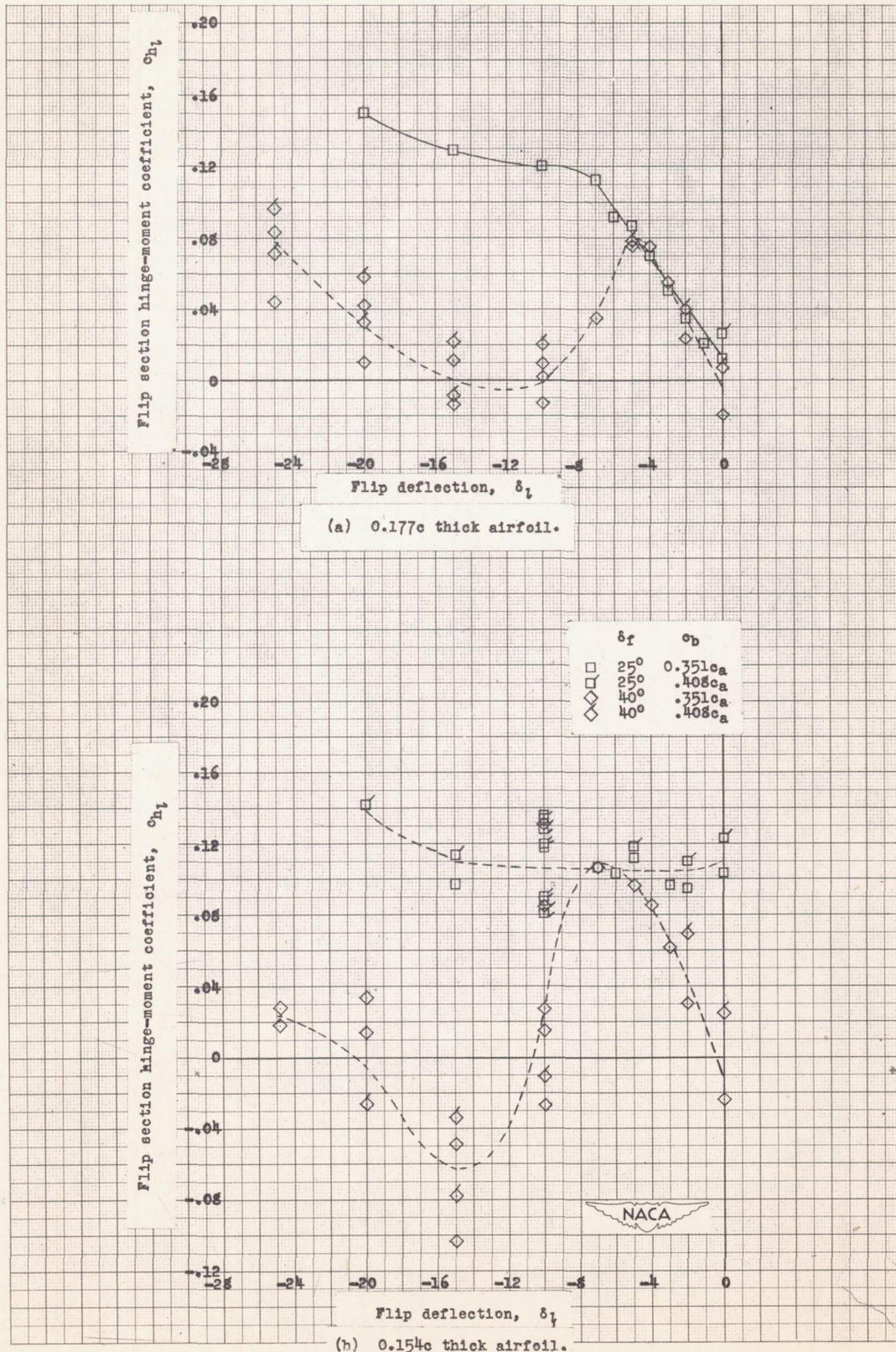


Figure 23.- Hinge-moment characteristics of a flap on two NACA 7-series-type airfoils with double slotted flap and straight-sided Frise aileron. $\alpha_0 = 0^\circ$; $\delta_a = 0^\circ$; $R = 6.0 \times 10^6$ (approx.).